7-1-2013

Role of Rab7 in the pathogenesis of Charcot-Marie-Tooth Type2B (CMT2B) Disease

Soumik BasuRay

SOUMIK BASURAY

Candidate

BIOMEDICAL SCIENCES- PATHOLOGY

Department

This dissertation is approved, and it is acceptable in quality and form for publication:

Approved by the Dissertation Committee:

ANGELA WANDINGER-NESS,Ph.D. , Chairperson

ERIC R. PROSSNITZ,Ph.D.

KEVIN K. CALDWELL,Ph.D.

DIANE S. LIDKE, Ph.D.

Role of Rab7 in the pathogenesis of Charcot-Marie-Tooth Type2B

(CMT2B) Disease

By

Soumik BasuRay

B.S., Biotechnology, Bangalore University, India, 2004

M.S., Biochemical Technology, Madurai Kamaraj University, India, 2006

DISSERTATION

Submitted in Partial Fulfillment of the

Requirements for the Degree of

Doctor of Philosophy

Biomedical Sciences

The University of New Mexico

Albuquerque, New Mexico

July, 2013

Dedication

The thesis is dedicated to the thousands of people suffering from Charcot-Marie-Tooth Disease. May this dissertation be a fruitful endeavor to balm their pain and suffering. I also dedicate this work to my Baba, Ma and Dada who have been a source of my strength and sustenance.

Acknowledgement

Piled higher and deeper, the process of obtaining a PhD degree was a long and tedious journey that met a fruitful culmination. The guiding light that helped me see the end of the tunnel was my mentor Dr. Angela Wandinger-Ness. I owe it her for shaping my career and guiding me move on to the next phase of scientific training. Her patience and support has been exemplary and I hope to receive her invaluable advice even in the future. I would also like to acknowledge my Dissertation Committee members Dr. Eric R. Prossnitz, Dr. Kevin K. Caldwell and Dr. Diane S. Lidke for their constructive inputs and advice during my dissertation work.

I thank all the present and past members of the Wandinger-Ness laboratory for providing a congenial and amiable environment during my stay. A special thanks goes to Elsa G. Romero for providing excellent technical support and being there as my "lab mom". I would also like to thank my colleagues in the lab Dr. Heather Ward, Dr. Jacob Agola, Ms. Stephanie Jerman and Ms. Yuna Guo who have been great to work with. Other members of the lab Ms. Patricia Jim, Mr. Chris Contreras, Ms. Anna Vestling, Ms. Shelly MacNeil, Mr. Anthony Arceci and Ms. Lauren Pincomb also deserve a mention. I would also like to extend my gratitude to past members of the lab Dr. Sanchita Mukherjee, Dr. Jianbo Dong, Dr. Mary-Pat Stein and Dr. Canhong Cao for laying the foundation of the Rab7 functional studies. My sincere thanks goes to Dr. Matthew N. J. Seaman at the University of Cambridge, UK for providing the stable cell lines expressing the Rab7CMT2B mutants and for his valuable inputs during the preparation of the manuscript that eventually got published in the Journal of Biological Chemistry. I would like to thank Dr. Michael C. Wilson for providing his input during the preparation of the

PLoS One manuscript. I would also like to acknowledge Dr. Tione Buranda for the lengthy intellectual discussions. Ms. Genevieve Phillips and Ms. Jamie Padilla provided technical support in conducting some of the experiments and are hereby acknowledged.

I take this opportunity to thank my teachers at St. Xavier's Collegiate School, Kolkata, Bangalore University and Madurai Kamaraj University. I also thank Indian Institute of Chemical Biology, Kolkata, National Center for Biological Sciences, Bangalore, Indian Institute of Science, Bangalore and Bose Institute, Kolkata for giving me the research opportunities to build up my scientific career. Among my academic and research mentors, I would like to especially thank Dr. Govindan Sadasivam Selvam, Dr. M. Hussain Munavar, Dr. G. Shanmugam (Madurai Kamaraj University, Madurai), Dr. Nahid Ali (IICB, Kolkata), Dr. Mathew K. Mathew (NCBS, Bangalore), Dr. Valakunja Nagaraja, Dr. Ashok Mohan Raichur, Dr. Manas Chanda (IISc, Bangalore), Dr. V. Veera Raghavan, Mr. Chethan Kumar K.V., Dr. Raghavendra Rao, Dr. Chandrashekhar Naik, Dr. Riya Dutta, Ms. Neetha D.C. and Ms. Bindu Rao (M.S.Ramaiah Degree College, Bangalore University). I would also like to acknowledge the direct and indirect funding support from the National Science Foundation for conducting this research.

A special thanks to my dear friend, Ms. Verena Fleischanderl who inspired me with the words "Well, you have to take small steps now, everything step by step.. And when you are done, you'll be able to look back from the mountain top, see where you walked and be able to enjoy the view". Lastly, I express my sincere gratitude to my mother, Ms. Rina BasuRay and my father, Dr. Kali Sankar BasuRay who sacrificed a lot to rear me up and make the person I am today, my elder brother, Mr. Saugata BasuRay whom I miss a lot and **GOD, THE ALMIGHTY**.

Role of Rab7 in the pathogenesis of Charcot-Marie-Tooth Type2B (CMT2B) Disease

By

Soumik BasuRay

B.S., Biotechnology, Bangalore University, India, 2004

M.S., Biochemical Technology, Madurai Kamaraj University, India, 2006

Ph.D., Biomedical Sciences, University of New Mexico, USA, 2013

Abstract

Charcot-Marie-Tooth (CMT) Disease is a group of peripheral neuropathies affecting 1 in 2500 individuals. It is characterized by progressive sensory loss and distal muscle weakness affecting mostly the lower extremities that lead to foot deformities. More than thirty genetic loci are affected in this disease, products of which are involved in axonal trafficking. *Rab7* is one such gene that gets mutated in CMT Type2B disease. To date four missense mutants of Rab7 have been identified. L129F, K157N, N161T and V162M amino acid substitutions of Rab7 occur in highly conserved regions. Rab7 is a ubiquitous protein but only the peripheral nerves get affected in this disease. This calls for an urgent need to study the pathogenesis of CMT2B disease, the awry molecular mechanisms of

which remain unknown. This thesis details for the first time the impaired trafficking, altered endosomal and nuclear signaling caused by Rab7CMT2B mutants through differential interaction with effector proteins. The work provides foundation for identifying potential molecular targets for therapeutic interventions in combating this disease.

Table of Contents

List of Figures

List of Tables

Abbreviations

CMT2B: Charcot-Marie-Tooth Type 2B

Rab7: Ras related protein in brain 7

NGF: Nerve growth factor

EGF: Epidermal growth factor

EGFR: Epidermal growth factor receptor

TrkA: Tropomyosin related kinaseA

ERK: Extracellular signal related kinase

Egr-1: Early growth response gene -1

SMN1: Survival motor neuron1

Mcl-1: Myeloid cell leukemia sequence1

FRAP: Fluorescence recovery after photobleaching

GFP: Green fluorescent protein

GDP: Guanidine diphosphate

GTP: Guanidine triphosphate

PI3K: Phosphatidyl inositol 3-kinase

MAPK: Mitogen activated protein kinase

TGF-β: Transforming growth factor beta

HER2: Human epidermal growth factor receptor-2

ESCRT: Endosomal sorting complexes required for transport

EEA1: Early endosomal antigen-1

MNCV: Motor nerve conduction velocity

CIN85: cbl -interacting protein of 85 kDa

Elk-1: ETS like gene 1 tyrosine kinase

Chapter 1: Introduction

Genetics of Neuropathies

Charcot-Marie-Tooth (CMT) disease is a clinically diverse, heterogenous group of inherited peripheral neuropathies that typically affect the peripheral nervous system with a prevalence of 40 in 100,000 individuals (1-3). These diseases affect both the sensory and motor neurons and hence are also known as hereditary Motor and Sensory Neuropathies. CMT disease is divided into Type 1 characterized by a demyelinating phenotype and Type 2 characterized by distinct axonal loss. Both these subtypes result in progressive sensory loss, distal muscle weakness, affecting mostly the lower extremities that lead to foot deformities (4-6). Type 1 subtypes affect myelination or cell communication principally in Schwann cells and include CMT1A-B, CMT3 (hypertrophic neuropathy of Dejerine-Sottas),some forms of CMT4A, CMT4B and CMTX (7). The CMT Type 2 is caused by mutations in 15 genetic loci that cause autosomal dominant or recessive forms of the disease (8). Type 2 subtypes result in axonal degeneration and include CMT2A-G, I-L, and intermediate CMT, DI-CMTB (9). The similarities in disease manifestation resulting from mutations in over thirty known genes may be ascribed to the extensive interdependence of Schwann cells and neurons, and to the fact that the gene products are operative on common pathways **(Figure 1)**. For example, multiple CMT disease associated genes affect proteins that regulate endocytic membrane transport and thereby impact neurons and Schwann cells in the maintenance of axon viability.

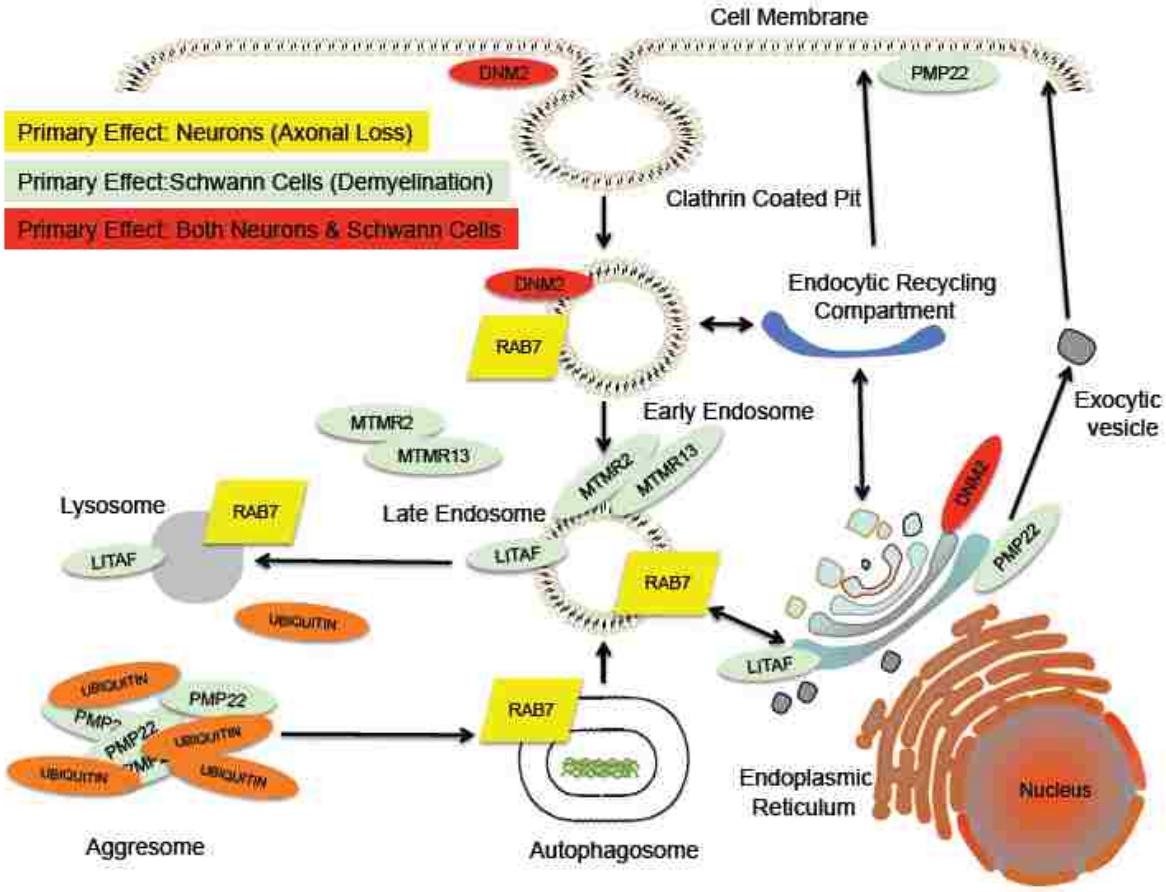

Figure 1: Charcot-Marie-Tooth Disease is a neurodegenerative disorder caused by defects in endocytosis. Charcot-Marie-Tooth (CMT) disease is heterogenous group of peripheral neuropathy affecting more than thirty genetic loci coding for proteins playing important roles in endocytic trafficking. The above diagram shows the different proteins mutant in this disease and their consequent phenotypic effects.

Systematic genetic screening in CMT affected patients enables diagnosis of 50-70% of patients suggesting that additional genes are involved in peripheral neuropathies (10). CMT patients have symmetric distal amyotrophy in lower limbs and hands, foot deformities and distal sensory loss (11). Spine deformities are not common but are seen in specific subtypes like CMT type 4C (12). CMT disease typically sets in the first or second decade of life and primarily affects the lower extremities.

According to the motor nerve conduction velocity (MNCV) and compound muscle action potential CMT can be divided into two types: demyelinating (CMT1) and axonal (CMT2). The demyelinating forms usually have MNCV lower than 38m/s in the upper extremities and the axonal form has higher MNCV although the compound muscle action potential is also affected in this form. The intermediate form of CMT disease is characterized by MNCV in the range of 38-45m/s (13-16).

About 90% of the dominant forms of CMT disease are more prevalent in Western countries whereas 30-50% of the recessive forms occur in countries with high incidence of consanguinity (eg. Mediterranean Basin, European gypsies) (17). A detailed list of the different forms of CMT disease is given in **Table1.**

Table1: Different forms of CMT Disease

Inheritance	Demyelinating Forms		IntermediateForms		Axonal Forms	
	Form	Genes	Form	Genes	Form	Genes
Autosomal Dominant	CMT1A CMT1B CMT1C CMT1D CMT1F	*PMP22* *MPZ* *LITAF* *EGR2* *NEFL*	DI-CMTA DI-CMTB DI-CMTC DI-CMTD DI-CMTE	*DNM2* *YARS* *MPZ* *INF2*	CMT2A1/2 **CMT2B** CMT2C CMT2D CMT2E CMT2F CMT2G CMT2I/2J CMT2K CMT2L CMT2M CMT2N CMT2O CMT2P	MFN2/KIF1B **RAB7** TRPV4 GARS NEFL HSP27 ? MPZ GDAP1 HSP22 DNM2 AARS DYNC1H1 LRSAM1
Autosomal	CMT4A	GDAP1	RI-		ARCMT2A2	MFN2

Recessive	CMT4B1 CMT4B2 CMT4C CMT4D CMT4E CMT4F CMT4G CMT4H CMT4J	MTMR2 MTMR13 SH3CT2 NDRG1 EGR2/MPZ PRX HK1 FGD4 FIG4	CMTA	*GDAP1*	CMT2B1 CMT2B2 CMT2H CMT2P	LMNA MED25 GDAP1 LRSAM1
X-linked Dominant			CMTX1	*GJB1*		
X-linked Recessive			CMTX2 CMTX3 CMTX4 CMTX5	? ? ? *PRPS1*		

Charcot-Marie-Tooth disease affects both the Schwann cells and the axons. The axonal forms of CMT affect both the dorsal root ganglion sensory neurons and spinal motor neurons. Axons can grow as long as 1meter from the soma to sensory receptors in the muscle or skin and to neuromuscular junctions with skeletal muscles (18). This is an Achilles' heel for the neuron as minor differences in endocytic trafficking can have a profound overall impact on its long term survival.

The complexity of CMT disease is underscored by the fact that more than thirty genetic loci are affected. Mutations in *DYNC1H1* gene that encodes the dynein heavy chain protein or *NEFL* and *LMNA* genes encoding the neurofilament and LaminA/C responsible for neurofilament homeostasis cause impaired axonal transport in CMT disease. Mutations in *MFN2* and *GDAP1* genes responsible for mitochondrial functions lead to CMT due to energy requirements for endocytic transport. There is close co-operativity between Rab32 and mitochondrial function (19, 20). Other genes responsible for protein synthesis and turnover (*GARS, AARS, LRSAM1*), calcium homeostasis (*TRPV4*), myelin assembly (*MPZ*), gene expression regulation (*MED25*) and endocytosis (*Rab7 and DNM2*) lead to the severe axonal forms of the disease (21, 22).

Rab7CMT2B Disease

Rab7 belongs to the Ras superfamily of GTPases that play a crucial role in cellular trafficking, signaling and cytoskeletal regulation. Rab7 controls the transport from early endosomes to late endosomes, lysosome maturation, phagolysosomal and

autophagosomal biogenesis. It also plays a critical role in growth factor mediated cell survival and apoptosis (23).

Mutation or dysfunction in the Rab7 gene causes endocytic trafficking disorders leading to Charcot–Marie-Tooth Type 2B (CMT2B) also known as heriditary Motor and Sensory Neuropathy type IIB. It causes prominent loss of sensory neurons and is often characterized by frequently occurring infections and ulcers hence it is also termed as ulceromutilating neuropathy (24). To date, four mutants associated with Rab7have been implicated in this disease. These are L129F, K157N, N161T and V162M, all amino acid substitutions of highly conserved amino acid residues (25-27) **(Figure 2)**. All these missense mutants reside outside the nucleotide binding pocket and adjacent to the switch II region in the C-terminal portion of the protein (28). Biochemical studies of the Rab7CMT2B mutants indicate that the disease mutants have reduced GTPase activity and predominantly occur in the GTP-bound state; hence they are presumed to be more active than the wild-type protein (29, 30).

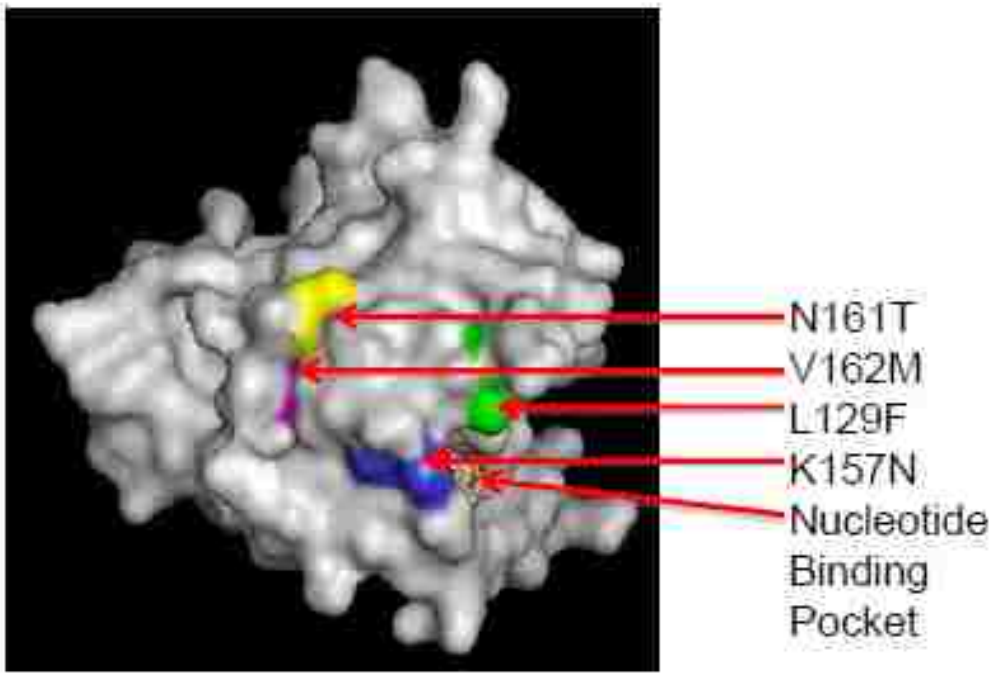

Figure 2: Structure of Rab7 with CMT2B disease mutants. Rab7 structure indicates the amino acid residues L129F, K157N, N161T and V162M substitutions in Charcot-Marie-Tooth Type2B Disease (Image: Oleg Ursu).

Rab7-the master regulator of endocytic traffic

Rab7 is one of the most studied endocytic Rab GTPases due to its pivotal roles in shunting molecules for recycling through the Golgi, back to the plasma membrane or to degradation **(Figure 3**). Typical of Ras-related GTPases, Rab7 undergoes a cycle of membrane association and dissociation that is closely linked to nucleotide binding and hydrolysis (31). In the membrane associated state, Rab7 is GTP-bound and active, while upon hydrolysis the GDP-bound Rab7 is inactive and recycles to the cytoplasm. The GDP/GTP dependent activation cycle is regulated by two sets of proteins, the guanine nucleotide exchange factors (GEFs) that catalyze the conversion to the active GTP-bound state and the GTPase activating proteins (GAPs) that stimulate the GTPase activity of the Rab protein to convert it to the inactive GDP-bound state. Early reports suggested Vps39 functioned as a Rab7 GEF. More recently, studies in yeast and *C. elegans* indicate that Ypt7p/Rab7 activation is linked to endosome conversion involving coordinate inactivation and loss of the early endosomal Rab5 and acquisition and activation of the late endosomal Rab7 through large multimeric complexes with overlapping components **(Figure 4)** (32).

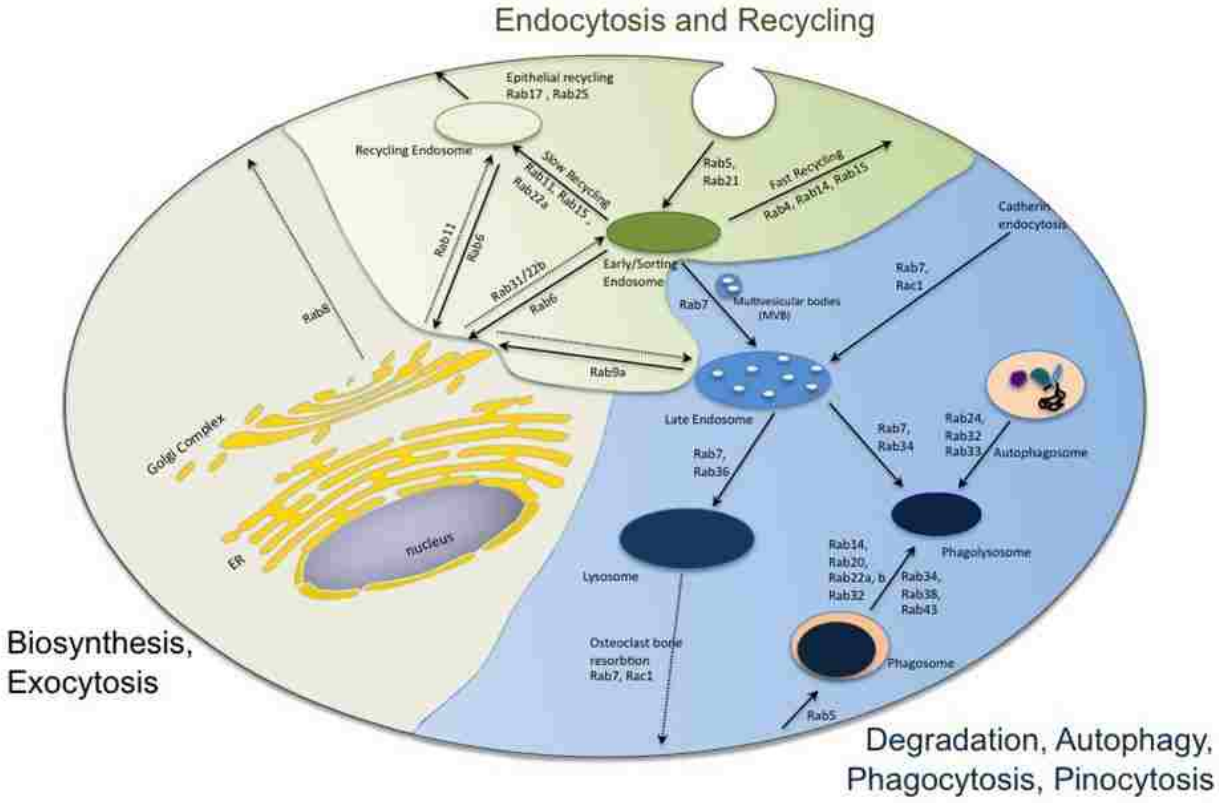

Figure 3: Intracellular trafficking pathways associated with Rab7. Rab7 regulates cargo trafficking to the lysosomes for degradation via late endosomes, cargo recycling through the Golgi back to the plasma membrane, autophagy, phagolysosome fusion and osteoclast-mediated bone resorption.

The activation of Rab7 is dynamically regulated through differential interactions of proteins first identified to be important in autophagy called Rubicon (RUN domain and cysteine-rich domain containing Beclin 1-interacting protein) and UVRAG (33, 34).Rubicon, a regulatory component of the phosphatidylinositol 3-kinase complex (PI3KC3;hVps34/hVps15), can bind and sequester UVRAG and thereby block Rab7 mediated transport (35, 36). Conversely, membrane-bound, active Rab7 can relieve the inhibition of its activation by binding Rubicon (33). Proteins of the Tre-Bub-CDC16 (TBC) family function as GTPase-activating proteins that stimulate nucleotide hydrolysis. Three family members (TBC1D2/Armus, TBC1D5, and TBC1D15) have all been shown to stimulate Rab7 nucleotide hydrolysis and may regulate Rab7 involvement in discrete functions in coordination with specific signaling (37-39). For example, on endosomes the recycling of mannose 6-phosphate receptor to the Golgi via retromer is thought to be regulated by Rab7/TBC1D5, while the disassembly of adherens junctions and degradation of E-cadherin depends on signal integration of Arf6 and a Rac1/TBC1D2/Rab7 complex. As illustrated by the specific examples given, the facilitated nucleotide binding and hydrolysis cycle brings about conformational changes in Rab7 that modulate its activity and localization.

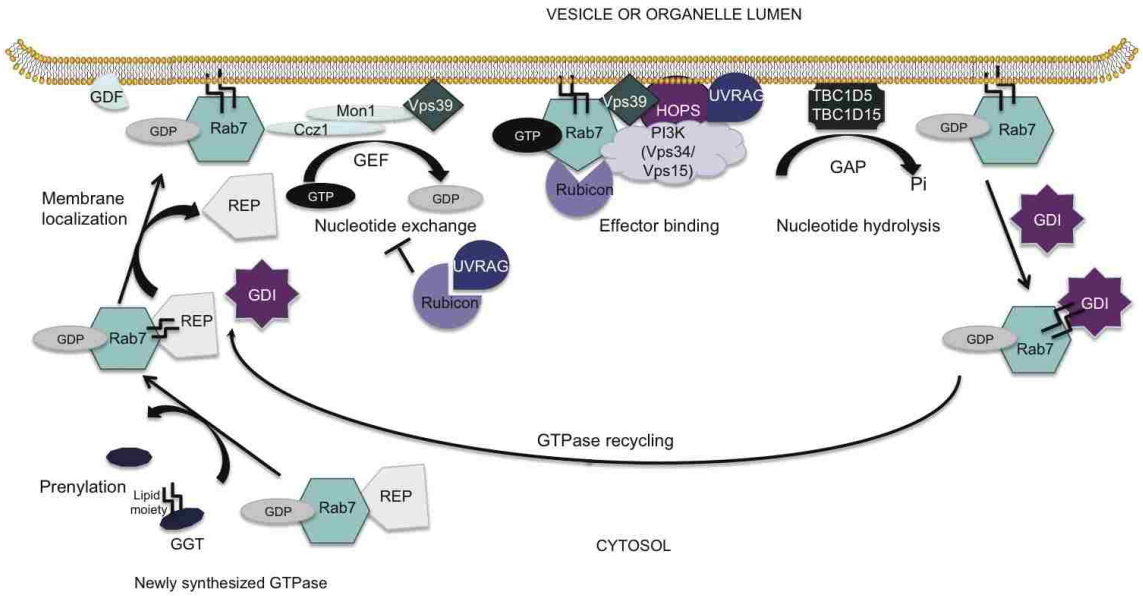

Figure 4: Rab7 activation cycle. Newly synthesized Rab7 is prenylated by geranylgeranyl transferase (GGT) and delivered to endosomal membranes by Rab escort protein (REP), thereafter Rab7 membrane cycling is facilitated by GDP dissociation inhibitor (GDI); pathways that are common to all Rab GTPases. A GDI displacement factor (GDF) has been implicated in membrane transfer of late endocytic Rab9 and Rab7. Rab7 activation is closely linked to Rab5 inactivation in a conversion process that involves Mon1. A Vps39-Mon1-Ccz1 complex likely acts as a guanine nucleotide exchange factor (GEF) to promote activation, while TBC1D5 or TBC1D15 act as GTPase-activating proteins (GAPs) to promote hydrolysis and inactivation. Active, GTP-bound Rab7 acts as a scaffold for sequentially binding multiple effectors phosphoinositide 3-kinase (PI3K, Vps34/Vps15), HOPS, Rubicon, UVRAG, among others to promote cargo selection, cytoskeletal translocation and membrane fusion.

Besides activation through nucleotide binding, another level of regulation occurs through membrane localization. Membrane localization is dependent on post-translational modification with a lipid anchor (prenylation). Nascent Rab7 synthesized on cytosolic ribosomes is inactive and GDP-bound. Prenylation on two C-terminal cysteine residues is mediated by the universal Rab geranyl geranyl transferase, through recognition of the last nine amino acid residues of Rab7 (40). The Rab escort protein (REP) serves as the intermediary for Rab7 presentation to the prenylating enzyme and first-time membrane association (28). GDP dissociation inhibitor (GDI) functions as a universal Rab recycling factor, binding preferentially to doubly prenylated, GDP-bound Rab7 (41). GDI binding masks the isoprenyl anchor in the cytosol and renders Rab7 membrane association a reversible process that is closely linked to the nucleotide bound status, based on the fact that GDI has a 3 order of magnitude higher affinity for Rab7-GDP than Rab7-GTP (42). A GDI-displacement factor (GDF) has been implicated in GDI release during endosomal Rab membrane association, though GEF proteins may also perform this function in conjunction with nucleotide exchange (42). Once on the membrane and in the GTP-bound state, Rab7 interacts with diverse effectors to carry out specific functions in late endocytic membrane trafficking.

Like other Rab GTPases, Rab7 GTPase is a molecular switch that cycles between a GTP-bound active state and a GDP-bound inactive state and serve as platforms to regulate membrane trafficking and intracellular signaling in a spatiotemporal manner (43-46). Rab7has a low molecular size (23kDa); however structural analyses reveal it has multiple

interaction surfaces through which it interacts with different effector proteins and regulatory molecules. The Rab7CMT2B disease mutants have been proposed to have a misregulated Rab7 activation cycle. According to this model, decreased affinity of the mutant Rab7 for GDP permits GTP exchange to occur independent of GEF activity and GTP dissociation to occur independent of GAP activity to inactivate the protein. Interestingly, since the relative affinity of the disease mutants for GTP is higher than GDP these presumably bind to GTP and undergo multiple activation cycles before membrane extraction. This would result in a subtle increase in the GTP to GDP ratio and increase Rab7 residence time on the target membranes thereby facilitating Rab7 binding to host of different effectors potentially preventing progression to the next phase due to reduced GTP hydrolysis (47). This might slow the trafficking of signaling endosomes and reduce temporal progression and fusion with lysosomes by differential interaction with effectors.

Rab7 Effectors in the Control of Endocytic Trafficking

Over the years, many effector proteins have been identified to interact specifically with active GTP-bound Rab7. Rab7 effectors orchestrate events ranging from cargo selection to microtubule translocation to downstream membrane tethering and endosomal membrane fusion **(Figure 5).** Emerging concepts are that Rab7 activation contributes to the dynamic assembly of large protein complexes in a spatially and temporally regulated manner (32). Specific protein complexes serve discrete functions in the transport process, yet handoffs and multiple layers of regulation are common. The importance of maintaining transport fidelity is evidenced by the increasing numbers of human diseases

attributable to defects in endosomal trafficking and Rab7 specifically (Charcot-Marie-Tooth disease type 2) (31, 48) **(Figure 6)**.

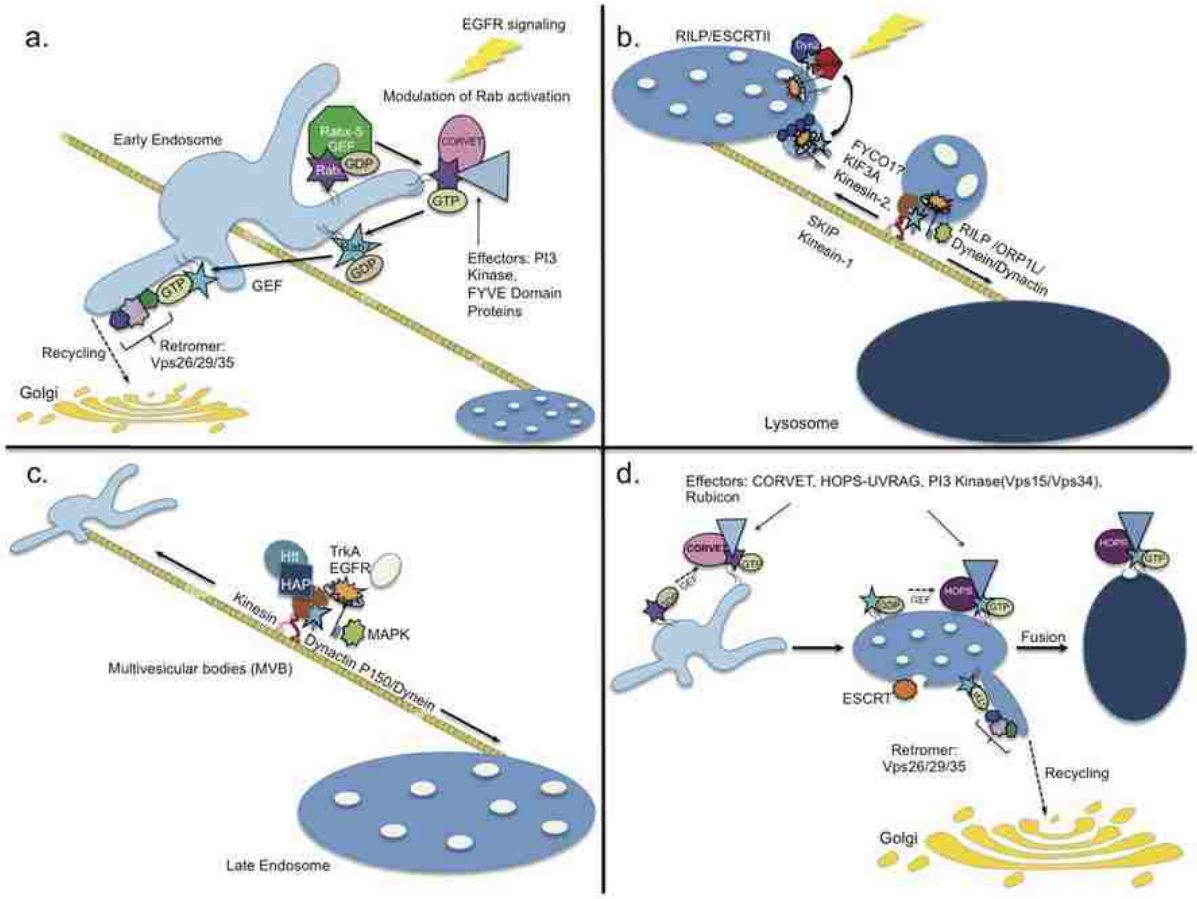

Figure 5: Rab7 regulated trafficking by coordinating with host of effectors. (a) Cargo recycling from early endosomes to the Golgi entails sequential Rab5 (via CORVET) and Rab7 activation and Rab7 mediated recruitment of a complex of VIPs proteins (26/29/35) known as retromer. Rab5 activation can be positively modulated by EGF receptor signaling. **(b)** Transport to lysosomes. Rab7 cooperates with the Dyn2-CIN85 complex to regulate signaling and lysosomal degradation of the ligand-receptor (EGF-EGF receptor) complex. Bidirectional transport on microtubules depends on kinesin and dynein motors. **(c)** Transport from early to late endosomes. Growth factor receptor signaling is intimately coupled to endocytic transport. As illustrated, nerve growth factor receptor TrkA and EGF receptor associate with MAPK on endosomes are translocated bidirectionally on microtubules. Transport toward perinuclear late

endosomes occurs through association with the Rab7 effector RILP and the p150/dynein motor complex. Association with HAP1/Http contributes to perinuclear late endosome positioning. Transport to the cell periphery is mediated in association with kinesin motor complexes (Kif3a/Kinesin-2 via FYCO1 or Kinesin-1 via SKIP). **(d)** Distinct multi-protein complexes regulate transport to and from late endosomes. Rab5-Rab7 conversion involves coordinate inactivation of Rab5 and activation of Rab7, transition of CORVET complex to HOPS complex, which ensures seamless cargo transport to late endosomes. Handoff to ESCRT machinery enables membrane invagination and sequestration of growth factor receptors on intraluminal vesicles of multivesicular bodies. Rab7-retromer complex enables Golgi recycling. Rab7-HOPS complex enables late endosome-lysosome fusion.

On multivesicular bodies and late endosomes, Rab7 facilitates coordinate cargo sorting and bidirectional transport on microtubules through interactions with effectors that differentially associate with dynein or kinesin motors **(Figure 5b–c).** Lysosomal sorting and perinuclear transport are mediated by the Rab7 interacting lysosomal protein (RILP) effector. RILP interacts with components of the endosomal sorting complex required for transport (ESCRT-II) (Vps22 and Vps36) and based on depletion studies, RILP is shown to participate in the sorting of ubiquitinated receptors into intraluminal vesicles (28, 32). In this manner, RILP sorts and sequesters the receptors from the cytosolic signaling machinery and targets them for lysosomal degradation. In a tripartite complex, Rab7, RILP, and a second effector known as oxysterol-binding protein-related protein 1 L (ORP1L) serve to recruit a dynein/dynactin motor complex that in association with betaIII spectrin facilitates the perinuclear transport of endosomes on microtubules (32) **(Figure 5b).** Endosomal lipids such as cholesterol and phosphoinositides are critical regulators of cargo sorting and transport on the late endosomal pathway that are integrated through Rab7 and associated motor proteins. In particular, cholesterol sensing is integrated with transport through the Rab7 effector ORP1L (32). When cholesterol levels are low, ORP1L promotes the association of late endosomes with the endoplasmic reticulum via the dissociation of minus end motor proteins. The ER protein VAPB contributes to motor dissociation and the peripheral movement of late endosomes. Being more peripherally localized, late endosomes are poised to receive cholesterol and other cargo internalized through early endosomes or association with the endoplasmic reticulum (ER). Conversely, when cholesterol levels are high, the conformation of ORP1L is altered and perinuclear transport is favored. Interestingly, Rab7CMT2B

mutants showed similar interaction with RILP (29) although they showed enhanced interaction with ORP1L compared to that of the wild type (47) .

Rab7 together with the early endosomal myotubularin lipid phosphatases (MTM1) and late endosomal myotubularin-related protein 2 (MTMR2) acts as a molecular switch controlling the sequential synthesis and degradation of endosomal PI(3)P (49). Direct binding of the phosphatases to the phosphatidylinositol 3-kinase complex leads to inactivation of the myotubularins. The lipid kinase myotubularin interaction also precludes the interaction of the activated Rab7 with the lipid kinase, illustrating the importance of protein handoffs in phosphoinositide 3-phosphate homeostasis on late endosomes. Together, the examples cited provide evidence for Rab7 function in endosomal lipid homeostasis in both metabolism and signaling, the disruption of which leads to CMT disease (50). Two Rab7 effectors participate directly in the regulation of cargo degradation. Rabring7 (Rab7 interacting ring finger protein) functions as an E3 ligase in conjunction with the Ubc4 and Ubc5 as E2 proteins (28, 32). Functionally, overexpression of Rabring7 increases epidermal growth factor receptor degradation and lysosome biogenesis. The proteasome alpha-subunit XAPC7 or PSMA7 in mammals has been found to interact specifically with Rab7 and is recruited to late multivesicular endosomes (28). Overexpression of XAPC7 impairs late endocytic transport of EGF receptor and hence is a negative regulator of trafficking. Together, Rabring7 and XAPC7 may coordinate the degradation of ubiquitinated growth factor receptors via a link to the proteasomal degradation machinery though further studies are required to elucidate mechanistic details. In addition to the described Rab7 effectors whose functional

activities have been detailed, there are many more putative effectors whose characterization remains to be documented.

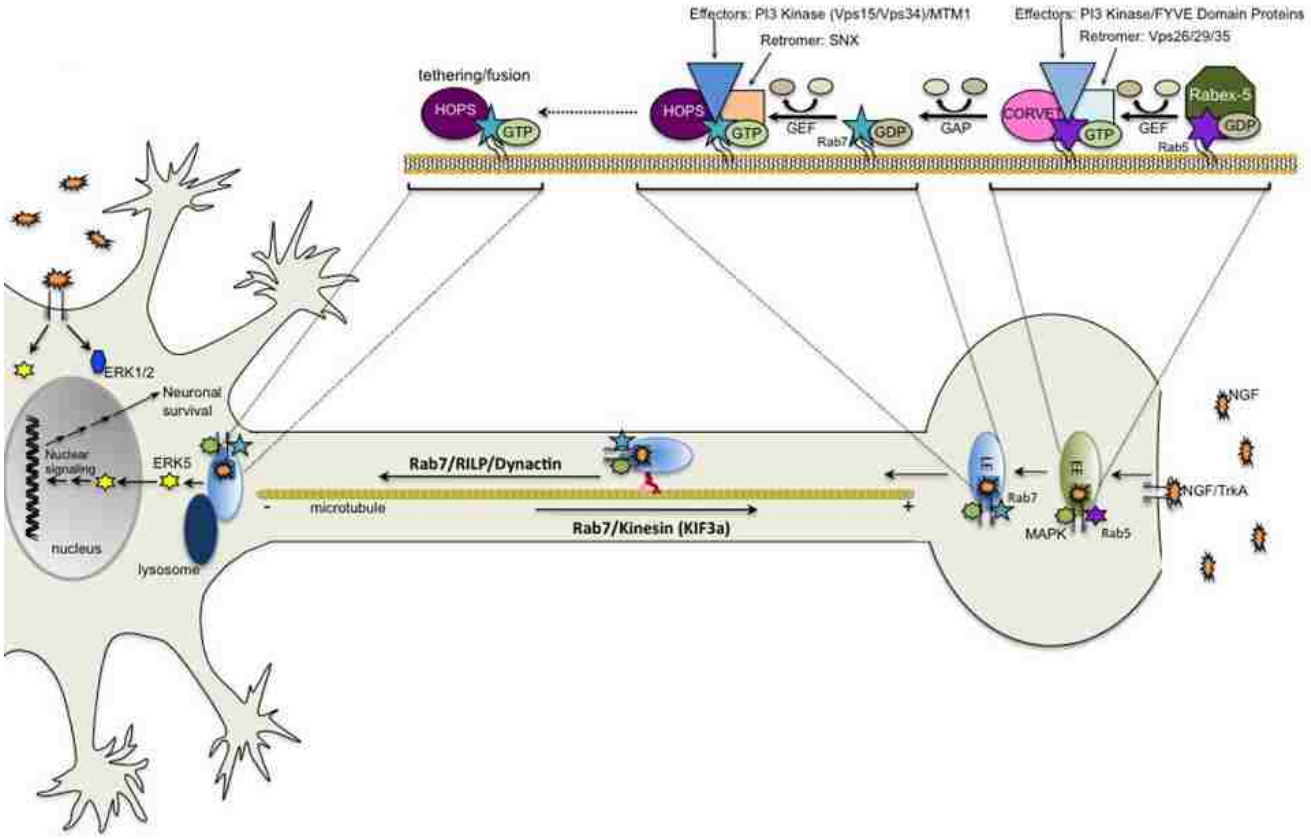

Figure 6: Axon viability depends on coordinated endocytic trafficking and signaling. Nerve growth factor (NGF) binds to the TrkA receptor tyrosine kinase and stimulates phosphorylation and internalization. Endocytosed TrkA is transported from Rab5-positive early endosomes to Rab7-positive late endosomes. In peripheral neurons long distance transport of late endosomes to the cell body is critical for growth factor degradation and proper nuclear signaling to maintain cell viability and differentiation. Transport occurs on microtubules through Rab7, the Rab interacting lysosomal protein

(RILP) effector and dynactin minus-end directed motor complex. Return transport to the synapse is mediated by Rab7 in conjunction with a plus-end directed kinesin motor, likely KIF3a. Inset illustrates endosomal membrane protein complexes involved in Rab conversion that allows transfer of cargo along the degradative pathway. Several conserved multimeric protein complexes first identified in yeast are thought to aid in Rab conversion, directed transport and fusion (RETROMER: endosome to Golgi; CORVET: early to late endosome;HOPS: late endosome to lysosome).

Therefore, further complexity in Rab7 mediated regulation of cargo sorting, cytoskeletal transport, and membrane fusion will emerge through continued study.

In sum, the function of the Rab7-RILP complex in sorting and cytoskeletal transport is best characterized and has been shown not to impair Rab7CMT2B interaction (29), while other Rab7 effector interactions like XAPC7 await further characterization.

Rab7 at the Nexus of Endocytosis and Endosomal Signaling

Endocytosis and endosomal signaling are intricately intertwined. Endocytosis of membrane receptors typically occurs via four major routes: macropinocytocis, clathrin mediated endocytocis, caveolin mediated endocytocis and clathrin and caveolin independent endocytocis. To date EGFR internalization has been studied extensively and it is known that on binding the EGF, EGFR gets activated and recruits clathrin coat proteins to undergo a clathrin mediated endocytocis and gets released in the cytosol following which the clathrin coat dismantles and the cargo resides in distinct endosomes (51). However the endocytic route adopted by the neurotrophins and TrkA receptors remains controversial. NGF stimulation increases the association of TrkA and clathrin with membranes as observed in both PC12 cells and dorsal root ganglion (DRG) neurons. Complexes of activated TrkA, clathrin heavy chain and clathrin adaptor protein AP-2 have been detected (52, 53). The clathrin coated vesicles isolated from NGF stimulated PC12 cells not only show NGF-TrkA complexes but also activated signaling mediators of MAPK pathway (53). Apart from clathrin mediated endocytocis, internalization of NGF-TrkA complex can occur through clathrin and caveolin independent routes. Recently,

identification of Pincher that mediates caveolin independent macropinocytosis of NGF-TrkA complexes shows the diverse nature of the internalization processes (54).

In a cellular context, the nature of ligand-receptor interaction, the concentration of the ligand and the magnitude of the ligand stimulated signal deeply influence the endocytic routes adopted by the activated receptors. During neuronal development the axons that are exposed to a concentration gradient of a particular neurotrophin might prefer different endocytic routes and hence form distinct signaling complexes (55).

At the late endosome, Rab7 coordinately regulates intracellular signaling through special scaffolds, selective endosome positioning and control of growth factor receptor trafficking. Epidermal growth factor receptor (EGF receptor) and nerve growth factor receptor (TrkA) all depend on Rab7 for their signaling and downregulation (31). For example, upon EGF stimulation, K-Ras is endocytosed and sorted to late endosomes where Rab7 and the p14-MP1-p18 scaffolding proteins recruit and activate MEK-ERK on late endosomes (56, 57). MAP kinase signaling is further regulated by Rab7 dependent late endosome positioning through dynactin such that peripheral mislocalization results in prolonged EGF receptor activation and downstream upregulation of ERK and p38 signaling. Retrograde endosomal signaling in neurons involves many steps starting with internalization of ligand-receptor complex, sorting of internalized cargo into active signaling vesicles, movement of these activated vesicles along the microtubule network to the cell body to elicit endosomal signaling and finally dismantling this machinery to terminate the signaling.

Rab7 regulates endosomal signaling

Rab7 plays a crucial role in concomitant neuritogenic signaling and trafficking of activated internalized growth factor receptors. In PC12 cells it interacts with endocytosed nerve growth factor (NGF) receptor TrkA in a growth factor and time dependent manner. Immediately after addition of growth factor, the NGF-TrkA complex is internalized. In the early endosome, the NGF-TrkA complex associates with Rab5 and provides a platform for MAPK signaling by sustaining Rap1 activation exclusively from endosomes (58). This recruits and activates B-Raf that facilitates recruitment of other components of the MAPK signaling module. The complex of Rap1, B-Raf, ERK1 and ERK2 localizes on the endosomal membrane and gets retrogradely translocated towards the cell body **(Figures 6 and 7)** (59). Apart from the MAPK module, components of the PI3kinase pathway have also been detected to be associated with the Trk vesicles and inhibition of the PI3kinase activity results in impaired NGF internalization and retrograde transport (60). Many proteins involved in endocytosis have phosphoinositide binding domains (FYVE, PX, PH, ENTH and FERM) (61). EEA1 is a prominent example that binds to PI3P via the FYVE domain, is known to move along with the retrograde NGF-TrkA complex and also interacts directly with Rab5 to sort proteins to early endosome (62). There is agreement that the Akt pathway gets activated by the surface TrkA receptors whereas the MAPK pathway is activated from the endosomes (63). In a nutshell, target derived NGF binds to TrkA that gets activated by tyrosine phosphorylation at the presynaptic terminal and gets endocytosed and trafficked along microtubules to the neuron cell body (64). Delivery of tyrosine phosphorylated TrkA to the soma activates

the ERK1/2 and Akt signaling pathways which effect changes in gene expression and metabolic activity required for neuritogenesis.

The localization of two signaling mediators of the TGF-β superfamily to Rab7-positive late endosomes (p-Smad1 and p-Smad2) is also suggested to be critical for regulation of growth factor signaling (65). At the conclusion of signaling, Rab7 may act cooperatively with dynamin 2 and CIN85 (cbl -interacting protein of 85 kDa) to promote the transfer of signaling receptors from late endosomes to lysosomes for degradation (66).

In neuronal cells, the receptor tyrosine kinase, TrkA is activated by nerve growth factor (NGF). On NGF stimulation, Rab7 interacts with TrkA as it transits through early and late endosomes. Cells expressing Rab7T22N, which is predominantly GDP-bound, showed prolonged ERK1/2 signaling due to impaired trafficking of activated TrkA (31, 67). Disease-causing Rab7 mutants that are constitutively activated have also been shown to exhibit enhanced NGF-stimulated ERK1/2 signaling (68). This apparent contradictory result can be explained by the duality of Rab7 in regulating transfer of cargo to lysosomes and interacting with scaffold proteins.

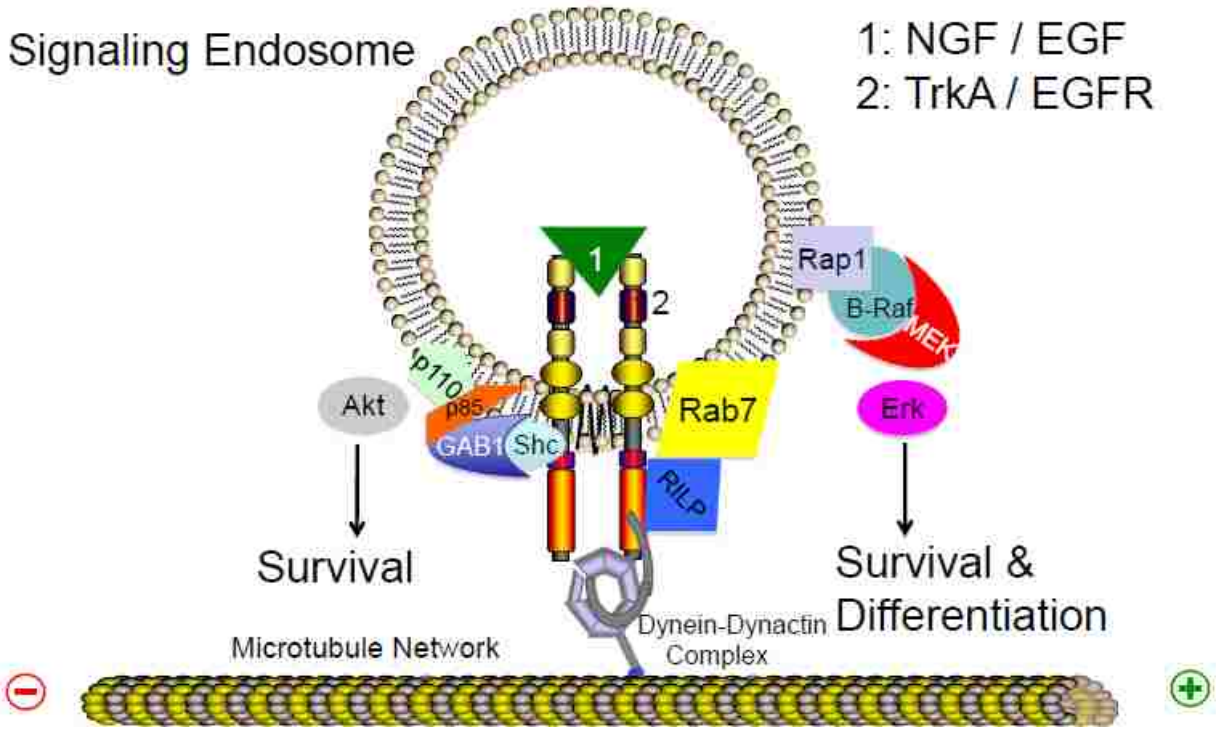

Figure 7: The Signaling Endosome. Signaling endosome showing the recruitment of the MAPK signaling module and the PI3K signaling mediators alongwith the NGF-TrkA complex. The singaling complex also interacts with dynein-dynactin complex for retrograde movement towards the cell body.

Phosphorylation of Rab7 in response to growth factor suggests a further layer of regulation. Large scale proteomics analyses have identified Rab7 to be both serine and tyrosine phosphorylated. In mouse liver extracts, Rab7 was found phosphorylated on serine 72 within highly conserved sequence near the GTP-binding pocket (69). Rab7 was phosphorylated in response to EGF stimulation on tyrosine 183 in the C-terminal region. Enhanced tyrosine 183 phosphorylation of Rab7 was also associated with mutant EGF receptor and HER2 overexpression in non–small cell lung carcinoma and mammary epithelia, respectively (70). The functional consequences of Rab7 serine and tyrosine phosphorylation with respect to membrane trafficking, GTP binding, and hydrolysis remain to be established.

Role of ubiquitination in receptor downregulation

Ubiquitination of activated growth factor receptors plays a crucial role in the endosomal sorting and lysosomal targeting to downregulate receptor levels and hence signaling. Such ubiquitination may depend on interaction with Rab7 and the Rabring7 E3 ubiquitin ligase. The sorting of ubiquitinated receptors into luminal vesicles of multivesicular bodies depends on the ESCRT0, ESCRTI, ESCRTII, and ESCRTIII complexes (71). EGF receptor and TrkA endolysosomal degradation are both ubiquitin and proteasome dependent. The K63-linked polyubiquitin chain on activated TrkA receptors gets shuttled by the p62 scaffolding protein, possibly in association with Rab7/XAPC7, to the proteasome for deubiquitination prior to degradation in lysosomes (72, 73). TrkA deubiquitination prior to lysosomal degradation may allow crucial recycling of ubiquitin

since the ubiquitin tagging is essential for optimum interaction of activated TrkA with the transport machinery and its delivery along the long axonal route from the tip to the cell body.

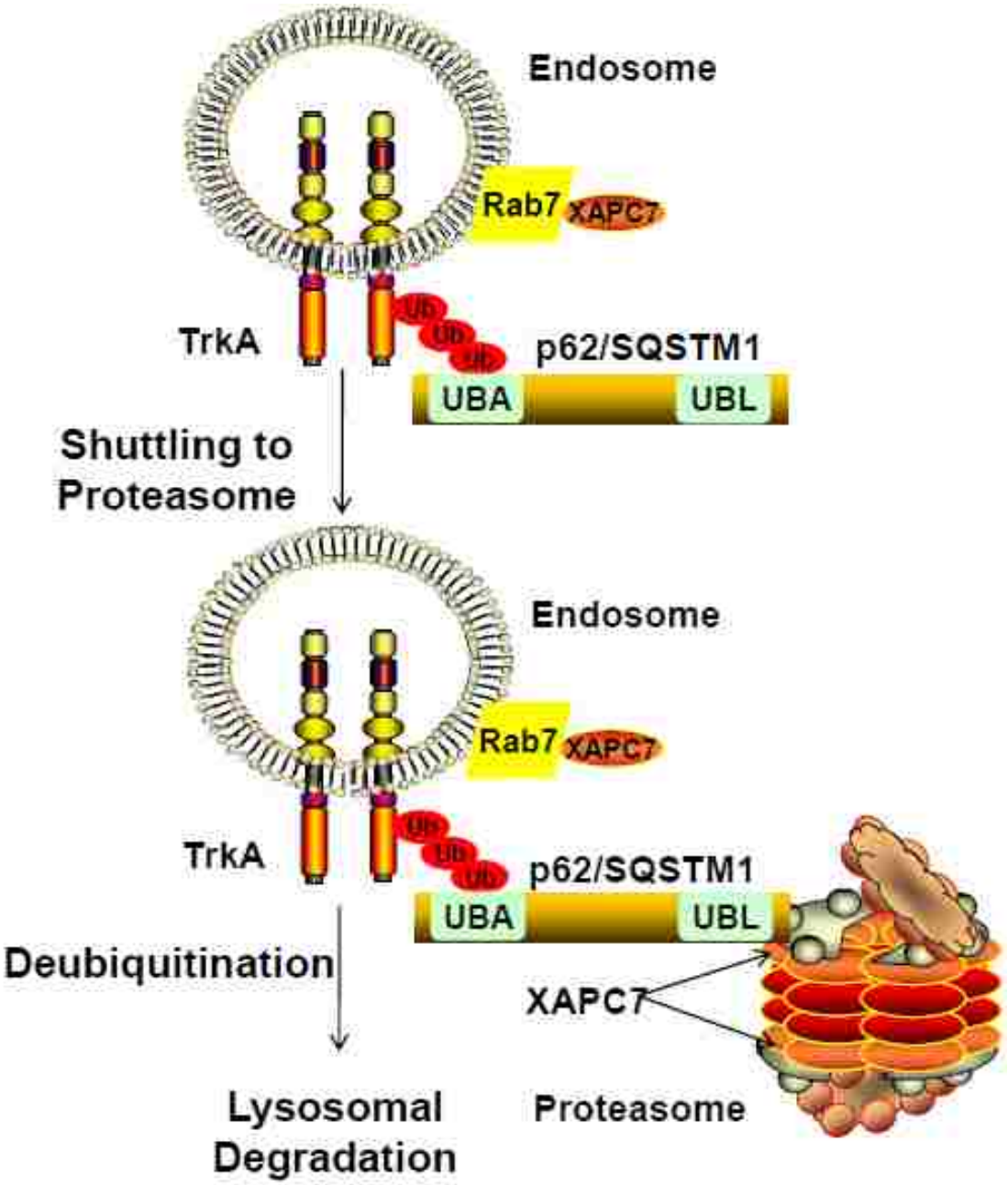

Figure 8: Proteasomal deubiquitination of TrkA is a prerequisite for its lysosomal degradation. TrkA receptors upon growth factor stimulation gets internalized and ubiquitinated. The ubiquitylated cargo is captured by the p62/SQSTM1 which shuttles it to the proteasome for deubiquitination. Following this step the cargo proceeds to lysosomal compartments for degradation.

Only after TrkA reaches the cell body, the termination of signaling calls for deubiquitination of the cargo prior to its lysosomal degradation. As illustrated, the reversible ubiquitination is an important component of growth factor receptor downregulation **(Figure 8)**. The Rab7-regulated, interdependent late endocytic trafficking and signaling pathways are indispensible for translating growth factor signals into appropriate cell responses, misregulation of which may cause this neurodegenerative disease (74).

In sum, Rab7, a crucial regulator of endocytosis interacts with a host of different effector proteins to orchestrate endocytic trafficking. Although ubiquitous, Rab7 mutants implicated in CMT2B disease affect only the peripheral neurons. This raises a question on the putative effects of differential effector interactions with Rab7 to alter endosomal trafficking and concomitant endosomal signaling to cause neurodegeneration.

Overall hypothesis

Rab7 plays a pivotal role in the pathogenesis of the peripheral neuropathy Charcot-Marie-Tooth Type 2B disease. Based on the available literature the overall hypothesis of the dissertation is **Rab7CMT2B mutants alter trafficking of activated growth factor receptors and spatiotemporal endosomal signaling through differential interactions with effectors.**

Specific Aims

Specific Aim 1: To biochemically characterize the modulation of endosomal signaling by Rab7CMT2B mutants.

Specific Aim 2: To measure the impact of Rab7CMT2B mutants on the spatiotemporal fidelity of endosomal signaling relative to late endocytic traffic regulation.

Specific Aim 3: To measure the effect of differential interaction with a Rab7 interactor (XAPC7-proteasome subunit)

Chapter 2: Methods

Mutagenesis and plasmid construction

Rab7 used in these studies was *Canis lupus familiaris* (NM_001003316) (75). GFP-tagged Rab7CMT2B mutants (L129F, K157N, N161T and V162M) were constructed by site directed mutagenesis of wild-type GFP-Rab7 in the pEGFP-C3 vector. The plasmids were used as templates for PCR-based mutagenesis. All amino acid substitutions were generated by a one-step reverse cyclic PCR method using the appropriate base changes in the synthetic oligonucleotides (76). The primer sequences used for generating the mutants were as follows:

Rab7L129F (Fwd-5'-ATTGACTTCGAAAACAGACAAGTGGC-3',

Rev-5'-CTTGTTTCCCAACACAACGAAAGGGA-3'),

Rab7K157N (Fwd-5'AGTGCCAACGAGGCCATCAATGTGG-3',

Rev-5'-GGTCTCGAAGTAGGGAATGTTGTTT-3'),

Rab7N161T (Fwd -5'-GCCATCACCGTGGAGCAGGCGTTCCA-3',

Rev -5'-CTCCTTGGCACTGGTCTCGAAGTAGG-3' and

Rab7V162M (Fwd -5'GCCATCAATATGGAGCAGGCGTTCCA-3' and

Rev -5'-CTCCTTGGCACTGGTCTCGAAGTAGG-3'.

Mutations were confirmed by sequencing the entire Rab7 gene.

Transient Transfection and Expression of Rab7CMT2B Mutants

Cell lines were cultured as described above and passed on consecutive days to maintain in logarithmic growth phase immediately prior to transfection. Transfections of PC12 cells were performed using Lipofectamine 2000 (Invitrogen) according to manufacturer's instructions. Rab7 expression was maximal 16–24h post-transfection and experiments were conducted during this time frame. Transfection efficiency of 35% was consistently observed.

The level of expression of GFP-tagged Rab7 wild-type and mutant proteins in transfected PC12 cells was 3-foldhigher than the endogenous Rab7 with transfection efficiencies of ~35% **(Figure 9)**.

Generation of stable cell lines

Stable PC12 cell lines were established using these canine Rab7 constructs with a G418 resistance marker. The Rab7 constructs used to generate stable HeLa cells was of murine origin, and mutagenesis was performed on Rab7 in pEGFP-C1. The constructs were subcloned into pIRESneo2 and transfected to generate stable HeLa cell lines expressing GFP-Rab7. The GFP-Rab7 expression in all the cell lines was similar on stimulating with EGF in a time dependent manner **(Figure10).**

A.

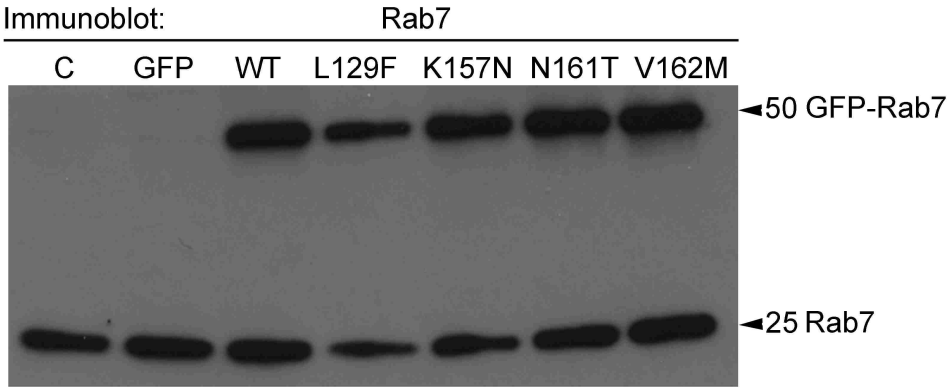

B.

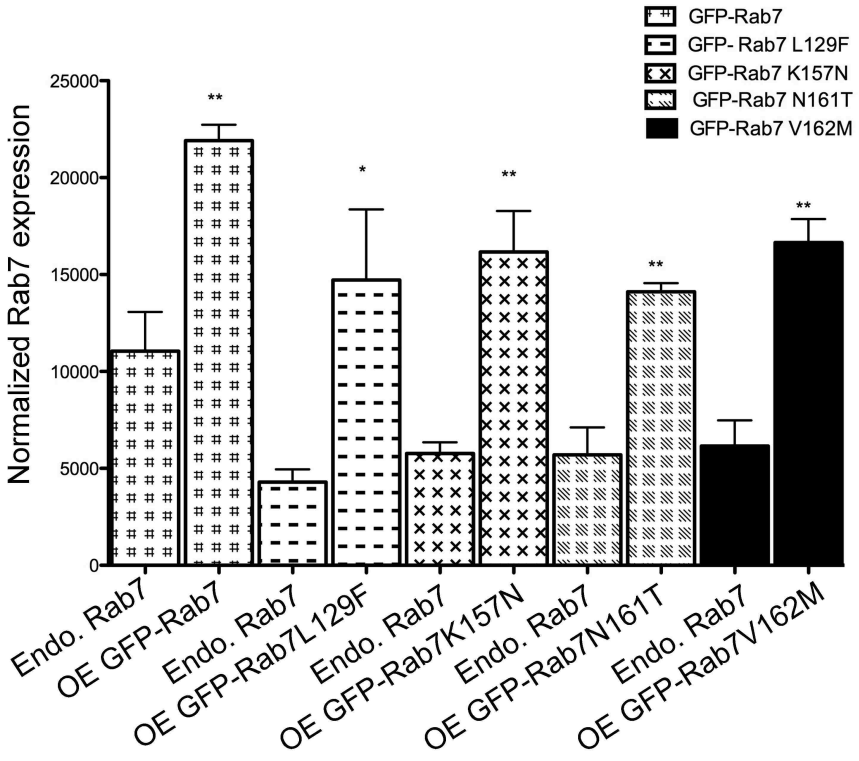

Figure 9: GFP-Rab7 wild-type and Rab7CMT2B mutant proteins are uniformly expressed in PC12 Cells 3-fold above endogenous levels. (A) Transiently transfected PC12 cells expressing GFP, GFP-Rab7wild-type, GFP-Rab7L129F, GFP-Rab7K157N, GFP-Rab7N161T and GFP-Rab7V162M were lysed 16h post-transfection and immunoblotted for Rab7 to probe for GFP-tagged proteins as well as the endogenous Rab7 levels. **(B)** Films from three independent experiments were quantified using Image J analysis. Values of overexpressed (OE) GFP-Rab7wt and GFP-Rab7CMT2B mutant protein expression were compared to endogenous (Endo.) Rab7 levels. Error bars indicating mean ±S.E.M. n=3, *$p<0.05$; **$p<0.01$.

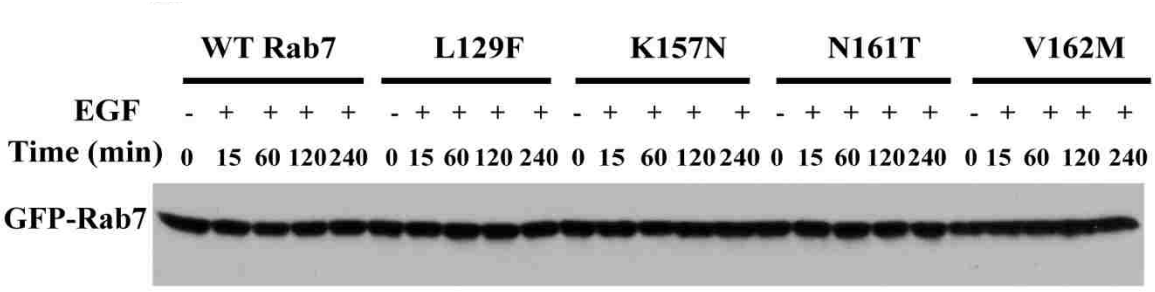

Figure 10: Similar levels of GFP-Rab7 expressed in all samples stably expressing Rab7 wild-type and CMT2B mutants. Samples from EGFR degradation assays were probed with antibody directed against GFP to assess the GFP-Rab7 expression levels for all the samples.

NGF stimulation protocol

NGF (200ng/ml) stimulation was performed as described previously (67).

For all NGF stimulations, a concentration of 200ng/ml of recombinant human NGF was used. Eighteen hours post transfection, PC12 cells were washed and stimulated with NGF for 10min in serum-free medium (DMEM and 0.1% BSA) to drive internalization of TrkA into endosomes. Subsequently, PC12 cells loaded with internalized activated TrkA bound to NGF (77) were chilled on ice to arrest endosomal trafficking, and the remaining surface bound NGF was removed by three washes with ice-cold "surface strip buffer" (0.2 M acetic acid and 0.5 M NaCl) (78), followed by three washes with ice-cold PBS. Afterward, cells were reincubated for the indicated time points in pre-warmed serum-free medium and subsequently processed for immunofluorescence or biochemical assays.

EGFR Degradation Assays

For degradation assays, stable HeLa, stable PC12 cells and A431 cells grown on six well plates were serum starved for 5h in DMEM with 25µg/ml cycloheximide and stimulated with serum free media containing 100ng/ml epidermal growth factor (EGF;Invitrogen) and 25µg/ml cycloheximide. At time points (0–4h), cells were lysed with 80µl SDS lysis buffer (10mM Tris, pH 7.5, 140mM NaCl, 1% [w/v] SDS, 5mM EDTA, 2mM EGTA, 1mM PMSF, 1mM Na_3VO_4,10mM NaF, 30mM sodium β-glycerophosphate and protease inhibitor cocktail CLAP: 10µg/ml of chymostatin, leupeptin, antipain, and pepstatin A) and brief sonication to shear DNA. Cellular debris was removed by centrifugation, and total protein concentration was quantified using a BCA protein assay (Pierce,Rockford, IL). For siRNA knockdown experiments a previously reported protocol for endogenous

Rab7 ablation was followed human Rab7 siRNA (Gene ID 7879) was purchased from Dharmacon Technologies (38).

Immunoprecipitation

BHK-21 cells were grown on 100-mm dishes and GFP-Rab7 wild-type or individual CMT2B mutants were co-transfected with XAPC7-DsRed plasmid using Lipofectamine 2000 (Invitrogen). Mock transfections were performed using a suitable vector lacking an insert. Cell homogenates were prepared in homogenization buffer (HB, 20mMhepes, pH 7.4 and 2mM $CaCl_2$) buffer by passage through a 27-gauge needle 10-20 times. Nuclei, cell debris and large organelles were removed by low speed centrifugation at 1000 rpm for 5min in an Eppendorf microcentrifuge at 4ºC. Mitochondria were removed by centrifugation at 1,950g for 20min, and a crude membrane fraction was collected by centrifugation at 105,000 g for 2h. The pellet was resuspended in RIPA buffer (1% (v/v) Nonidet P-40, 0.5% (w/v) deoxycholate, 0.1% (w/v) SDS, 50mM Tris pH 7.4, and 150mM NaCl) containing a protease inhibitor cocktail (1mM phenylmethylsulfonyl fluoride, 1mM benzamidine, 1µg/ml CLAP) and immunoprecipitation of XAPC7 was performed using polyclonal rabbit anti-Rab7 as described (79-81). Immunoprecipitates were recovered with Protein A-Sepharose (Sigma-Aldrich) and resolved on 12% gels and transferred to hybond-C membrane (Amersham Biosciences). Immunoblot analysis was performed with a mAb directed against XAPC7 or with our rabbit polyclonal antibody directed against Rab7 (NW112) (82).

Gel electrophoresis and Immunoblot Analyses

Samples were resolved by SDSPAGE on 8% gels for EGFR degradation assays and 12% gels for p38 and ERK1/2, transferred to nitrocellulose, blocked with 3% newborn calf serum in Tris Buffer Saline Tween-20 (pH-8). Samples comparing wild-type and mutant lysates were resolved on a single gel for each experiment. Actin, phospho-proteins, total p38 and ERK1/2 were analyzed on a single blot.

Fluorescence Recovery after Photobleaching (FRAP) Assay

BHK-21 cells were seeded and grown to 50-60% confluency on coverslips. GFP-tagged wild-type Rab7, dominant negative Rab7T22N, constitutively active Rab7Q67L and individual CMT2B mutants were overexpressed in BHK-21 cells using transient transfection. FRAP experiments to monitor GTPase activation were performed based on published procedures at 37°C and using cells on glass coverslips mounted in a chamber suited for inverted microscopic imaging (83). Live cell images were collected using a BioRad Radiance 2100 mounted on a Nikon TE2000 inverted microscope. A subset of GFP-Rab7 vesicles were bleached for 10s by a high-intensity light illumination at 488 nm, and the fluorescence recovery in the bleached spot was quantified. Fluorescence recovery was measured every 20s for a total of 600s for each sample. The FRAP measurements were performed on n=30 cells for each Rab7 mutant and repeated a total of n=3. FRAP measurements were made both near the nucleus as well as on peripheral vesicles with no significant differences. The recovery curves were corrected for loss of

total fluorescence due to bleaching induced by repeated imaging on a control area without GFP-Rab7 decorated endosomes.

Immunofluorescence Microscopy

Cells transfected with GFP-tagged Rab7 wild-type and CMT2B mutant plasmids were starved for 14h and incubated with Alexa555-tagged EGF for 1h at 4°C. Cells were kept at 37°C for 10min followed by wash in DMEM and reincubated at 37°C for 20, 60, and 120min. Cells were fixed with 3% paraformaldehyde and permeabilized for 5min in 0.1% (v/v) Triton X-100. Blocking and antibody incubations included 0.4% fish skin gelatin (Sigma-Aldrich). Coverslips were viewed on a Zeiss LSM 510 confocal microscope using plan-Neofluor 40X/1.30 oil or plan-Neofluor 63X/1.30 numerical aperture oil objectives, taking 0.4-µm optical sections. All images were exported as tiff files and compiled in Adobe Photoshop (San Jose, CA). For comparative analyses, cells were imaged under identical parameters, and fluorescence intensity was analyzed using Slidebook 4.1 software (Intelligent Imaging Innovations, Denver, CO). The percentage of colocalization was analyzed using Slidebook 4.1 software. Masks were created for each channel for all of the *z*-stacks acquired for each image, and the overlap was assessed with AND functions to determine the percentage of colocalization of the two channels.

Subcellular Fractionation

Nuclear and cytosolic fractions were prepared as previously described with minor modifications (84). PC12 cells and HeLa cells stably expressing GFP-Rab7CMT2B mutants were plated on 60mm dishes. For NGF stimulated cells were transiently

transfected with GFP-tagged Rab7CMT2B mutants. To separate the nuclear and cytosolic pools of ERK1/2, the cells were serum starved for 5h and stimulated with NGF for 10min followed by surface stripping of the ligand. The cells were then incubated in starvation medium (DMEM containing 0.1% BSA) for 2h, 6h or 24h at 37°C. The cells were washed thrice in ice cold PBS and scraped in 750µl of lysis buffer (10mM Tris-HCl, pH 7.4, 10mM NaCl, 3mM $MgCl_2$ 0.3% (v/v) NP-40, 1mM PMSF, 1mM Na_3VO_4,10mM NaF, 30mM sodium β-glycerophosphate, 10mg/ml chymostatin, 10mg/ml leupeptin, 10mg/ml antipain and 10mg/ml pepstatin). Cells were incubated on ice for 5min followed by centrifugation at 500g for 5min to pellet the nuclei. The remaining supernatant was taken as the cytosolic fraction. Nuclear pellets were washed in the same lysis buffer without NP-40. The cytosolic and nuclear fractions were boiled in 2X Laemmli sample buffer and resolved on 10% SDS polyacrylamide gels and probed with a phospho ERK1/2 antibody. The purity of the nuclear fraction was verified with an antibody directed against nuclear lamin B.

Expression and purification of GST-RILP.

Competent *E.coli* BL21 cells were transformed with a plasmid encoding GST-RILP. Cultures were grown at 37°C to an absorbance of 0.5O.D. measured at 595 nm and protein expression induced by transfer to room temperature and addition of 0.2mM isopropyl-beta-D-1-thiogalactopyranoside (IPTG) for 16-18h to maximize the yield of properly folded active fusion protein. Purification of GST-RILP was performed according to standard procedures as previously described (85, 86). The harvested bacterial cell pellet was resuspended in phosphate buffer saline. Cells were lysed using

lysozyme and microtip sonicator (Misonix Inc., Newtown, CT, U.S.A.).The samples were kept on ice. The power setting was kept at 50% with intermittent pulse of 5s repeated twice with a gap of 30s in between. The cell lysates were mixed with 10% TritonX-100 end over end for 30min at 4°C. Cells were then centrifuged at 8,000*g* for 10min to pellet the cellular debris. The supernatant was mixed with glutathione Sepharose 4B slurry and bound at 4°C for 2h using gentle agitation to keep the resin suspended in the lysate solution. Glutathione sepharose 4B beads with bound protein was settled using low speed centrifugation (500*g*) followed by multiple washes before eluting the glutathione Sepharose 4B bound GST-tagged protein with 10mM Glutathione in 50mM Tris-HCl elution buffer. Eluted protein was concentrated by passing through Millipore Amplicon Ultra Tubes (MWCO 30,000). The purified protein was quantified using the BCA protein estimation kit (Pierce). Single use aliquots stored at -80ºC were used in experiments.

Stimulation, cell lysis and flow cytometry analysis of active GTPases by effector beads

HeLa cells were plated in 48-well plates and incubated overnight at 37°C with 5% CO_2 and 90% humidity. Cells were starved for overnight in serum-free medium followed by stimulation with EGF at 100 ng/ml and inhibitor concentration at 10µM. After incubating cells for desired time points, cells were lysed with 100µL ice-cold RIPA buffer. The plates are scraped, and the lysate collected. For the purposes of standardization, a fraction of the supernatant was collected, quantified using BCA protein estimation kit (Pierce). Lysates were kept ice cold at all times to limit hydrolysis of active GTPases. Lysates were sonicated briefly, and then centrifuged at 14,000rpm in Eppendorf mirocentrifuge for 10min to clear the lysate of debris and DNA. 10,000 beads for each effector assay

were used and added to a lysate. The beads were synthesized as described earlier (87). If probing for more than one protein, the lysate was divided into desired tubes and probed individually. The beads and lysate were allowed to incubate for 1h at 4°C. After incubation, the beads were pelleted in a cold centrifuge. The bead pellets were resuspended in RIPA buffer and incubated with a primary monoclonal antibody for the target GTPase, with gentle shaking for 1h. The beads were than centrifuged and resuspended in RIPA buffer with an Alexa 488 secondary antibody at a 1:200 dilution for 1h with shaking at 4°C. Finally the beads were centrifuged once and resuspended in 100µL RIPA buffer for quantification in the flow cytometer. The assay concept is illustrated below **(Figure 11)**.

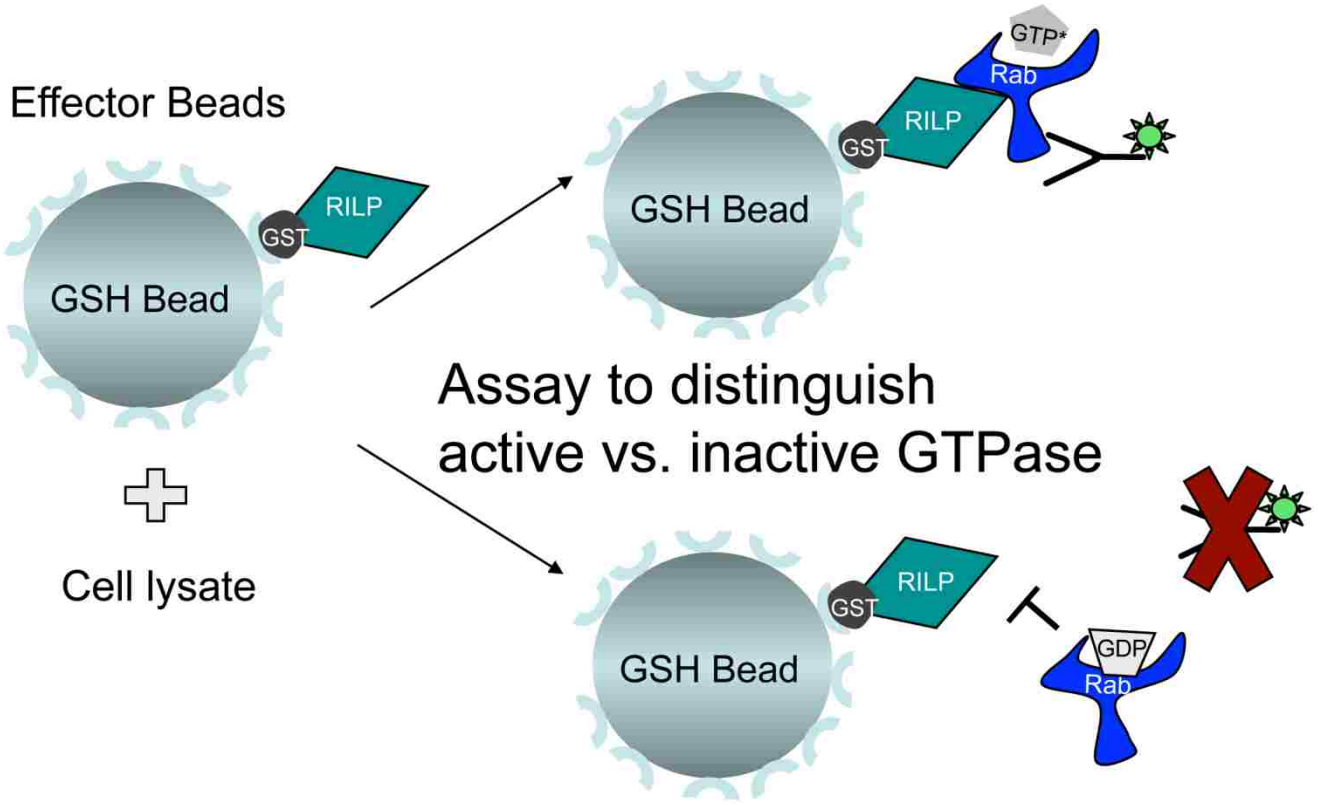

Figure 11: Flow cytometry based assay to determine Rab7-RILP interaction.

Chapter 3: Results- Rab7CMT2B mutants alter endocytic trafficking

It may be postulated that the process of maturation of the internalized cargo from early endosome to late endosome or from late endosome to lysosome is delayed under diseased conditions. Previous studies have indicated misregulation of intracellular trafficking cause defects in axonal transport and hence impair supply and clearance. This slowed axonal transport gradually leads to progressive neuronal cell death (93). Neurons expressing mutant form of mitofusin found in Charcot-Marie-Tooth Type 2A (CMT2A) dramatically hampers the mitochondrial mobility resulting in their redistribution in the soma and proximal axon (94). This leads to redistributed mitochondria that directly impact the aerobic respiration (i.e. generation of ATP) and calcium buffering. Hence a neuron might eventually die due to starvation. Studying the intracellular trafficking and hence its impact on endosomal signaling is key in determining the pathogenesis of CMT2B disease.

Rab7CMT2B mutants show perinuclear distribution

As shown in **Figure 12,** all of the CMT2B associated Rab7 mutants were observed to accumulate with a perinuclear distribution consistent with localization to endosomes. HeLa cells were transiently transfected with GFP-tagged Rab7 wild-type and CMT2B mutants and analyzed for their subcellular distribution by confocal microscopy.

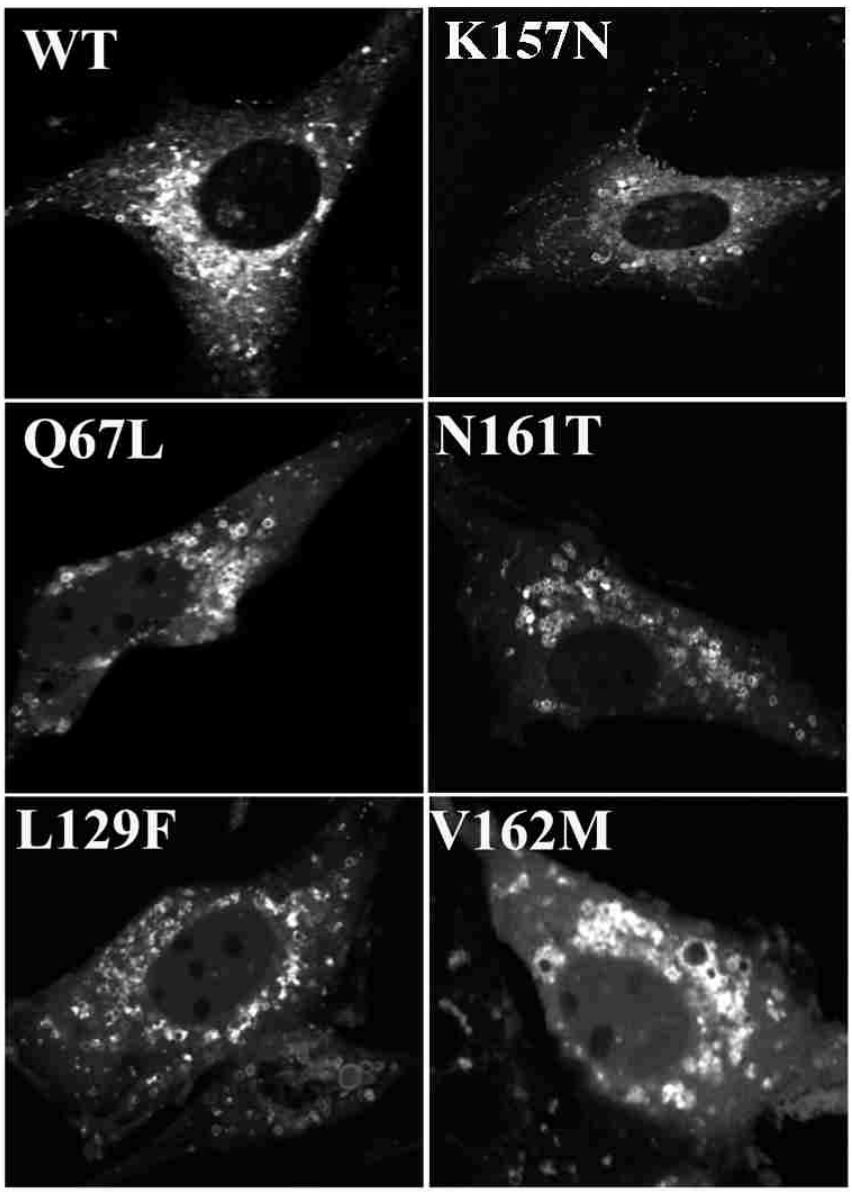

Figure 12: Rab7CMT2B mutants show a perinuclear distribution consistent with localization to endosomal membranes.

Rab7 Mutants Display Altered Membrane Association Kinetics

Rab7, like other Rab GTPases, exists in an active, GTP-bound state that is membrane-bound and an inactive, GDP-bound state that is cytosolic. To investigate the membrane association and cytosolic cycling of the Rab7CMT2B mutants, BHK-21 cells were transiently transfected with

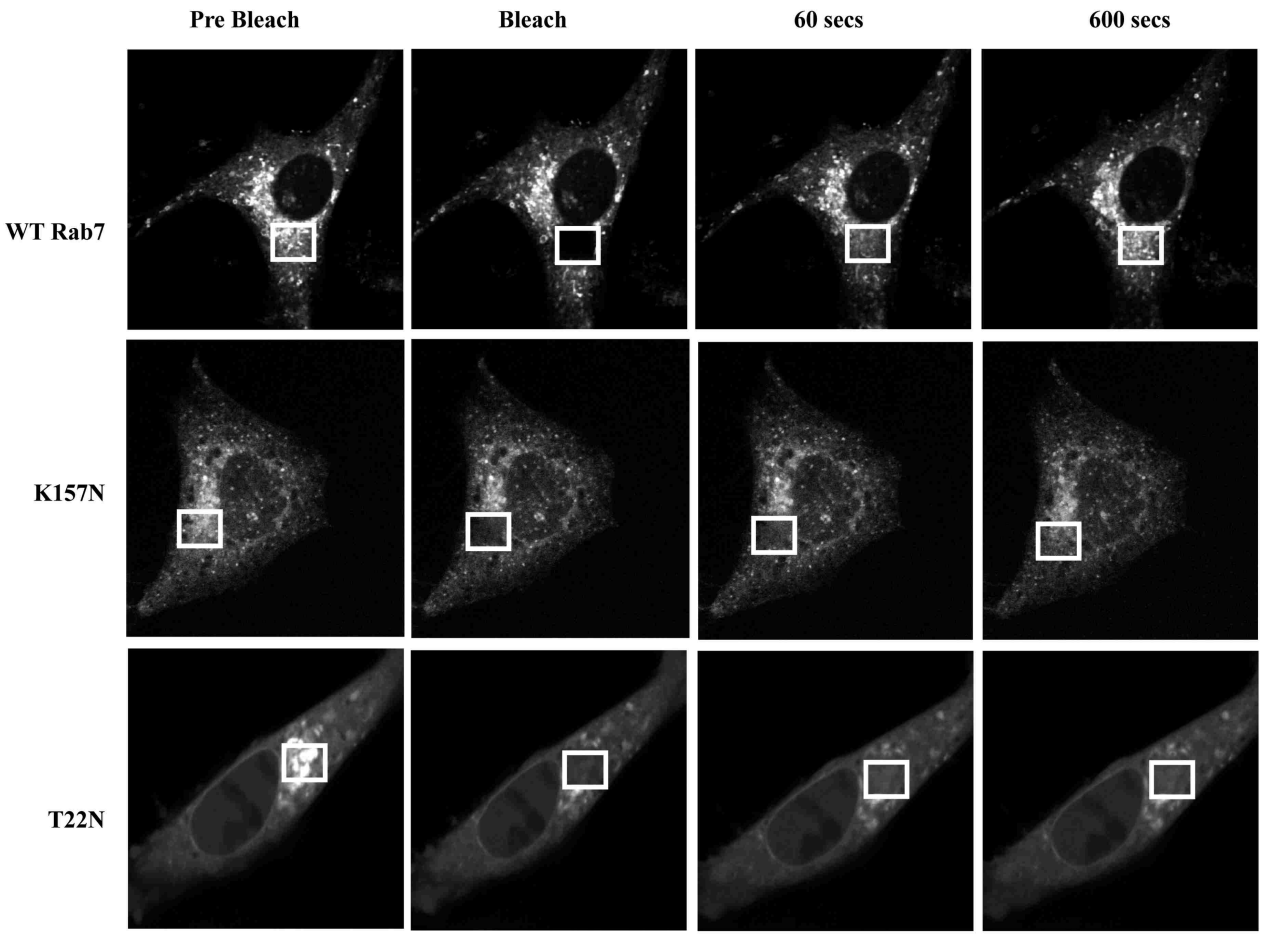

Figure 13: Rab7CMT2B mutants show differential membrane cycling. BHK-21 cells transfected with GFP-Rab7 wild-type (WT) and CMT2B mutants were used for Fluorescence Recovery After Photo bleaching (FRAP) studies. Regions of transfected cells were photobleached with a high intensity laser and recovery of fluorescence tracked over time. Representative time lapse images of GFP-Rab7 vesicles before and after photobleaching are shown. At least 30 cells were analyzed for each cell condition in each trial and results are representative of three independent experiments.

GFP-tagged wild-type Rab7 and CMT2B mutants, and FRAP analyses were conducted as described previously (83). Regions of the transfected cell were photobleached by high intensity laser, and the recovery of fluorescence was tracked over time **(Figure 13)**. The time of recovery of 50% of the fluorescence measured for Rab7 wild-type ($t_{1/2}$=40.6 s) was comparable with published literature ($t_{1/2}$= 52 s)**.** Three of the Rab7CMT2B mutants showed a slower rate of fluorescence recovery compared with wild-type Rab7 **(Figure 14 and Table 2)**.

The L129F and V162M showed similarly slow recoveries compared with the wild-type ($t_{1/2}$=134.3 s and $t_{1/2}$=127.6 s). Our finding is consistent with a previous report (83), although recovery rates for the two mutants were not explicitly stated. Among the previously untested mutants, K157N also showed a dramatically decreased fluorescence recovery ($t_{1/2}$ =130.7 s), whereas the half-time of fluorescence recovery of N161T (57.7 s) was similar to that of the wild type (40.6 s). As expected, the predominantly GDP-bound, cytosolic dominant negative Rab7T22N mutant showed little or no fluorescence recovery.

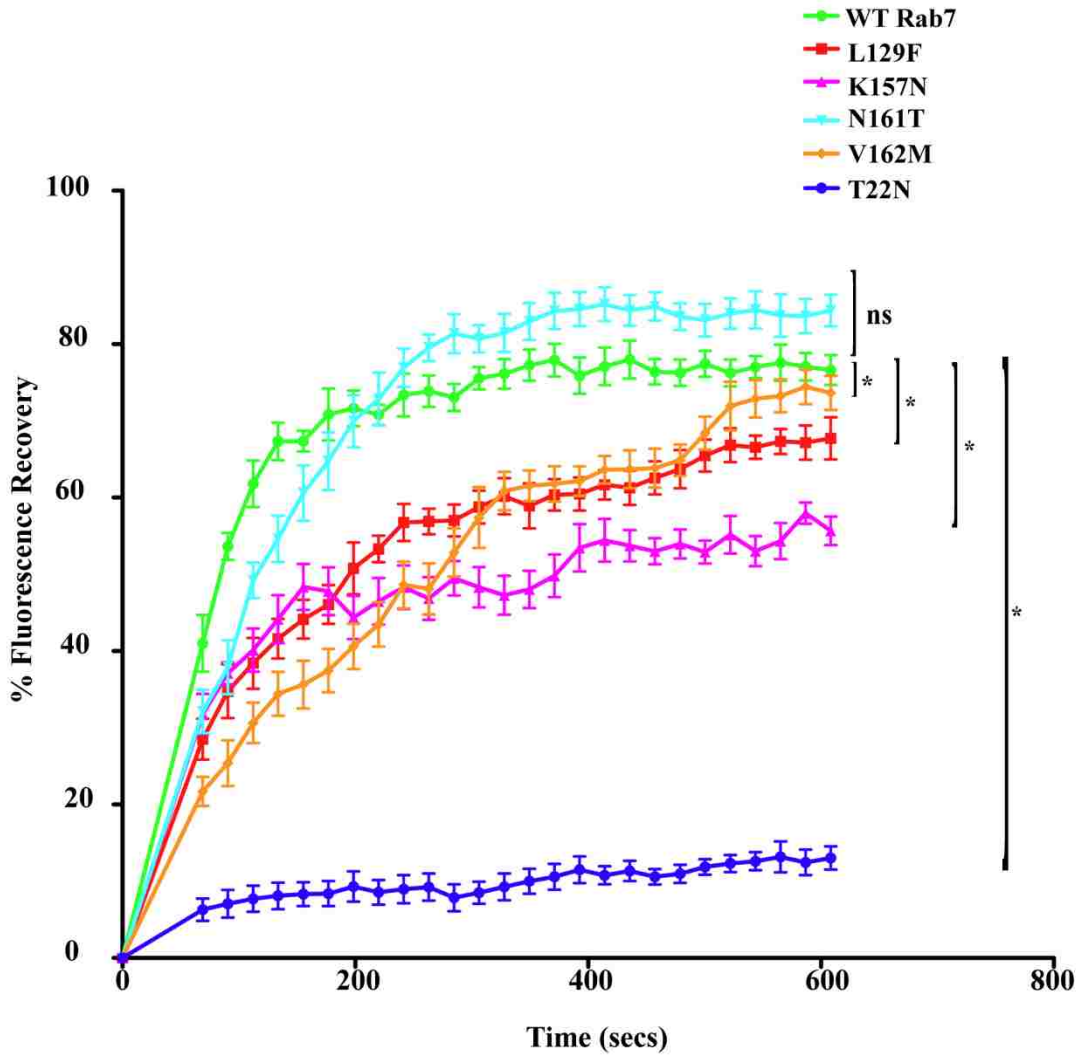

Figure 14: Quantitative analysis of differential membrane cycling of Rab7CMT2B mutants. FRAP analyses show a decreased rate of fluorescence recovery of all the Rab7CMT2B mutants compared to the wild-type. Rab7T22N mutant showed little or no fluorescence recovery. The differences in fluorescence recovery from three independent

trials and 30 cells per trial are plotted ± S.E.M. Asterisks denote $p<0.05$ based on one-way ANOVA with Dunnett's post-test and relative to Rab7 wild-type control.

The differences were statistically significant for Rab7V162M and Rab7L129F, in agreement with previous studies (47), and also for the previously untested Rab7K157N and dominant negative Rab7T22N mutants. The slower recovery rates are indicative of increased membrane residence times for three of the four Rab7CMT2B mutants, which would be expected to impact endocytic trafficking.

Table 2: FRAP measurements of Rab7 wild-type and other mutants

Rab7	$T_{1/2}$ (sec)	Mobile Fraction (%)
WT	40.62±19.4	73.46±10.45
L129F	134.3±9.7	56.59±9.79
K157N	130.7±6.1	53.27±5.75
N161T	57.7±20.5	81.71±4.52
V162M	127.6±13.6	48.8±8.34
T22N	59.5±9.6	11.18±2.32

The Rab7CMT2B mutants interact with TrkA

The interaction of Rab7 with the receptor tyrosine kinase, TrkA is NGF dependent and furthermore the association is time dependent following nerve growth factor (NGF) stimulation (67). To study the impact of the CMT2B associated Rab7 mutants on TrkA interaction, the GFP-tagged versions of Rab7 bearing L129F, K157N, N161T and V162M substitutions were generated.

Based on previous studies, GFP-Rab7 fusion proteins preserve the functional properties of the untagged proteins (89). To see if the disease Rab7CMT2B mutants impair interaction with TrkA on NGF stimulation a set of co-immunoprecipitation assays were done.

In agreement with the published literature (67), endogenous Rab7 was found to coimmunoprecipitate with TrkA following NGF stimulation and the maximum interaction occurred 1h after stimulation **(Figure 15)**.

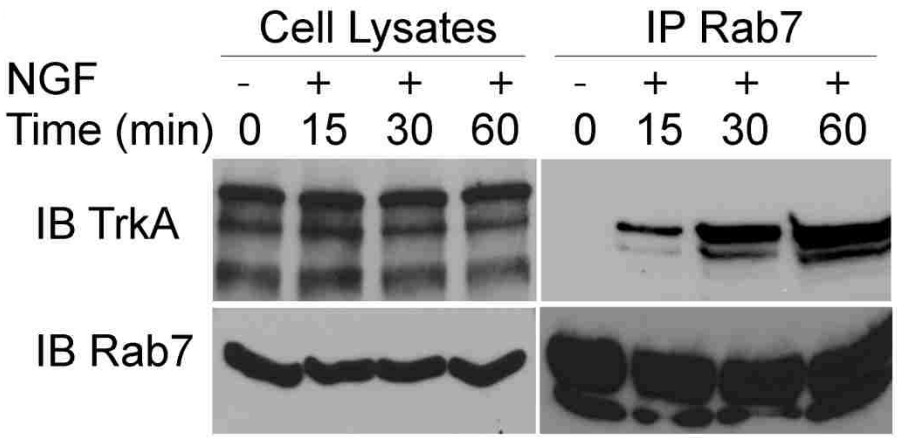

Figure 15: Rab7 interacts with TrkA in a time dependent manner. PC12 cells were stimulated with NGF (200ng/ml) for 15-60min as indicated. Cells were lysed and samples of cell lysates were immunoblotted for TrkA and Rab7 as a measure of degree of protein-protein interaction. Lysate samples containing equal amounts of protein were immunoprecipitated (IP) with a pAb directed against Rab7 and immunoblotted for TrkA. Subsequently, the membrane was stripped and re-blotted for Rab7.

Therefore, 1h NGF stimulation was used to test for an interaction between TrkA and GFP-tagged wild-type Rab7 as well as the CMT2B GFP-Rab7 mutants. GFP-tagged wild-type Rab7 and the Rab7CMT2B mutants were all seen to co-immunoprecipitate with TrkA at similar levels **(Figure 16)**, indicating that the mutant proteins were not impaired in their ability to bind to TrkA receptor.

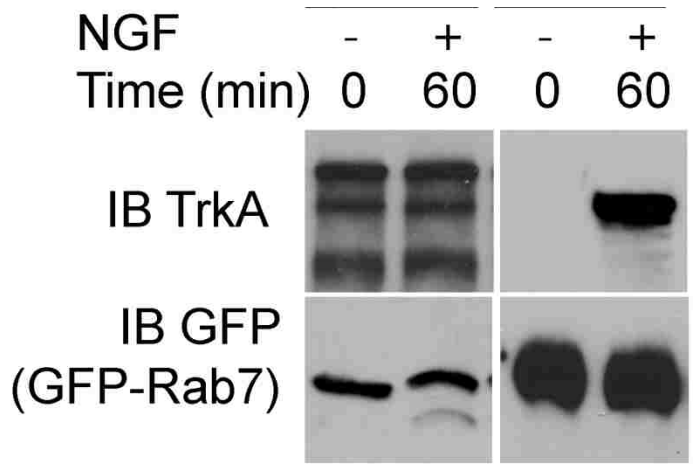

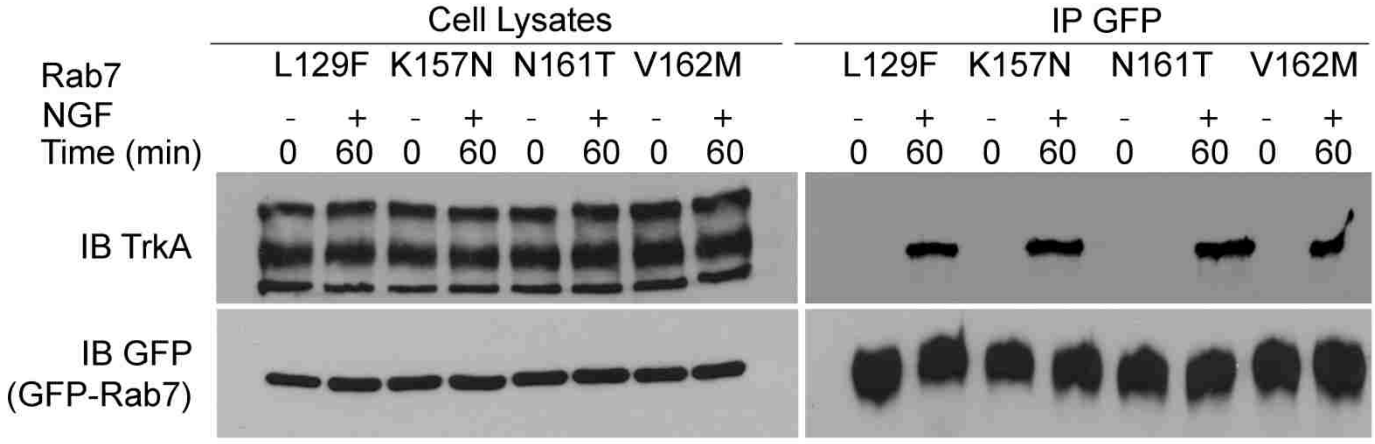

Figure 16: Rab7CMT2B mutants interact with TrkA on NGF stimulation. PC12 cells were transfected with GFP-tagged Rab7CMT2B disease mutants and stimulated with NGF for 60min. Equal amounts of lysate samples were immunoprecipitated with antibodies against GFP to precipitate the GFP-tagged Rab7

and subsequently immunoblotted for TrkA. The membrane stripped and reprobed with antibodies against GFP.

Rab7CMT2B Mutants Delay TrkA Degradation

The effect of the Rab7CMT2B mutants on endocytosis and transport of EGFR was monitored in PC12 cells stably expressing GFP tagged wild-type Rab7 and CMT2B mutants. Cells were serum-starved and NGF-stimulated, and TrkA degradation was traced over time as a measure of transport to lysosomes **(Figure 17).** The inclusion of cycloheximide precluded further synthesis of EGFR upon stimulation.

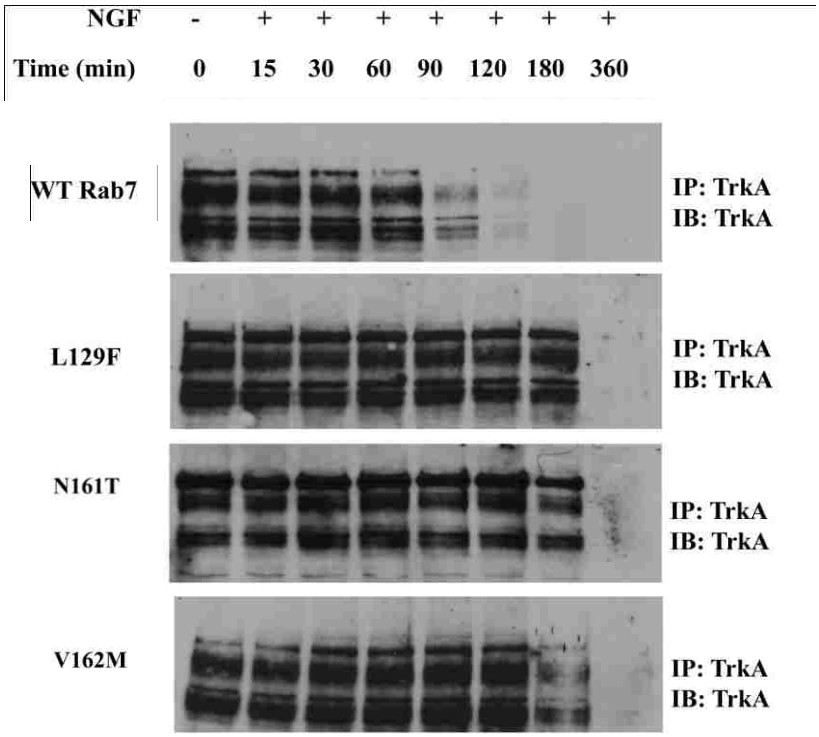

Figure 17: Rab7CMT2B mutants delay TrkA degradation. PC12 cells stably expressing GFP-tagged Rab7 wild-type and CMT2B mutants were serum starved, treated with cycloheximide for 30min and stimulated with 100ng/ml NGF for the indicated time points. Cells were lysed and probed with anti TrkA antibody.

The cells expressing GFP-Rab7 wild-type showed complete degradation of TrkA around 90min post NGF stimulation whereas the cells expressing the disease mutants showed a delay in degradation. The amount of undegraded TrkA present at 120min was in the order N161T>L129F>K157N>V162M>WT.

Rab7CMT2B Mutants Delay EGFR Degradation

The effects of the Rab7CMT2B mutants on endocytosis and transport of EGFR were monitored in HeLa cells and PC12 cells stably expressing GFP-tagged wild-type Rab7 and CMT2B mutants. Cells were serum-starved and EGF-stimulated, and EGFR degradation was traced over time as a measure of transport to lysosomes. The inclusion of cycloheximide precluded further synthesis of EGFR upon stimulation. The levels of EGFR at 15min post-stimulation were considered to be 100%, and subsequent levels at each time point were calculated accordingly. Expression of all Rab7CMT2B mutants kinetically delayed EGFR degradation in HeLa cells compared with the wild-type control (Figure 18 A-D).

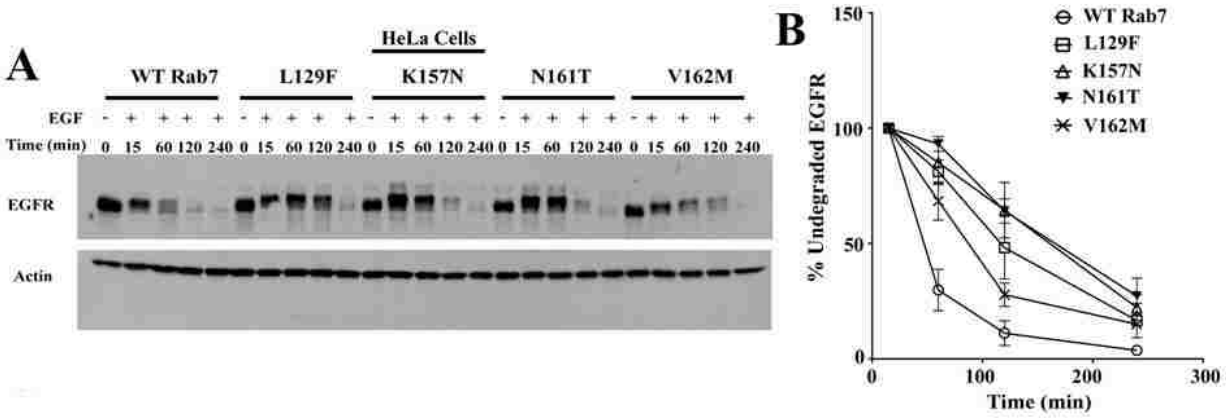

Figure 18: Rab7CMT2B mutants delay EGFR degradation. (A) HeLa cells stably transfected with GFP-tagged wild-type (WT) Rab7 and CMT2B disease mutants were starved in DMEM for 5h and pretreated with cycloheximide for 1h followed by EGF stimulation (100ng/ml) in a time dependent manner as indicated. Representative blots from one of three independent experiments are shown. Subsequently, cells were lysed and equal amounts of protein were immunoblotted and probed for EGFR with actin as the loading control. (**B)** Films from three independent experiments were quantified by Image J analysis. Line graphs show levels of undegraded EGFR in GFP-WT Rab7 and CMT2B mutant expressing cells. In each case the amount of EGFR was normalized to the amount of actin. (**C)** Neuronal PC12 cells stably transfected with GFP-tagged wild-type (WT) Rab7 and CMT2B disease mutants were starved in DMEM for 5h and pretreated with cycloheximide for 1h followed by EGF stimulation (100ng/ml) in a time dependent manner as indicated. Representative blots from one of three independent experiments are shown. Subsequently, cells were lysed and equal amounts of protein were immunoblotted and probed for EGFR with actin as the loading control. (**D)** Films from at least three independent experiments were quantified by Image J analysis. Line graphs show levels of undegraded EGFR in GFP-WT Rab7 and CMT2B mutant expressing cells. In each case the amount of EGFR was normalized to the amount of actin.

Rab7N161T mutant-expressing cells showed the slowest EGFR degradation kinetics, whereas the Rab7V162M mutant exhibited the fastest degradation kinetics among the mutants.

The levels of overexpressed GFP-Rab7 were similar in all of the cell lines under the given experimental conditions **(Figure 10).** To confirm the results in additional cell lines, we tested the effects of Rab7CMT2B mutants on EGFR degradation in stable PC12 cells **(Figure 18 C and D)** and transiently transfected A431 keratinocytes **(Figure 19 A and B).** A delay in EGFR degradation was found in both cell types overexpressing the Rab7CMT2B mutants. The K157N, N161T, and L129F mutants showed significantly delayed EGFR degradation rates compared to wild-type, with the V162M mutant exhibiting degradation rates most similar to wild-type **(Figure 18D).** The cumulative data strongly suggest that the disease mutants impair endosomal trafficking and degradation of EGFR and that the effect is not a cell type specific while also observed in a cell model commonly used for studying neuronal differentiation.

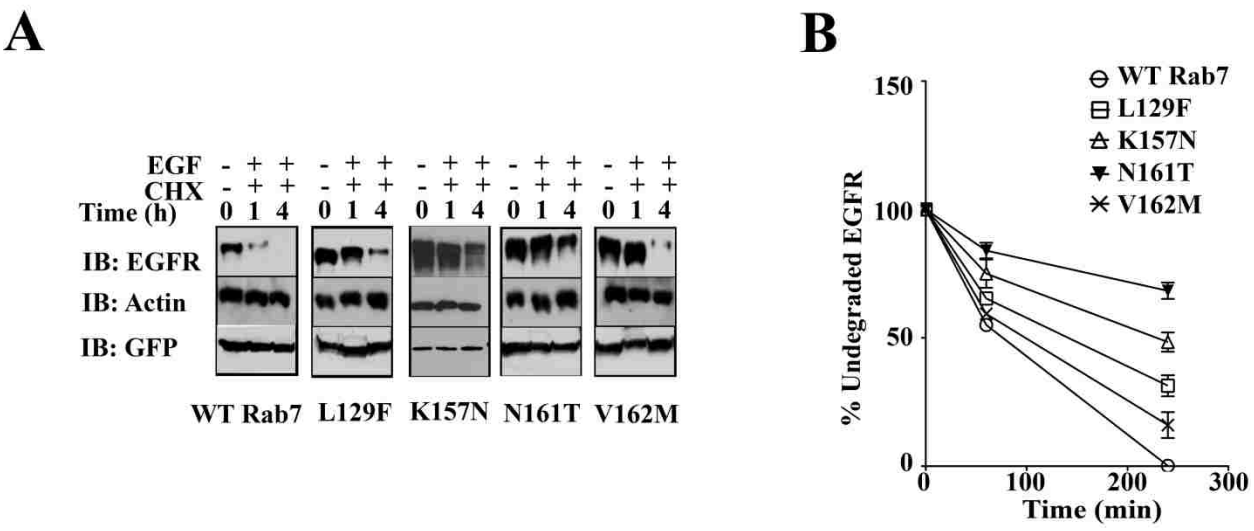

Figure 19: Rab7CMT2B mutants delay EGFR degradation in A431 cells. (A) A431 cells transfected with GFP-tagged Rab7 wild-type and CMT2B mutants were starved for 5h and pretreated with cycloheximide and stimulated with EGF for 1h and 4h. A431 cell lysates were collected at the indicated time points as described in experimental procedures. Samples were resolved by SDS-PAGE and then subjected to immunoblotting to detect EGFR and actin. Same samples were resolved by 12% SDS-gel to detect GFP Rab7 expression using rabbit polyclonal GFP antibody as shown at the bottom of the each box. **(B)** EGFR levels were quantified densitometrically and normalized to actin.

The milder impairment in EGFR trafficking caused by the disease mutants in the HeLa cells relative to PC12 cells or A431 keratinocytes might be attributed to differences in EGFR levels or the presence of endogenous wild-type Rab7 that can still serve to facilitate normal endocytic trafficking in the cells stably overexpressing the Rab7CMT2B mutants.

Coexpression of mutant allele and wild-type alleles is the expected genotype in autosomal dominant CMT2B. Nevertheless, to further confirm that the slowed EGFR transport and degradation were directly attributable to the Rab7CMT2B mutants. Therefore, HeLa cells overexpressing mutant GFP-tagged Rab7N161T protein of murine origin were treated with siRNA to specifically deplete the endogenous human wild-type Rab7 or with a scrambled.

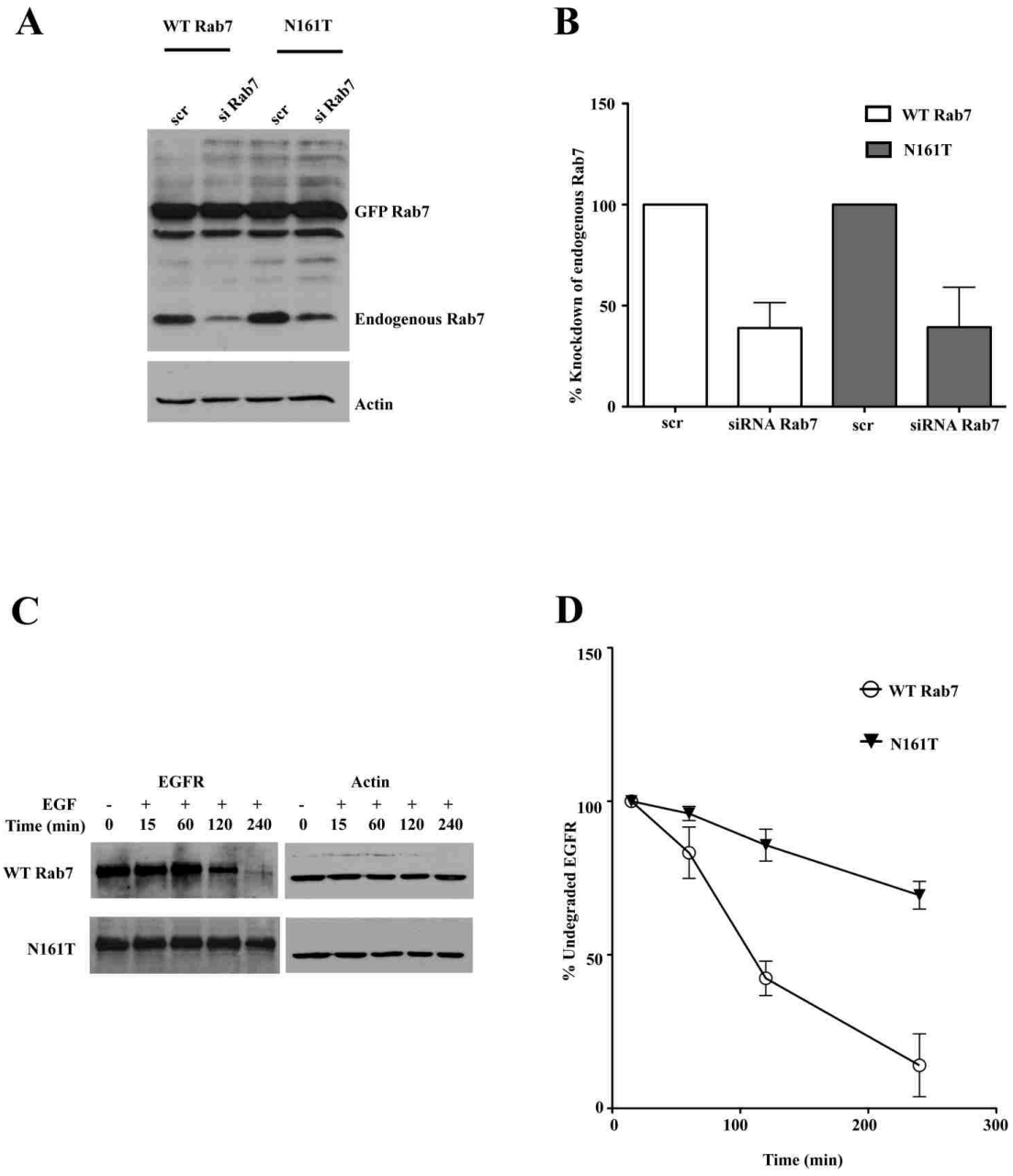

Figure 20: Knockdown of endogenous wild-type Rab7 showed a pronounced delay in EGFR degradation of Rab7N161T mutant compared to Rab7 wild-type. (A) HeLa cells stably expressing murine GFP-Rab7 wild-type (WT) and CMT2B mutants were transfected with scrambled siRNA (scr) and siRNA targeted against human Rab7a (siRab7) to knockdown the endogenous Rab7. Cells were kept for 48h to bring about effective knockdown. Representative western blot is shown showing the unaltered expression of murine GFP-Rab7 (~50kDa) and knockdown of endogenous Rab7

(~25kDa). **(B)** Densitometric quantification of the western blots showed ~50% knockdown of endogenous Rab7 in both GFP-Rab7 wild-type and N161T expressing cells. **(C)** HeLa cells stably expressing murine GFP-Rab7 wild-type and CMT2B mutants were transfected with siRNA targeted against endogenous Rab7. The cells were incubated for 48h following transfection to bring about effective knockdown of endogenous Rab7 following which cells were starved for 5h and pretreated with cycloheximide for 1h and stimulated with EGF for the indicated time points. Rab7 N161T showed a pronounced delay in EGFR degradation compared to the wild-type. **(D)** Densitometric quantitation of films from at least three independent experiments showed a faster kinetics of EGFR degradation in cells expressing wild–type Rab7 compared to those expressing Rab7N161T.

Knockdown of endogenous human Rab7 in cells overexpressing Rab7N161T showed a more pronounced delay in EGFR degradation than was seen in the presence of endogenous wild-type Rab7 protein **(Figure 20 C and D).** It was somewhat surprising that there was also a mild slowdown of EGFR degradation in the cells where endogenous Rab7 was depleted but GFP-tagged Rab7 wild-type protein was overexpressed, suggesting that the GFP tag may have a mild effect on protein function, as has been noted for Arf GTPases (90)**.**

Overall, the siRNA data support the conclusion that the Rab7CMT2B mutants directly impair the trafficking and degradation of EGFR.

Rab7CMT2B Mutants Slow Endocytic Transport of EGF

To assess the stage where growth factor transport was being delayed by the Rab7CMT2B mutants, we tracked the time-dependent transit of internalized EGF from the early endosome to late endosomes/lysosomes. HeLa cells were transiently transfected with GFP-tagged Rab7 wild- type or CMT2B mutants.

Post-transfection, cells were serum-starved and stimulated with Alexa555-labeled EGF for 10min, followed by washing and reincubation in serum-free medium for 20 or 60min, respectively. At the 20min time point, internalized EGF was significantly associated with EEA1-positive early endosomes in the Rab7CMT2B mutant cells seen as purple punctate structures in the merged images **(Figure 21A).**

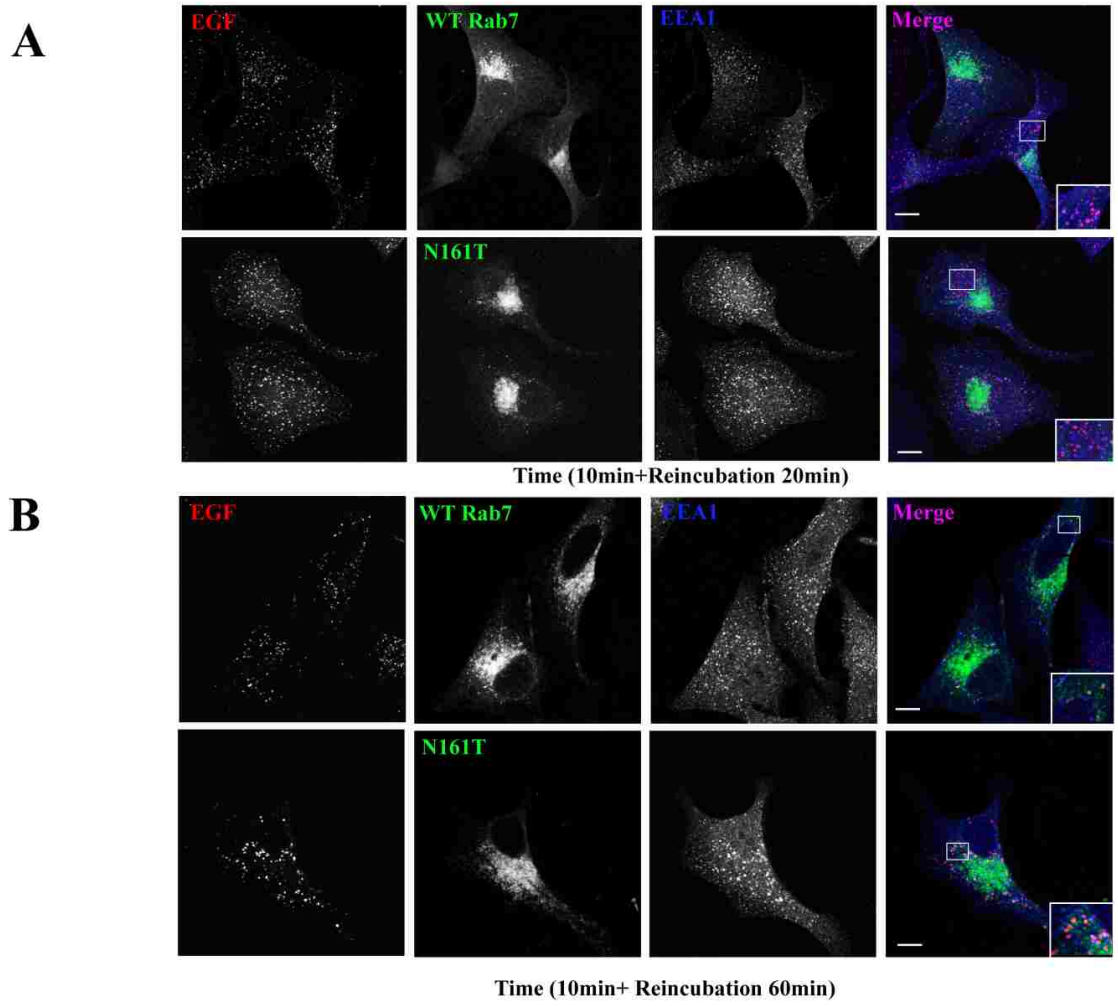

Figure 21: Rab7CMT2B mutants show a delay in EGF transport from early to late endosomes. HeLa cells transfected with GFP-tagged wild-type (WT) Rab7 and Rab7CMT2B mutants were starved for 14h and stimulated with Alexa555-tagged EGF for 10min followed by reincubation in DMEM for 20min and 60min **(A, B)** at 37ºC, permeabilized with Triton X-100 and stained with anti-EEA-1 antibody. **(C)** Bar graphs showing the degree of colocalization of EGF and EEA-1 at 20min and 60min. At least 30 cells were scored for each construct of one experiment for a total of three independent experiments. The degree of colocalization of EGF with EEA-1 was analyzed by Slidebook 4.1 software and the differences are represented as ± S.E.M. Scale Bar =10µm. **(D)** Bar graphs showing the degree of colocalization of EGF and Lamp1 at 60min and 120min. At least 30 cells were scored for each construct of one experiment for a total of three independent experiments. The degree of colocalization of EGF with Lamp1 was analyzed by Slidebook 4.1 software and the differences are represented as ± S.E.M. Values in all cases are from three independent experiments plotted ± S.E.M. Asterisks denote $p<0.05$ based on one-way ANOVA with Dunnett's post-test and relative to Rab7 wild-type control.

Quantitative analyses of the degree of colocalization of EGF with EEA1 at 20min post stimulation were essentially identical in cells expressing wildtype and mutant proteins, suggesting no impairment in internalization or delivery to early endosomes. However, the degree of colocalization of EEA1 and EGF was significantly higher in the Rab7CMT2B mutants at the longer time point (60min) compared with the wild-type Rab7 cells, as can be seen from more purple punctuate structures in the Rab7N161T mutant compared with the wild-type **(Figure 21B and C).** The Rab7K157N mutant exhibited the greatest retention and accumulation of EGF in the EEA1-positive early endosomes, followed by V162M, N161T, and L129F. The data indicate a delay in the transit of the internalized EGF from early to late endosomes when the Rab7CMT2B mutant proteins are expressed. The transport of internalized EGF to late endosomes/lysosomes was measured by stimulating with Alexa555-labeled EGF for 10min, followed by washing and reincubation in serum-free medium for 1–3h and staining for Lamp1-positive structures. Quantitative analyses at two time points showed a marginally higher degree of colocalization of EGF and Lamp1 in cells expressing wild-type Rab7 compared with the disease mutants **(Figure 21D).** This is consistent with the protracted localization of EGF in EEA1-positive early endosomes. At a longer time point (3h), the Rab7CMT2B mutants showed a higher degree of colocalization of EGF and Lamp1, consistent with a kinetic delay in progressing to lysosomal degradation. It is worth noting that the difference in the degree of colocalization between the wild-type and Rab7CMT2B mutants is about 10–15% and is statistically significant.

These data further support a delayed trafficking of EGF and its associated receptor to late endocytic compartments in the Rab7CMT2B mutant-expressing cells compared to the wild type.

Chapter 4: Results-Rab7CMT2B mutants alter endosomal signaling

Endocytosis and cell signaling are interdependent and bidirectionally linked cellular processes. These intertwined processes influence cell motility and cell fate determination (91, 92). Cells respond to external stimuli by activation of signaling receptors which get endocytosed and sorted into distinct endosomal compartments. Endocytosis regulates the availability of a number of receptors available for stimulation at the plasma membrane and the endocytosed ligand stimulated receptors activates downstream mediators that in turn regulate the process of endocytocis. Endosomes serve as decision forks involved in recycling, secretion and degradation that determines the receptor level and activity. Endosomes have the unique feature to serve as signaling scaffolds during signal transduction. The small volume of endosomes allows for optimum interaction of ligand with receptor and the slow process of sorting facilitates longer duration of signaling. Impaired trafficking of activated growth factor receptors would be expected to alter endosomal signaling through differential interaction with effectors.

Rab7CMT2B mutants are gain of function mutations (88) hence would be expected to interact with TrkA on NGF stimulation. On activation with NGF, TrkA would be expected to undergo phosphorylation and activate the downstream signaling pathways to upregulate the differentiation genes. It may be postulated that the disease mutants would differentially activate the downstream mediators of activated TrkA receptors.

Previous studies have shown that Rab7 interacts with TrkA in a nerve growth factor (NGF) and time dependent manner. Overexpressing the Rab7T22N dominant negative mutant that is predominantly GDP-bound was shown to prolong ERK1/2 signaling and stimulate neurite outgrowth. Under diseased conditions, Rab7 would be expected to

impair trafficking of activated growth factor cargos. As such disease mutants would expect to alter the endosomal signaling of activated TrkA receptors. Hence it is postulated that Rab7CMT2B mutants alter the subcellular partitioning of activated mediators of Trk signaling.

It was observed that Rab7CMT2B mutants delay the trafficking of activated, internalized EGFR. This would increase the membrane residence time of the signaling endosomes. As such activation of EGFR and its downstream signaling mediators like ERK1/2 would be expected to be enhanced and account for differential activation of endosomal signaling. The ligand induced stimulation of EGFR leads to activation of MAPK signaling scaffold that gets recruited on the activated, internalized cargo. Thus the appropriate trafficking of activated EGFR to endosomes controls the spatio-temporal regulation of MAPK signaling. Typically the activated ERK1/2 gets translocated to the nucleus and activate Elk-1 transcription factor. However the activation of Elk-1 in the CMT2B mutants may be impaired and the positioning of the signaling endosomes might be critical in determining the outcome of nuclear signaling i.e. enhanced Elk-1 or reduced Elk-1 activation **(Figure 22)**.

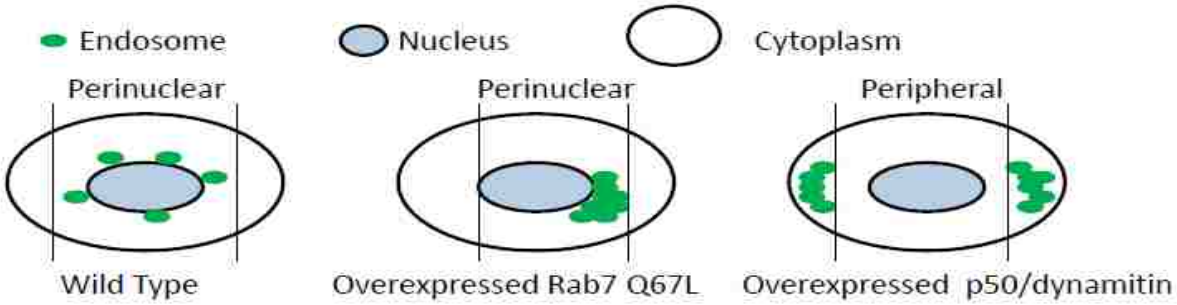

Figure 22: Intracellular positioning of signaling endosomes determine the signal output. Distribution of endosomal system in wild type (perinuclear), Rab7Q67L overexpressed (perinuclear and clustered) and p50 overexpressed cells (peripheral) and altered ERK and nuclear signaling in the different systems.

Rab7CMT2B mutants show differential TrkA and EGFR phosphorylation following growth factor stimulation

Rab7 is known to control endosomal trafficking of TrkA as well as receptor signaling. To assess the effect of the Rab7CMT2B mutants on NGF signaling, PC12 cells expressing the mutant proteins were briefly stimulated with NGF followed by removal of residual surface bound NGF ('surface stripping of ligand' as described in Materials and Methods) to maximize detection of signaling from activated, internalized TrkA receptors over the course of 2–24h.higher phospho-TrkA levels were consistently observed across multiple time points in cells expressing the GFP-tagged Rab7CMT2B mutants as compared to GFP-Rab7 wild-type or GFP only expressing control cells **(Figure 23)**. Expression levels of all GFP proteins were constant at all time points. Quantification of replicate experiments showed that Rab7L129F, Rab7K157N, Rab7N161T and Rab7V162M expressing cells had 2.1–3.9 fold higher levels of phospho-TrkA than the GFP only expressing control cells and 1.3–1.8 fold higher levels than the GFP-Rab7 wild-type expressing cells at the 2h and 6h time points **(Figure 23B, numerical values are provided in Table 3).** At the 24h time points, the pTrkA signal was greatly diminished and the differences between the mutants and the controls were no longer statistically significant. There was no down regulation of total TrkA levels in the lysates, similar to previous reports where Rab7 dominant negative mutant was expressed (67). Nevertheless, the higher TrkA phosphorylation is suggestive of differential interaction of

the Rab7 mutants with signaling complexes that leads to an increase in activated TrkA receptors in endosomes.

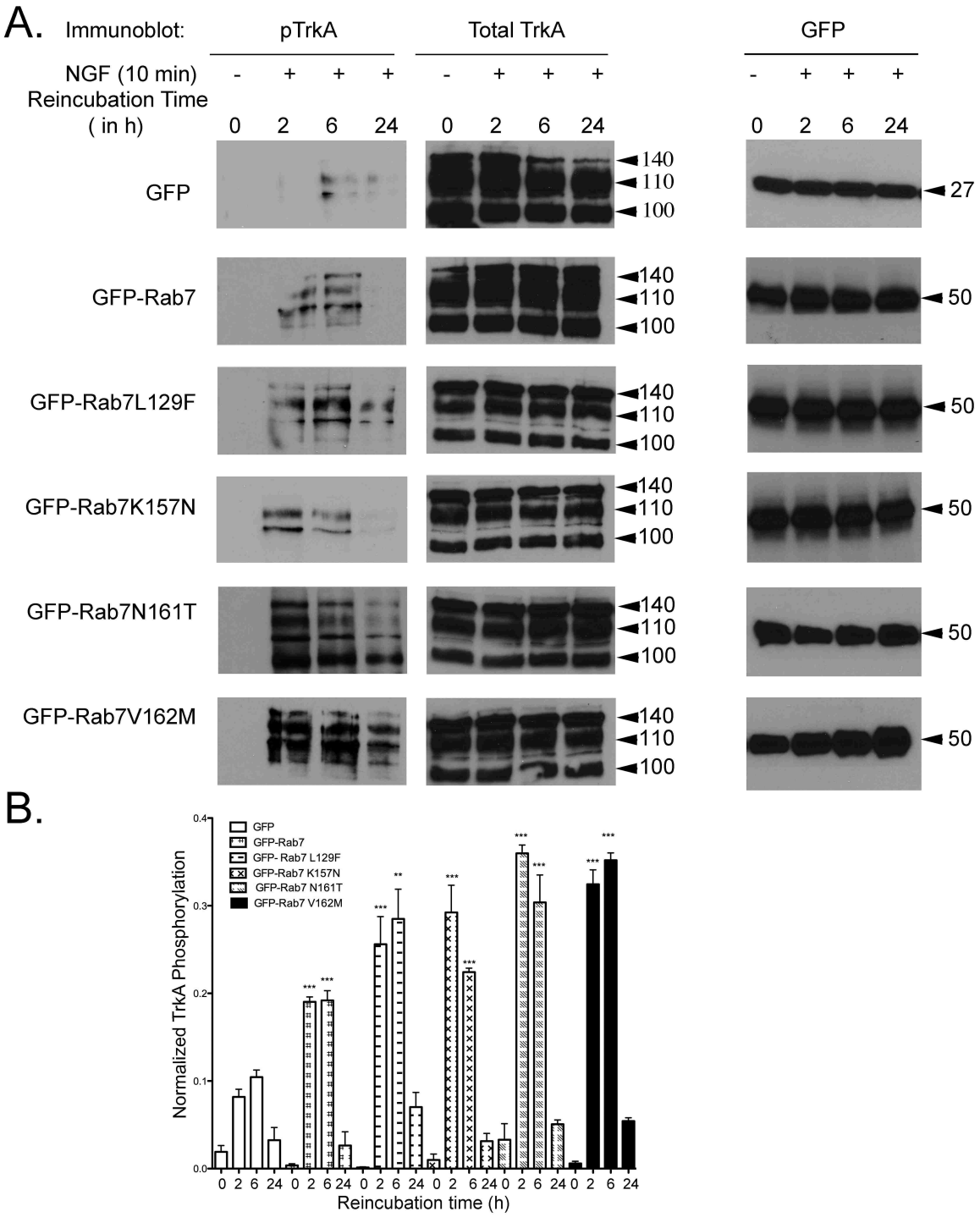

Figure 23: Cells expressing Rab7CMT2B mutants exhibit higher levels of phospho-TrkA following NGF stimulation. (A) Transiently transfected PC12 cells expressing GFP, GFP-Rab7 wild-type, GFP-Rab7L129F, GFP-Rab7K157N, GFP-Rab7N161T, GFP-Rab7V162M were briefly stimulated with NGF (200ng/ml) followed by surface stripping of ligand and reincubation in 0.1% BSA-DMEM for 2h,6h and 24h respectively. Subsequently, cells were lysed and equal amounts of protein were immunoblotted and probed for total and phosphorylated TrkA. Significantly, higher levels of phosphorylated TrkA were found at 2h and 6h. Equal amounts of protein from cell lysates were probed with antibodies against GFP. GFP-Rab7 wild-type and GFP-Rab7CMT2B mutant proteins are uniformly expressed in PC12 cells under these conditions as shown in the adjacent representative blot. **(B)** Films from four independent experiments were quantified by Image J analysis. Bar graphs show pTrkA in GFP-Rab7 wild-type and CMT2B mutant expressing cells. In each case the amount of pTrkA was normalized to the amount of GFP protein expressed. The bar graph shows the fold-change in pTrkA as a function of pTrkA in the GFP only control at each respective time point. Error bars indicating mean ± S.E.M., n=4, **p<0.01, ***p<0.001.

Table 3. Fold-changes in phospho-TrkA and phospho-ERK1/2 due to Rab7CMT2B mutants.

Expressed Protein	Phospho-TrkA Fold change relative to GFP			Phospho-TrkA Fold change relative to GFP-Rab7wt			Phospho-ERK1/2 Fold change relative to GFP			Phospho-ERK1/2 Fold change relative to GFP-Rab7wt		
	2h	6h	24h	2h	6h	24h	2h	6h	24h	2h	6h	24h
GFP	1.0	1.0	1.0				1.0	1.0	1.0			
GFP-Rab7 wt				1.0	1.0	1.0				1.0	1.0	1.0
GFP-L129F	3.1 p<0.001	2.72 p<0.01		1.34 p<0.05	1.48 p<0.05		2.58 p<0.001	2.15 p<0.01	2.67 p<0.05	1.62 p<0.01	1.75 p<0.01	2.17 p<0.05
GFP-K157N	3.57 p<0.001	2.14 p<0.001		1.53 p<0.01	1.52 p<0.05		2.49 p<0.001	2.14 p<0.001	2.84 p<0.05	1.57 p<0.001	1.74 p<0.01	2.3 p<0.05
GFP-N161T	4.39 p<0.001	2.9 p<0.001		1.88 p<0.001	1.58 p<0.01		2.98 p<0.001	1.82 p<0.01	2.54 p<0.05	1.87 p<0.01	1.48 p<0.01	2.06 p<0.05
GFP-V162M	3.96 p<0.001	3.37 p<0.001		1.70 p<0.001	1.83 p<0.001		3.14 p<0.001	2.6 p<0.001	2.65 p<0.05	1.97 p<0.001	2.12 p<0.001	2.15 p<0.05

Data from 4 independent experiments measuring TrkA phosphorylation and 3 independent experiments assessing ERK1/2 phosphorylation were evaluated using unpaired, one-tailed Student's t-test.

Changes in the activation status of the EGFR in the context of Rab7CMT2B mutants were assessed by probing the time-dependent phosphorylation. A phospho-EGFR antibody relative to cells expressing wild-type Rab7 directed against the tyrosine 1045 residue that is phosphorylated on EGF stimulation was used to monitor changes in the status of phosphorylation. The levels of phosphorylated EGFR were normalized to the levels of total actin. The Rab7CMT2B mutants showed 2–3-fold higher levels of phosphorylated EGFR within 15min of EGF stimulation compared with the wild-type **(Figure 24 A and B).** The Rab7N161T mutant showed the highest level of EGFR phosphorylation followed by V162M, L129F and K157N. The rate of dephosphorylation of EGFR measured over 240min was found to be up to 3-fold slower in the disease mutants WT > K157N > V162M > L129F > N161T **(Figure 25 and Table 4).**

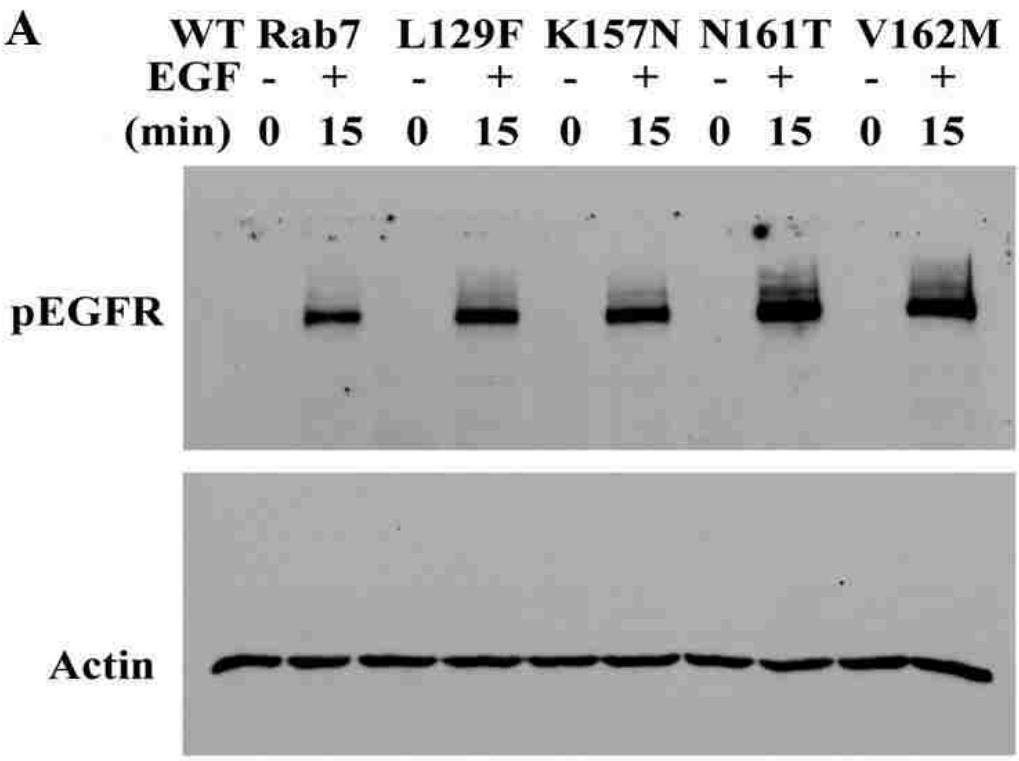

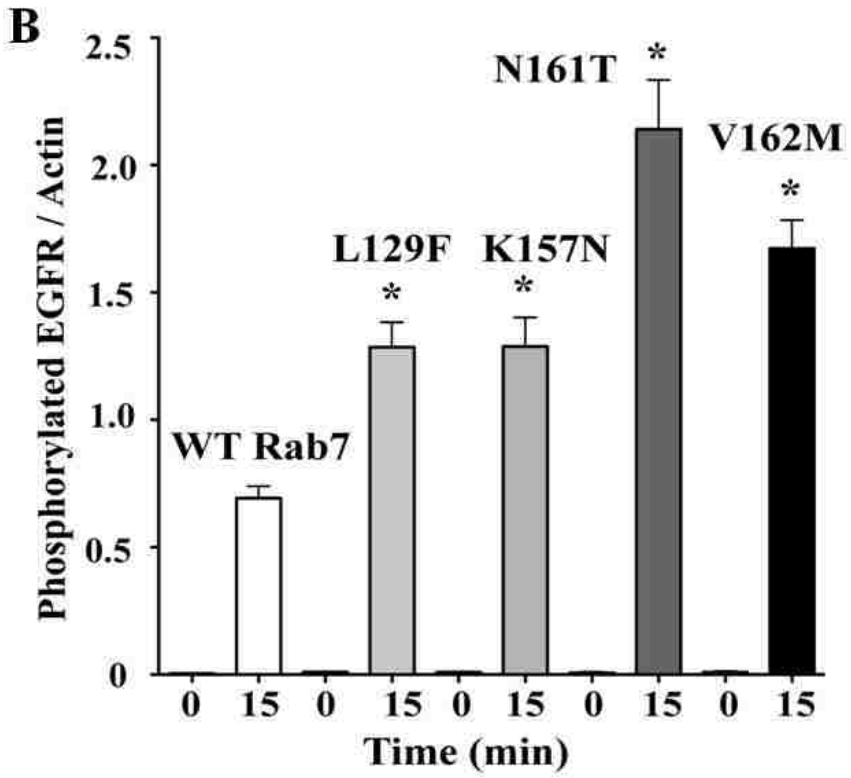

Figure 24: Rab7CMT2B mutants show enhanced EGFR phosphorylation

(A) Samples from EGFR degradation assays were probed for phospho-EGFR with actin as the loading control. **(B)** Films from at least three independent experiments were quantified by Image J analysis. Line graphs show levels of phospho-EGFR in GFP-Rab7 wild-type and CMT2B mutant expressing cells. In each case the amount of phospho-EGFR was normalized to the amount of total actin. Values in all cases are from three independent experiments plotted ± S.E.M. Asterisks denote $p<0.05$ based on one-way ANOVA with Dunnett's post-test and relative to Rab7 wild-type control. Non-linear curve fits were used to analyze degradation rates and obtain half-lives in Graphpad Prism version 5.0.

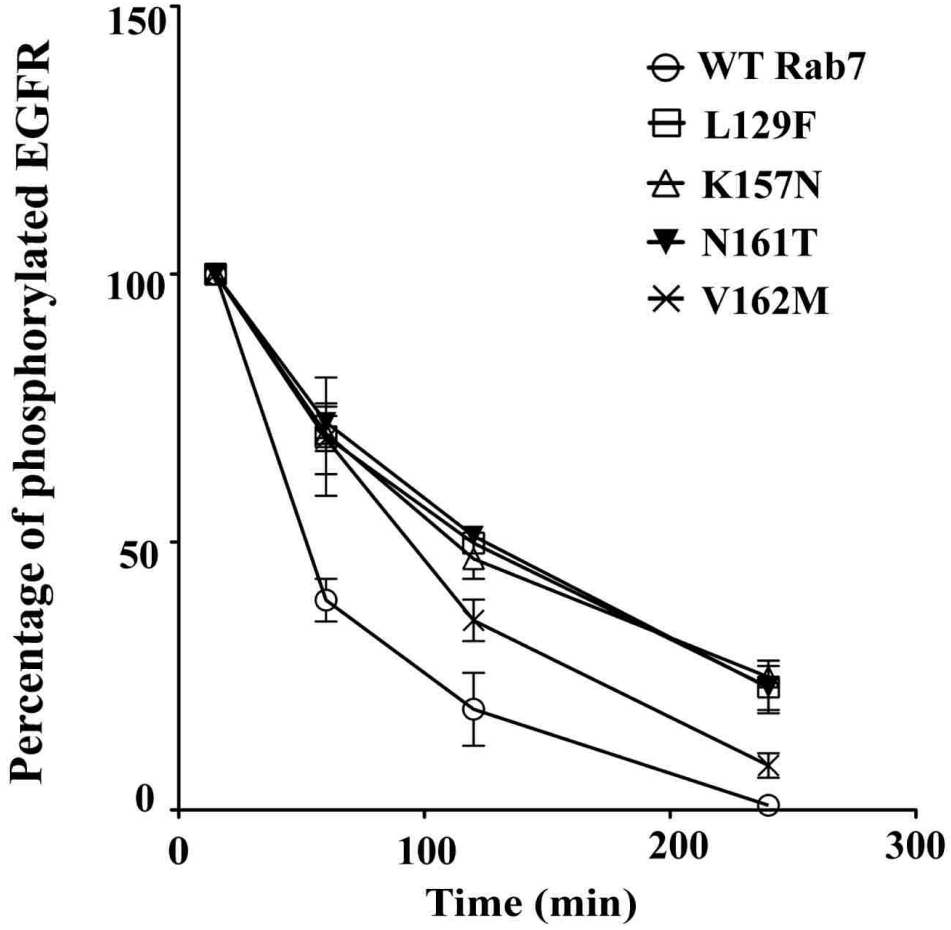

Figure 25: Rab7CMT2B mutants show delayed EGFR dephosphorylation. Samples from EGFR degradation assays were probed with antibody against tyrosine 1045 of EGFR to analyze the rate of dephosphorylation of the EGFR in the given time points. Line graphs represent the levels of phosphorylated EGFR normalized to actin.

Table 4: Half lives of activated EGFR, p38 and ERK1/2 in stable HeLa cells expressing the GFP-Rab7 wild-type and CMT2B mutants on EGF stimulation

Rab7	EGFR Dephosphorylation $T_{1/2}$ (sec)	Phospho p38 Dephosphorylation $T_{1/2}$ (sec)	Phospho Erk1/2 Dephosphorylation $T_{1/2}$ (sec)
WT	35.14±8.68	43.76±17.37	69.39±7.08
L129F	87.57±8.47	187.9±9.1	94.59±3.28
K157N	74.41±3.59	188.4±4.17	222.7±4.41
N161T	103±3.70	177.9±4.02	236.3±2.62
V162M	86.42±5.71	72.29±10.62	138.4±6.58

Rab7CMT2B mutants show no significant changes in Akt phosphorylation on NGF stimulation

The effect of NGF stimulation on the second major downstream signaling pathway regulated by phosphorylation of Akt was also analyzed in PC12 cells transiently expressing the Rab7CMT2B

mutants. There was no significant change in the Akt phosphorylation levels in the cells expressing the disease mutants when compared to cells expressing GFP alone or GFP-Rab7 **(Figure 26A–B).** The activation of Akt was similar in all samples at early time points and diminished uniformly at 24h.

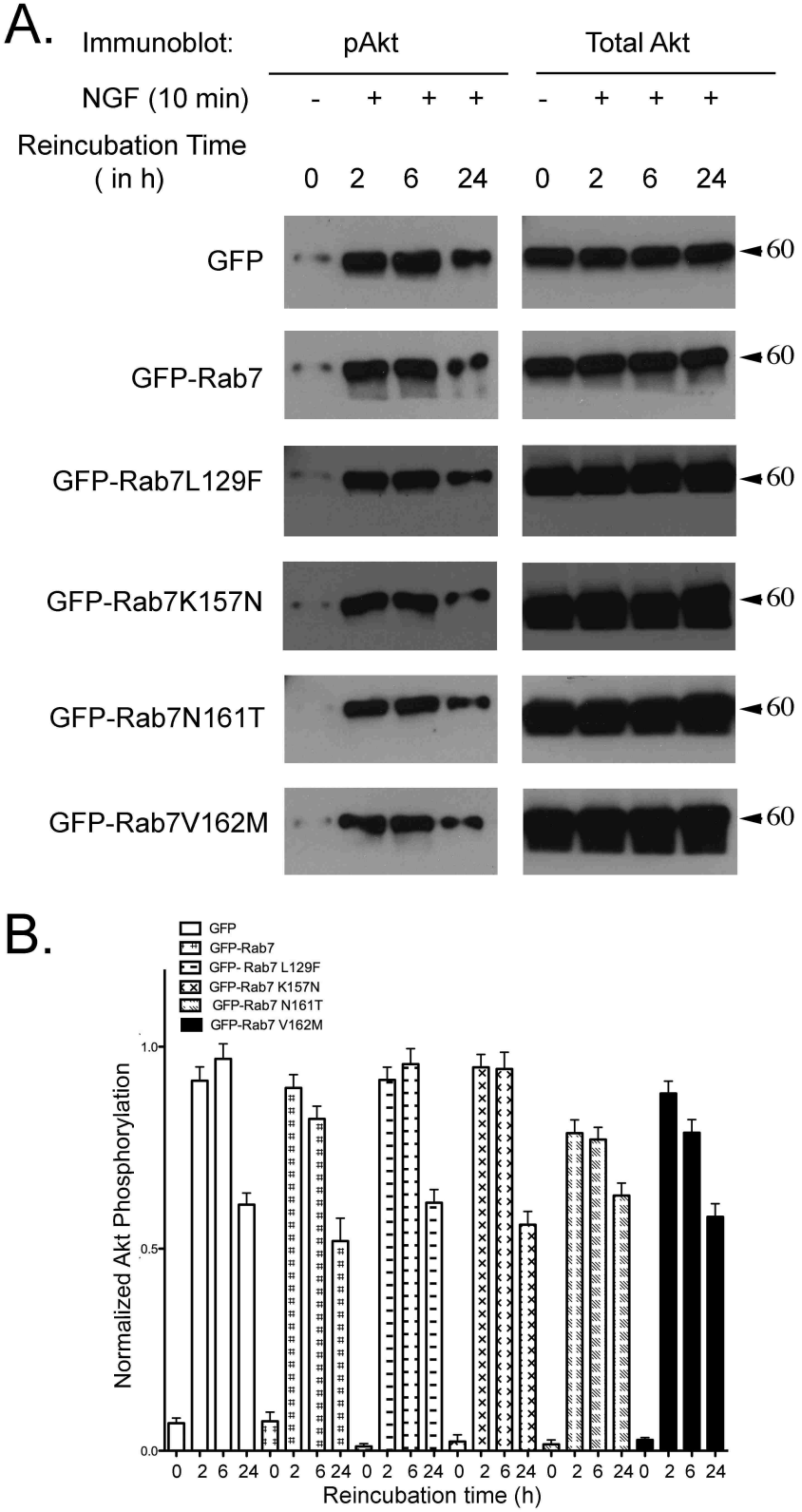

Figure 26: Cells expressing Rab7CMT2B mutants have no effect on Akt Signaling. **(A)** Transiently transfected PC12 cells expressing GFP, GFP-Rab7, GFP-Rab7L129F, GFP-Rab7K157N, GFP-Rab7N161T, GFP-Rab7V162M were briefly stimulated with NGF (200ng/ml) followed by surface stripping of ligand and reincubation in 0.1% BSA-DMEM for 2-24h. Subsequently, cells were lysed and equal amounts of protein were immunoblotted and probed for total and phosphorylated Akt. **(B)** Films from three independent experiments were quantified by Image J analysis. Bar graph shows levels of pAkt in GFP-Rab7 and CMT2B mutant expressing cells. In each case the amount of pAkt was normalized to the amount of GFP protein expressed. The bar graph shows the fold-change in pAkt as a function of pAkt in the GFP only control at each respective time point. Error bars indicating mean ± S.E.M. n=3, p values were not significant.

The findings are in agreement with a previous observation indicating that NGF stimulated Akt signaling occurs at the cell surface and is not triggered on the endosomes (95). The combined data suggest that alterations in TrkA downstream signaling are confined to endosomes and the ERK module, and are independent of Akt. Recent report suggested that Akt activation is typically triggered at the plasma membrane and is dependent on EGFR internalization. The MAPK activation in EGFR internalization defective mutants were not affected thereby reiterating the point that MAPK activation occurs from the internalized signaling endosomes (96).

Rab7CMT2B mutants expressing PC12 cells and HeLa show enhanced ERK signaling on growth factor stimulation

Upon NGF stimulation, PC12 cells stop proliferating and start differentiating (97). NGF-mediated TrkA signaling in PC12 cells typically activates ERK1/2 and Akt downstream signaling. The ERK activation module is located on endosomes (95, 98, 99) and is instrumental in NGF stimulated differentiation signaling from TrkA containing endosomes (100). To investigate the activation of the ERK1/2 signaling mediators, PC12 cells transiently expressing Rab7CMT2B mutants were briefly stimulated with NGF followed by surface stripping of ligand. Compared to control cells expressing GFP only or GFP-Rab7 wild-type protein, PC12 cells expressing the GFP-tagged Rab7CMT2B mutants consistently showed 1.5–2.2 fold higher levels of phosphorylated ERK1/2 at all time points examined **(Figure 27A-B, numerical values are provided in Table 2)**, providing evidence for the higher levels of phosphorylated receptors leading to enhanced downstream signaling.

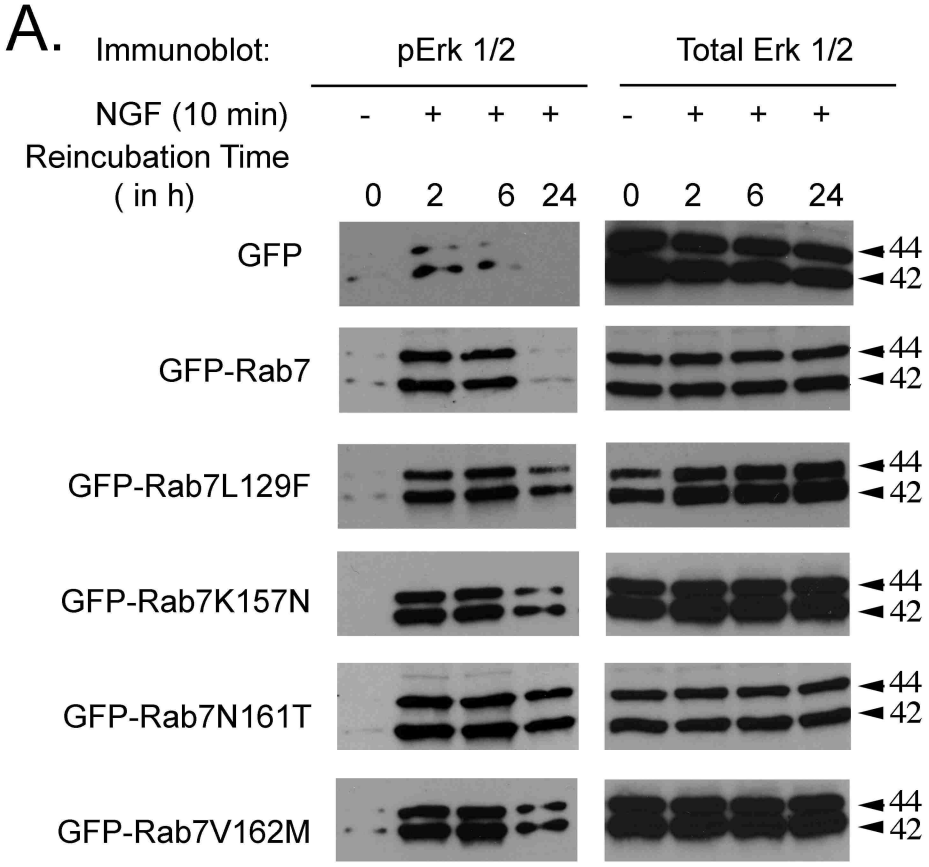

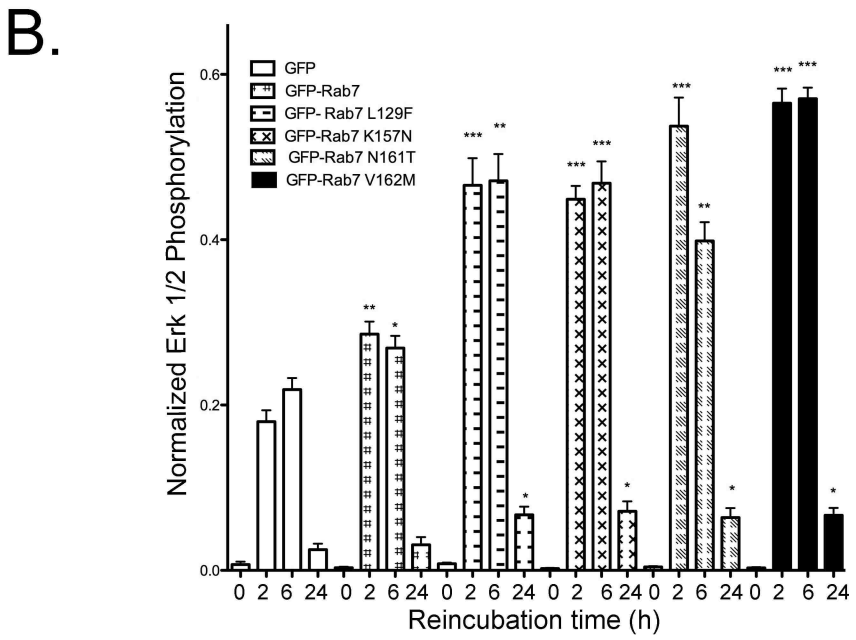

Figure 27: Cells expressing Rab7CMT2B mutants exhibit prolonged ERK signaling following NGF stimulation. (A) Transiently transfected PC12 cells expressing GFP, GFP-Rab7wild-type, GFP-Rab7L129F, GFP-Rab7K157N, GFP-Rab7N161T, GFP-Rab7 V162M were briefly stimulated with NGF (200ng/ml) followed by surface stripping of ligand and reincubation in 0.1% BSA-DMEM for 2-24h. Subsequently, cells were lysed and equal amounts of protein were immunoblotted and probed for total and phosphorylated ERK1/2. **(B)** Films from three independent experiments were quantified by Image J analysis. Bar graph shows levels of pERK1/2 in GFP-Rab7wt and CMT2B mutant expressing cells. In each case the amount of pERK1/2 was normalized to the amount of GFP protein expressed. The bar graph shows the fold-change in pERK1/2 as a function of pERK1/2 in the GFP only control at each respective time point. Error bars indicating mean ±S.E.M., n=3,*p<0.05; **p<0.01, ***p<0.001. For detailed numerical values see Table 2.

The effects of overexpression of Rab7CMT2B mutants on EGF-stimulated ERK1/2 signaling was assessed. HeLa cells and PC12 cells stably expressing the Rab7CMT2B mutants were starved and stimulated with EGF in a time-dependent manner. Rab7CMT2B mutants showed enhanced activation of p38 compared with the wild-type in both the stable HeLa and PC12 cells overexpressing Rab7CMT2B mutants **(Figure 28 A–D)**.

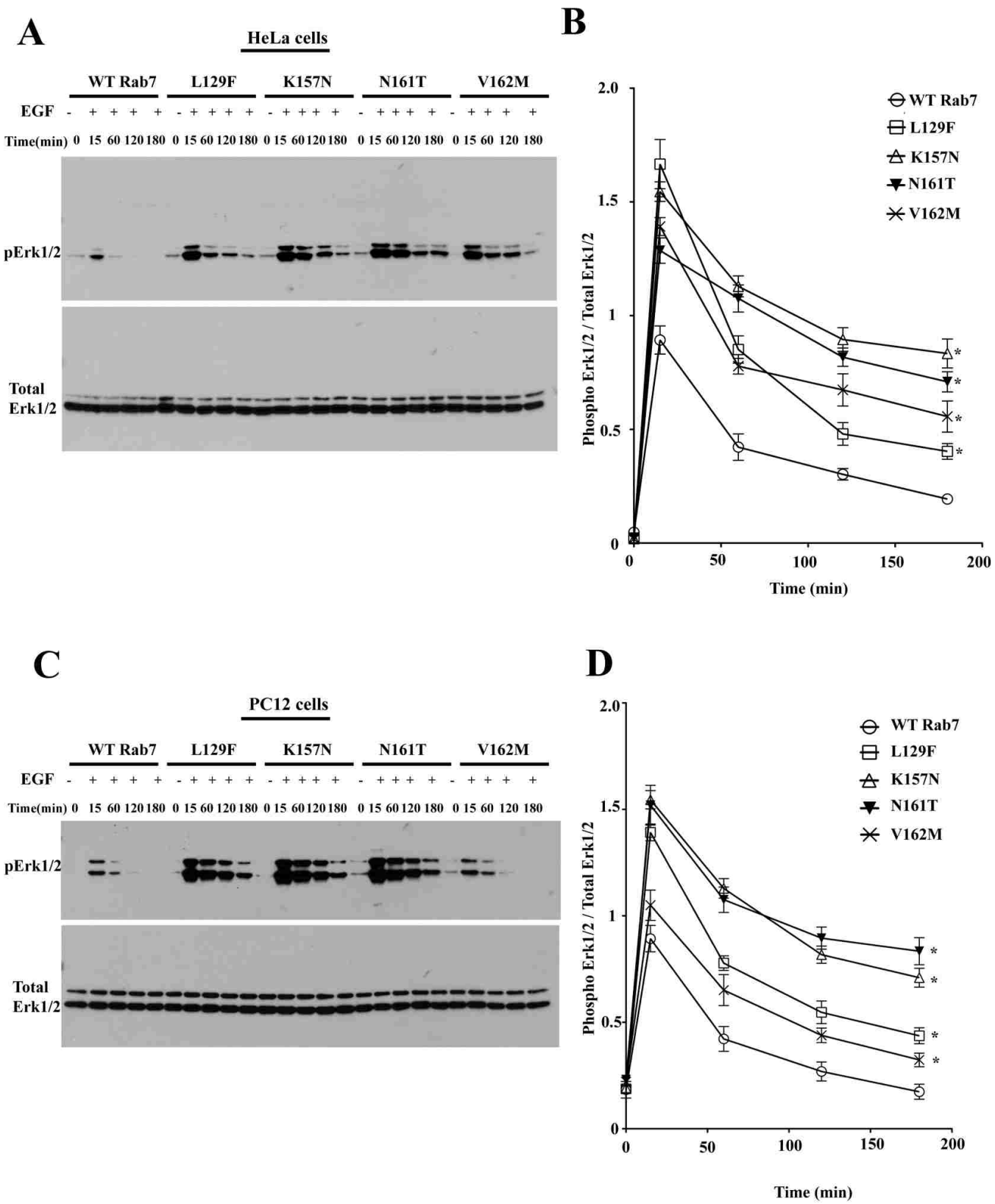

Figure 28: Rab7CMT2B mutants show enhanced ERK1/2 activation. (A) HeLa cells stably expressing GFP-Rab7 wild-type, GFP-Rab7L129F, GFP-Rab7K157N, GFP-Rab7N161T and GFP-Rab7V162M were starved with DMEM for 5h and stimulated with EGF (100ng/ml) for indicated time points. Subsequently, cells were lysed and equal amounts of protein were immunoblotted and probed for total and phosphorylated ERK1/2. **(B)** Films from three independent experiments were quantified densitometrically. Line graph shows levels of pERK1/2 in GFP-Rab7 wild-type and CMT2B mutant expressing cells. In each case the amount of pERK1/2 was normalized to the total ERK1/2 protein expressed. Differences are represented as ± S.E.M. **(C)** PC12 cells stably expressing GFP-Rab7 wild-type, GFP-Rab7L129F, GFP-Rab7K157N, GFP-Rab7N161T and GFP-Rab7V162M were starved in DMEM for 5h and stimulated with EGF (100 ng/ml) for indicated time points. Subsequently, cells were lysed and equal amounts of protein were immunoblotted and probed for total and phosphorylated ERK1/2. **(D)** Films from three independent experiments were quantified densitometrically. Line graph shows levels of pERK1/2 in GFP-WT Rab7 and CMT2B mutant expressing cells. In each case the amount of pERK1/2 was normalized to the total ERK1/2 protein expressed. Differences are represented as ± S.E.M. Asterisks denote $p<0.05$ based on one-way ANOVA with Dunnett's post-test and relative to Rab7 wild-type control.

Quantification showed higher levels of phosphorylated ERK1/2 at all time points in the cells expressing Rab7CMT2B mutants compared with the wild-type Rab7 **(Figure 28 B and D)**. The rates of dephosphorylation of activated ERK1/2 were up to 3.4-fold slower in the CMT2B mutants as compared with the Rab7 wild-type **(Table 4).**

Rab7CMT2B Mutants Enhance p38 Activation

Previous studies have shown that overexpression of the GTP-locked Rab7Q67L mutant leads to impaired degradation of EGFR with enhanced ERK1/2 signaling but no change in p38 activation but reduced nuclear signaling (101). In contrast when p50/dynamitin was overexpressed signaling endosomes were dispersed to the cell periphery were they showed enhanced ERK1/2 and p38 activation, delayed EGFR degradation but enhanced nuclear signaling. Although the Rab7CMT2B mutants are competent to bind GTP, their phenotype in the EGFR trafficking assays was reminiscent of dominant negative Rab7, overexpression of which impairs endocytic trafficking (102). To further study the effect of overexpression of Rab7CMT2B mutants on EGF-stimulated endosomal signaling, HeLa cells and neuronal PC12 cells stably expressing Rab7 wild-type or CMT2B mutants were starved and stimulated with EGF in a time-dependent manner. Rab7CMT2B mutants showed enhanced activation of p38 compared with the wild-type in both the stable HeLa and PC12 cells overexpressing Rab7CMT2B mutants **(Figure 29 A–D)**. Quantification showed higher levels of phosphorylated p38 at all time points in the cells expressing Rab7CMT2B mutants compared with the wild-type Rab7 **(Figure 29 B and D**). The rates of dephosphorylation of activated p38 were up to 4.3-fold slower in the CMT2B mutants as compared with Rab7 wild-type **(Table 4).**

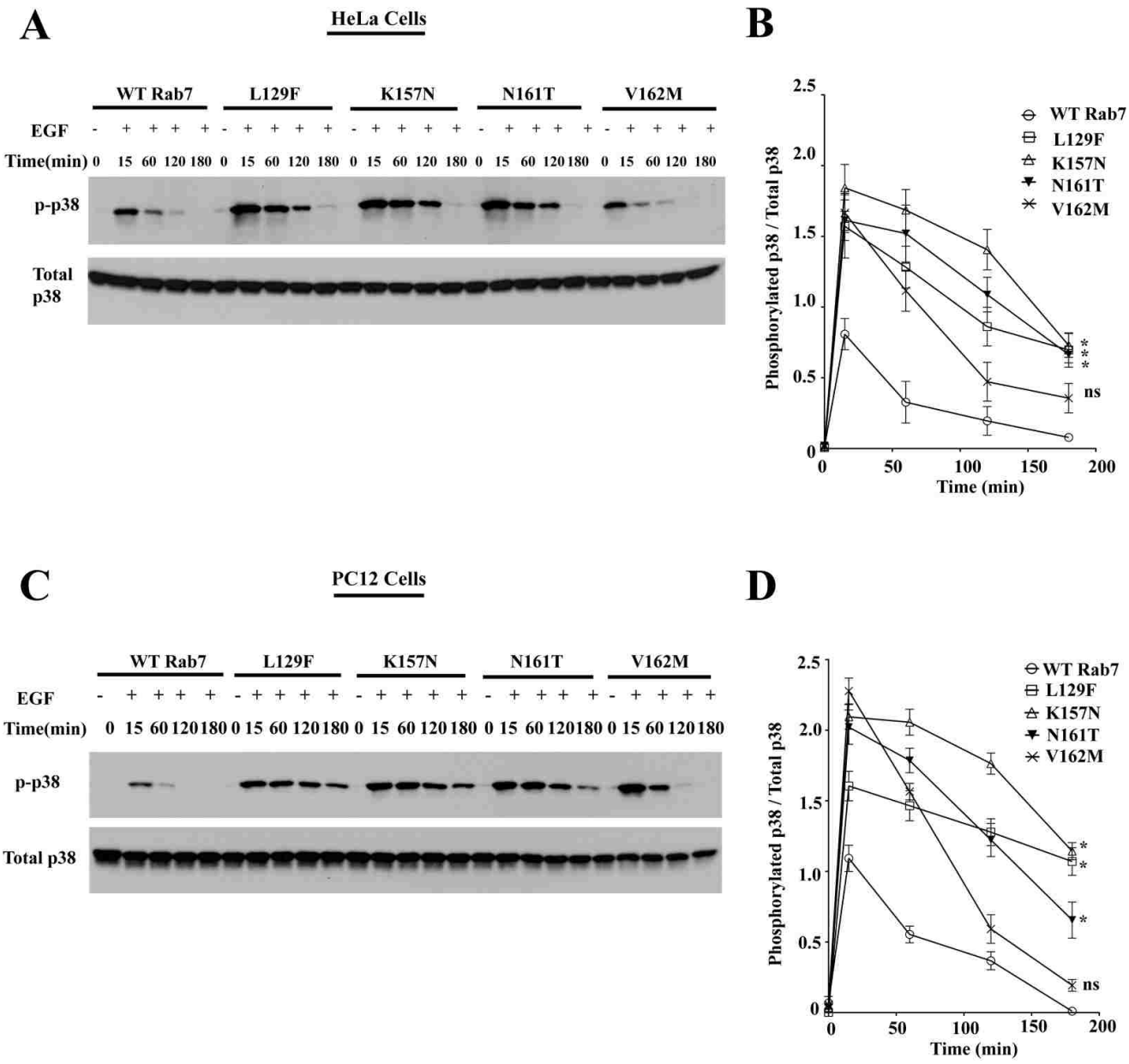

Figure 29: Rab7CMT2B mutants show enhanced p38 activation. (A) HeLa cells stably expressing GFP-Rab7 wild-type, GFP-Rab7L129F, GFP-Rab7K157N, GFP-Rab7N161T and GFP-Rab7V162M were starved with DMEM for 5h and stimulated with EGF (100 ng/ml) for indicated time points. Subsequently, cells were lysed and equal amounts of protein were immunoblotted and probed for total and phosphorylated p38. **(B)** Films from three independent experiments were quantified densitometrically. Line graph shows levels of p-p38 in GFP-Rab7 wild-type (WT) and CMT2B mutant expressing cells. In each case the amount of p-p38 was normalized to the total p38 protein expressed. Differences are represented as ± S.E.M. **(C)** PC12 cells stably expressing GFP-WT Rab7, GFP-Rab7L129F, GFP-Rab7K157N, GFP-Rab7N161T and GFP-Rab7V162M were starved in DMEM for 5h and stimulated with EGF (100 ng/ml) for indicated time points. Subsequently, cells were lysed and equal amounts of protein were immunoblotted and probed for total and phosphorylated p38. **(D)** Films from three independent experiments were quantified densitometrically. Line graph shows levels of phosphorylated p38 in GFP-WT Rab7 and CMT2B mutant expressing cells. In each case the amount of phosphorylated p38 was normalized to the total p38 protein expressed. Differences are represented as ± S.E.M. Asterisks denote $p<0.05$ based on one-way ANOVA with Dunnett's post-test and relative to Rab7 wild-type control.

Chapter 5: Rab7CMT2B mutants impair nuclear signaling

It is worth noting that the GTP-bound dominant active mutant of Rab7Q67L cause tight perinuclear clustering of endosomes and delays the entry to late endosomes and hence the degradation of internalized EGFR (101). As a consequence, the MAPK signaling is sustained yet nuclear signaling is downregulated (decreased activation of Elk-1). In contrast, repositioning the signaling endosomes containing activated internalized EGFR to cell periphery by overexpressing p50/dynamitin, a dynein subunit results in sustained MAPK signaling and enhanced nuclear signaling (increased activation of Elk-1). Thus the appropriate trafficking of activated EGFR to endosomes controls the spatio-temporal regulation of MAPK signaling **(Figure 9)**. It is therefore necessary to measure the impact of Rab7CMT2B mutants on the spatiotemporal fidelity of the endosomal signaling relative to late endocytic traffic regulation.

Rab7CMT2B Mutants Decrease Elk-1-driven Gene Activation and Downstream c-fos and Egr-1 Expression

Activated ERK1/2 translocates to the nucleus to activate the transcription factor Elk-1 to drive gene activity (103). To investigate the impact of the enhanced endosomal activation of p38 and ERK1/2 on nuclear signaling, HeLa cells stably expressing the Rab7CMT2B mutants were co-transfected with plasmids encoding the Elk-1 and luciferase gene controlled by the Elk-1-driven promoter. Following a 14h starvation, cells were stimulated with EGF for 15–240min, and luciferase activity was measured. Cells overexpressing the Rab7CMT2B mutants showed lower Elk-1-driven gene activity at all time points compared with the cells overexpressing wild-type Rab7 **(Figure 30)**.

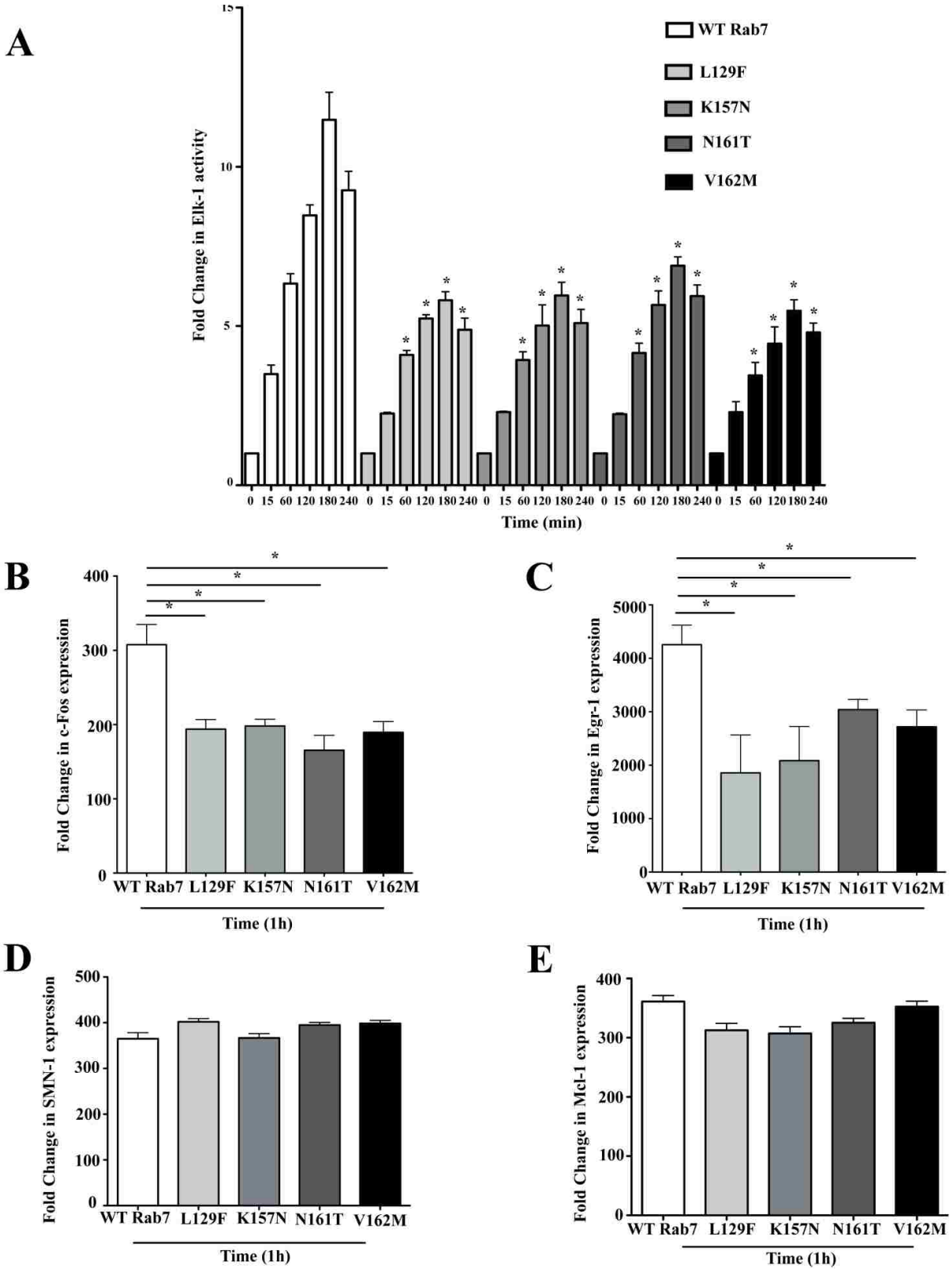

Figure 30: Rab7CMT2B mutants show lower Elk-1 driven gene activation and *c-fos* and *Egr-1* expression on EGF stimulation. (A) HeLa cells stably expressing GFP-tagged wild-type (WT) Rab7 and CMT2B mutants were transfected with plasmids pFR Luc and pFA2 Elk-1 to study Elk-1 driven gene activity. Cells were starved in DMEM for 14h followed by EGF stimulation (100ng/ml) in a time dependent manner. Following stimulation, cells were kept in serum free medium for 6h, lysed and luciferase activity was determined in a luminometer. Each time point was performed twice and measured in triplicates. Relative light units are normalized to the protein amounts. Disease mutants showed lower Elk-1 driven gene activity. Rab7CMT2B mutants were compared to the wild-type Rab7 at respective time points. Differences are represented as ± S.E.M. **(B)** HeLa cells stably expressing GFP-Rab7 wild-type and CMT2B mutants were serum starved, EGF stimulated for 1h and processed for RT-PCR as detailed in Experimental Procedures. Bar graphs showing the lower expression of *c-fos* on EGF stimulation in cells expressing GFP-Rab7CMT2B mutants compared to the wild-type. Differences are represented as ± S.E.M. **(C)** Bar graphs showing the lower expression of *Egr-1* on 1h EGF stimulation in cells expressing GFP-Rab7CMT2B mutants compared to the wild-type. Differences are represented as ± S.E.M. **(D,E)** Bar graphs showing no difference in expression levels of SMN1 and Mcl-1 on 1h EGF stimulation in cells expressing GFP-Rab7CMT2B mutants compared to the wild-type. Asterisks denote $p<0.05$ based on one-way ANOVA with Dunnett's post-test and relative to Rab7 wild-type control.

Although disease mutants exhibited enhanced ERK activation, the downstream Elk-1 target showed decreased activation. The altered Elk-1-driven gene activity in Rab7CMT2B-expressing cells would be expected to influence downstream genes under the transcriptional control of Elk-1. Therefore, we also analyzed the expression of two genes directly targeted by active Elk-1, c-fos and Egr-1. Quantitative real-time PCR analyses showed that all of the Rab7CMT2B mutants have significantly lower levels of c-fos and Egr-1 gene expression compared with the wild-type following 1h of EGF stimulation (**Figure 30 B and C)**.however, not all genes that have important neuronal functions and have been reported to be subject to Elk-1 regulation were uniformly affected. There was no apparent decrease in SMN1 (survival- of-motor neuron 1) and decreases in Mcl-1 (myeloid cell leukemia-1) transcription were too small to reach statistical significance **(Figure 30 D and E).** This suggests that the CMT2B mutants cause selective changes in Elk-1-regulated transcription.

Rab7CMT2B mutants expressing PC12 cells show altered subcellular localization of phosphorylated ERK1/2 and p38 on growth factor stimulation

To examine the subcellular distribution of activated ERK1/2 on NGF stimulation in PC12 cells we used subcellular fractionation to separate the cytosolic and nuclear fractions. Probing with lamin B, a nuclear envelope protein, tested the purity of the fractions. Following brief NGF stimulation and surface stripping of ligand, cells expressing the Rab7CMT2B mutants were reincubated in starvation medium for 2h and 24h. At the shorter time point, the Rab7CMT2B mutant expressing cells showed diminished levels of the activated ERK1/2 in the nucleus compared to GFP expressing control cells and consequently predominant cytoplasmic distribution of activated ERK1/2 **(Figure**

31A).however, after a 24h post stimulation chase period, activated ERK1/2 was no longer detected in the nuclear fraction in either the Rab7CMT2B mutant or the wild-type Rab7 expressing cells **(Figure 31B).** Interestingly, the level of phosphorylated ERK1/2 remained higher in the cytosolic fraction of the disease mutants relative to cells expressing the wild-type Rab7, suggesting either enhanced phosphorylation or decreased dephosphorylation of the ERK1/2 in the cells expressing the disease mutants.

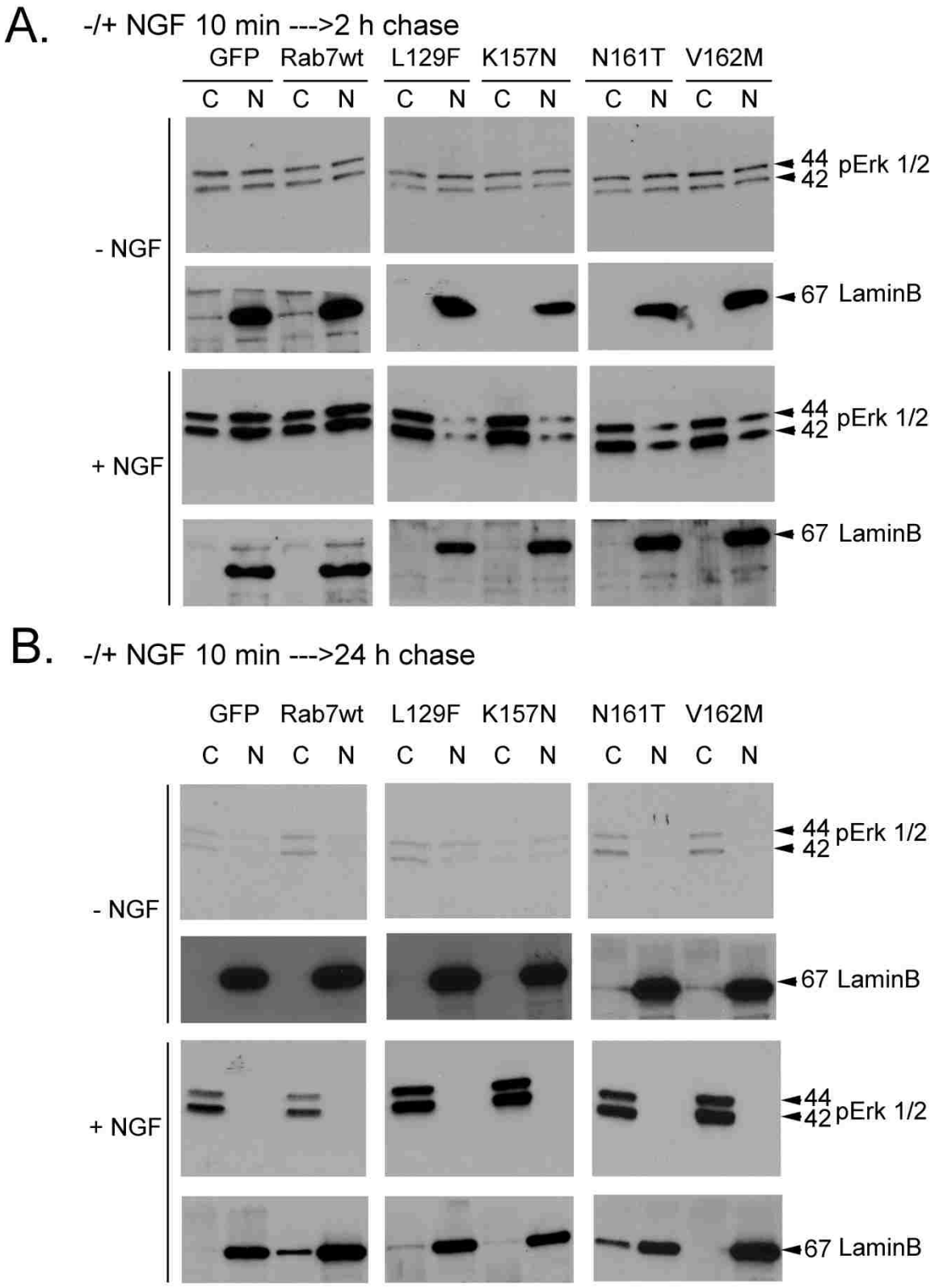

Figure 31: Cells Expressing Rab7CMT2B Mutants Exhibit Altered Cytoplasmic and Nuclear Partitioning of Activated ERK1/2. (A) Transiently transfected PC12 cells expressing GFP, GFP-Rab7 wild-type, GFP-Rab7L129F, GFP-Rab7K157N, GFP-Rab7N161T, GFP-Rab7 V162M were briefly stimulated with NGF (200ng/ml) followed by surface stripping of ligand and reincubation in 0.1% BSA-DMEM for 2h and **(B)** 24h. Subsequently, cells were lysed and subjected to subcellular fractionation and immunoblotted with antibodies directed against phosphorylated ERK1/2. The purity of fractions was confirmed by probing for the nuclear marker lamin B.

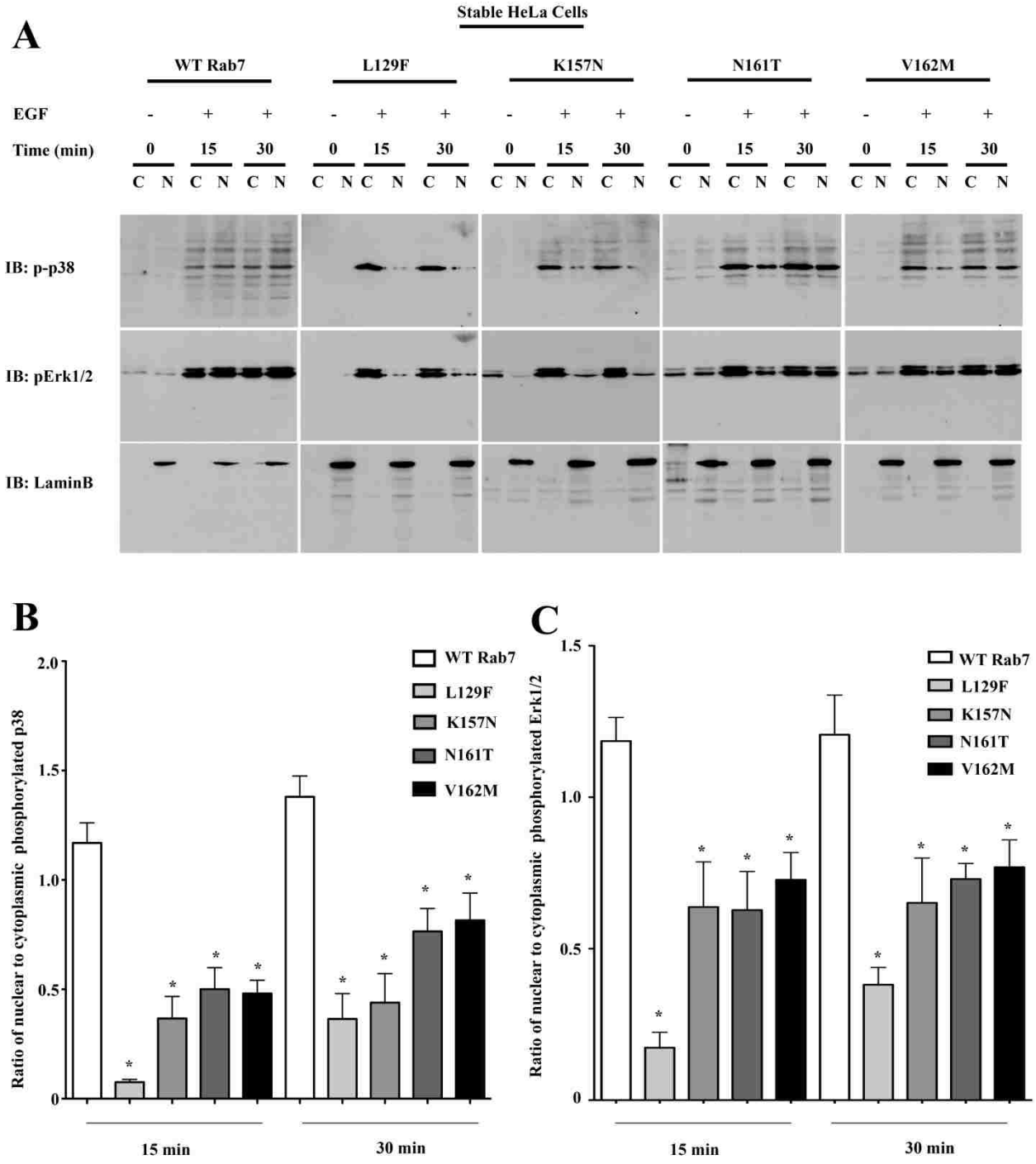

Figure 32: Rab7CMT2B mutants show delayed nuclear shuttling of activated MAPKs in HeLa cells. (A) Stable HeLa cells expressing GFP-tagged wild-type (WT) and Rab7CMT2B mutants were serum starved for 5h and stimulated with EGF (100 ng/ml) for 15min and 30min respectively. Subsequently, cells were lysed, subjected to subcellular fractionation to separate the cytosolic (C) and nuclear (N) fractions and immunoblotted with antibodies directed against phosphorylated p38 and phosphorylated ERK1/2. The purity of fractions was confirmed by probing for the nuclear marker lamin B. Rab7CMT2B mutants showed an impaired nuclear translocation of p-p38. Rab7L129F and Rab7K157N showed an impaired translocation of pERK1/2 and to a lesser extent in Rab7N161T and Rab7V162M expressing cells. **(B, C)** Bar graphs showing the differences in the nuclear to cytoplasmic ratio of activated p38 and ERK1/2 following 15min and 30min of EGF stimulation. Differences are represented as ± S.E.M. Asterisks denote $p<0.05$ based on one-way ANOVA with Dunnett's post-test and relative to Rab7 wild-type control. Comparison between CMT2B mutants was based on one-way ANOVA with Tukey's post-test and showed L129F significantly different from N161T and V162M for p38 activation at 15min of EGF stimulation, $p<0.05$.

Therefore it was tested if a similar delay in nuclear translocation of activated p38 and ERK1/2 exists in response to EGF signaling and might account for the observed decrease in Elk-1-driven gene activity in the disease mutants. HeLa cells and neuronal PC12 cells stably expressing the GFP-tagged Rab7CMT2B mutants were serum starved and stimulated with EGF for 15 and 30min prior to subcellular fractionation to separate the nuclear and cytosolic fractions. ERK1/2 nuclear translocation was impaired most significantly in the L129F and K157N mutants and to a lesser extent in the N161T and V162M mutants. Activated p38 nuclear translocation was markedly delayed in cells expressing all of the Rab7CMT2B mutants. The nuclear marker Lamin B and actin (not shown) served as a control for purity of the nuclear and cytosolic fractions. In both the HeLa **(Figure 32)** and PC12 **(Figure 33)** cells stably expressing the Rab7CMT2B mutants, the nuclear/cytoplasmic ratio of activated p38 distribution was significantly lower than in cells expressing Rab7 wild-type . Furthermore, in HeLa cells, Tukey's posthoc test showed that the nuclear/cytoplasmic ratio of activated p38 was significantly lower in the L129F mutant compared with N161T and V162M mutants. In PC12 cells, no statistically significant differences were observed between the individual CMT2B mutants. Similar trends were observed for the distribution of activated ERK1/2 **(Figure 32C and 33C)**. These results indicate that the Rab7CMT2B mutants have similar effects in different cell lines in impairing nuclear signaling.

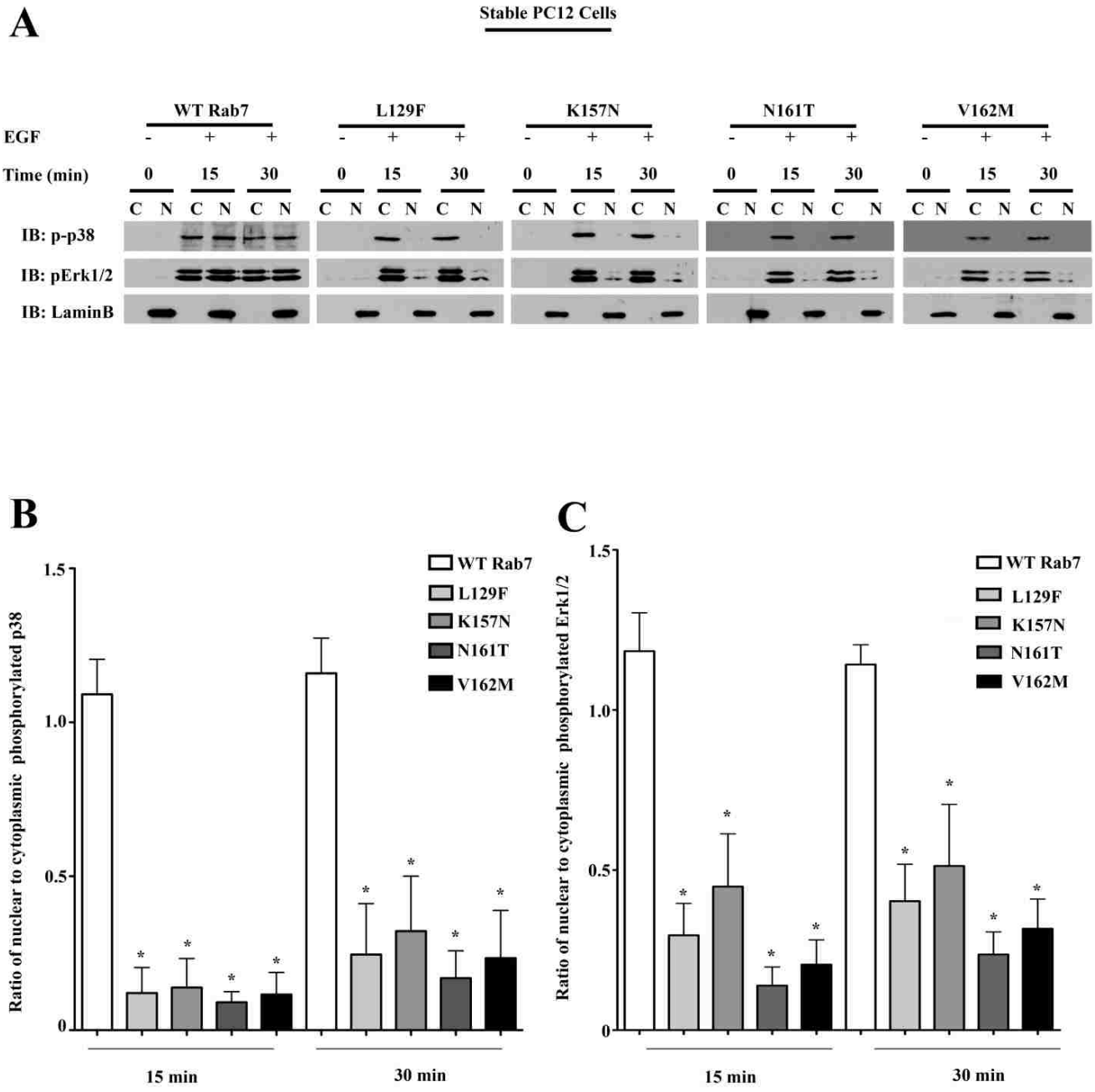

Figure 33: Rab7CMT2B mutants show delayed nuclear shuttling of activated MAPKs in neuronal PC12 cells. (A) Stable PC12 cells expressing GFP-tagged wild-type (WT) and Rab7CMT2B mutants were serum starved for 5h and stimulated with EGF (100ng/ml) for 15min and 30min respectively. Subsequently, cells were lysed, subjected to subcellular fractionation to separate the cytosolic (C) and nuclear (N) fractions and immunoblotted with antibodies directed against phosphorylated p38 and phosphorylated ERK1/2. The purity of fractions was confirmed by probing for the nuclear marker lamin B. Rab7CMT2B mutants showed an impaired nuclear translocation of p-p38 and pERK1/2. **(B, C)** Bar graphs showing the differences in the nuclear to cytoplasmic ratio of activated p38 and ERK1/2 following 15min and 30min of EGF stimulation. Differences are represented as ± S.E.M. Asterisks denote $p<0.05$ based on one-way ANOVA with Dunnett's post-test and relative to Rab7 wild-type control. Comparison between CMT2B mutants based on one-way ANOVA with Tukey's post-test showed no significant differences between the mutants.

Chapter 6: Results-Rab7CMT2B mutants alter ubiquitination of activated growth factor receptors

Disease mutants of Rab7 occur predominantly in the GTP-bound state. Active Rab7 binds to different effector proteins. The disease mutants of Rab7 showed enhanced interaction with different interactor proteins like ORP1L, Vps13c and clathrin heavy chain compared to the wild-type (47). This implies that Rab7CMT2B mutants would be expected to have differential interaction with a host of effectors. One such interactor is XAPC7, an alpha subunit of proteasome, that interacts specifically with Rab7 and colocalizes with it on the endosomal membrane thereby providing a link between cytoplasmic and lysosomal degradation pathways (80).

Interestingly trafficking of activated TrkA receptor is mediated by a scaffolding protein called p62/SQSTM1 that shuttles the ubiquitylated TrkA cargo to the proteasome for deubiquitination **(Figure 8).** This step is a prerequisite for the lysosomal degradation of the activated, internalized TrkA (72). SQSTM1/p62has been shown to colocalize with late endosomal markers like Rab7 and Lamp1 and EGFR following EGF stimulation and internalization (104). It is thus postulated that Rab7CMT2B mutants differentially interact with XAPC7 and have a delayed association with p62 for deubiquitylating the internalized, activated TrkA cargo creating a bottleneck that results in the observed delay in degradation. p62 has been shown to colocalize with endosomal markers. It is thus postulated a complex of Rab7, XAPC7 and p62 form a complex at late endosomal membrane and regulate trafficking of growth factor receptors.

Rab7CMT2B mutants are postulated to delay growth factor receptor trafficking. Since p62 serves as a shuttling scaffold to deubiquitinate the ubiquitylated cargo prior to lysosomal degradation, Rab7CMT2B mutants would be expected to delay this process.

To further dissect the mechanism responsible for the delayed degradation of growth factor receptors upon expression of Rab7CMT2B mutant proteins, we analyzed the ubiquitination status and interactions with proteasomal linker p62 protein.

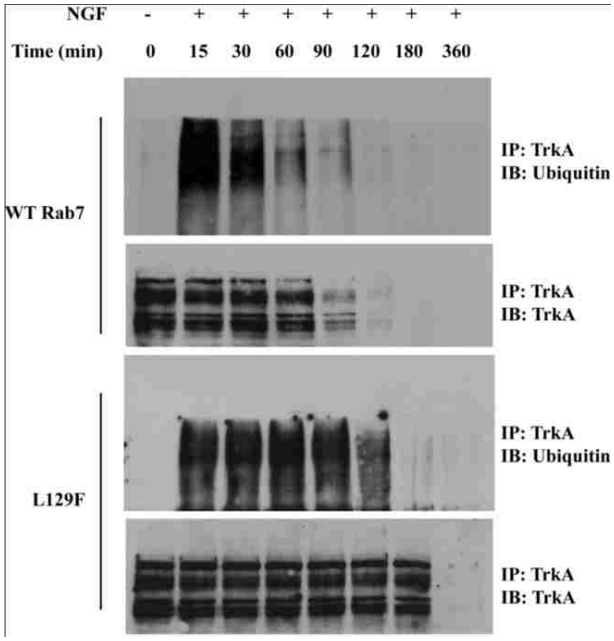

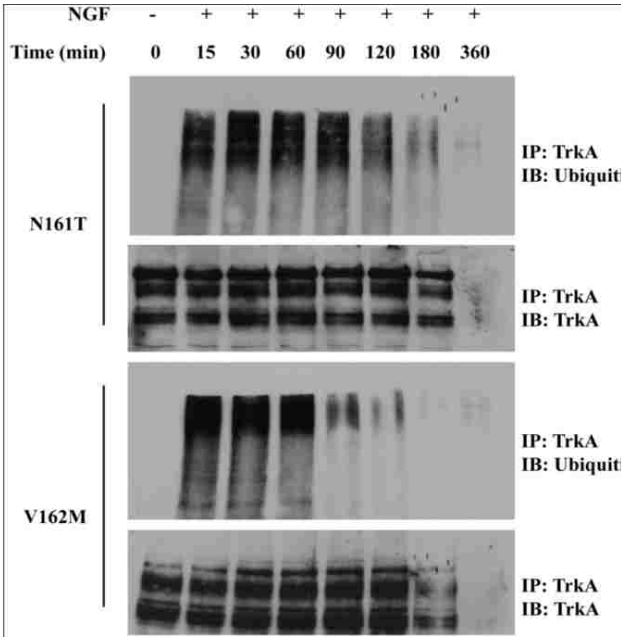

Figure 34: Expression of Rab7CMT2B mutants causes accumulation of ubiquitinated TrkA.

Stable cell lines expressing wild-type Rab7 or Rab7CMT2B mutants were serum starved and stimulated with nerve growth factor receptor for various times (0-360min). Cell lysates were prepared, immunoprecipitated for TrkA, and probed for ubiquitinated receptor at each time point. n=3.

A possible link through the proteasomal degradative pathway is suspected because the CMT2BV162M mutant failed to interact with the Rab7 interacting protein and alpha proteasome subunit, XAPC7 (68, 80,81).

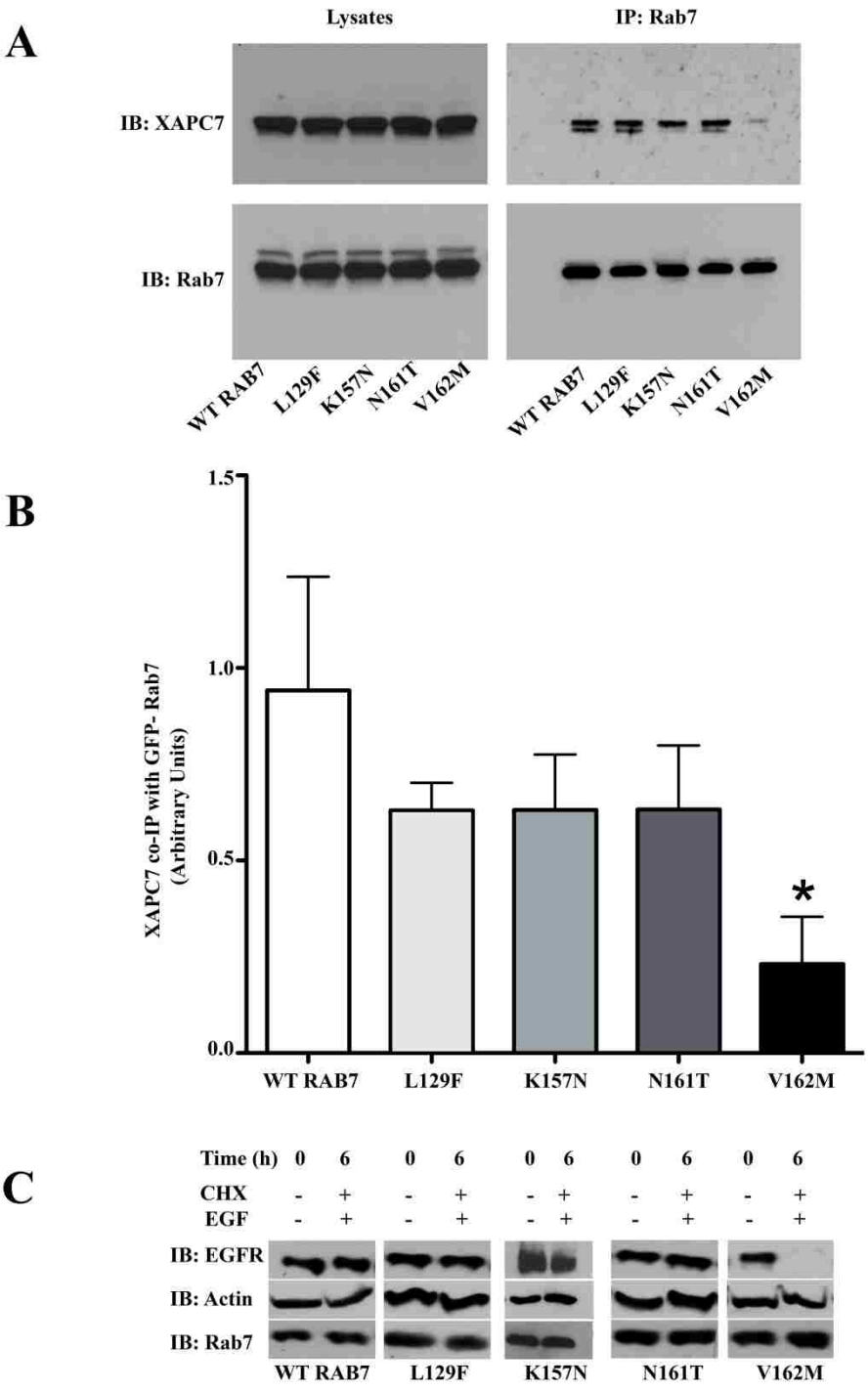

Figure 35: Two adjacent Rab7CMT2B mutants differentially affect binding to XAPC7, an alpha proteasome subunit XAPC7. (A) BHK-21 cells were transfected with plasmids encoding full length human XAPC7 in combination with GFP-tagged wild-type and Rab7CMT2B mutants. BHK-21 cell lysates were immunoprecipitated with rabbit antibody directed against Rab7 and the immunoprecipitated samples were resolved by 12 % SDS-PAGE and immunoblotted for XAPC7 and Rab7. **(B)** The data from three experiments were quantified by densitometry (normalizing to the respective GFP-Rab7 signal) and the average is shown in the bar graphs. Error bars represent S.E.M. **(C)** A431 cells were co-transfected with XAPC7 plasmid and Rab7 wild-type or Rab7CMT2B mutants as described in Experimental Procedures. Samples were resolved by SDS-PAGE and then subjected to immunoblotting to detect EGFR and actin as a control. Same samples were examined for XAPC7 expression level using mouse antibody.

The results suggest that the endosomal traffic is not completely blocked in the presence of endogenous wild-type protein but instead is slowed. Such a phenotype is consistent with the slow but progressive nature of CMT2B disease. One possible mechanism for the delayed transport could be differential Rab7 effector protein interactions with the Rab7CMT2B mutants and could account for the autosomal dominant phenotype **(Figure 34)**.

Expression of all four CMT2B mutants was found to prolong the lifetime of ubiquitinated nerve growth factor receptor, TrkA relative to wild-type Rab7 expression (**Figure 34**). All mutants except V162M exhibited reduced colocalization and interaction with the TrkA proteasomal linker protein p62 (**Figure 36**). Therefore, p62 interaction is crucial for chaperoning the ubiquitinated TrkA for proteasomal degradation.

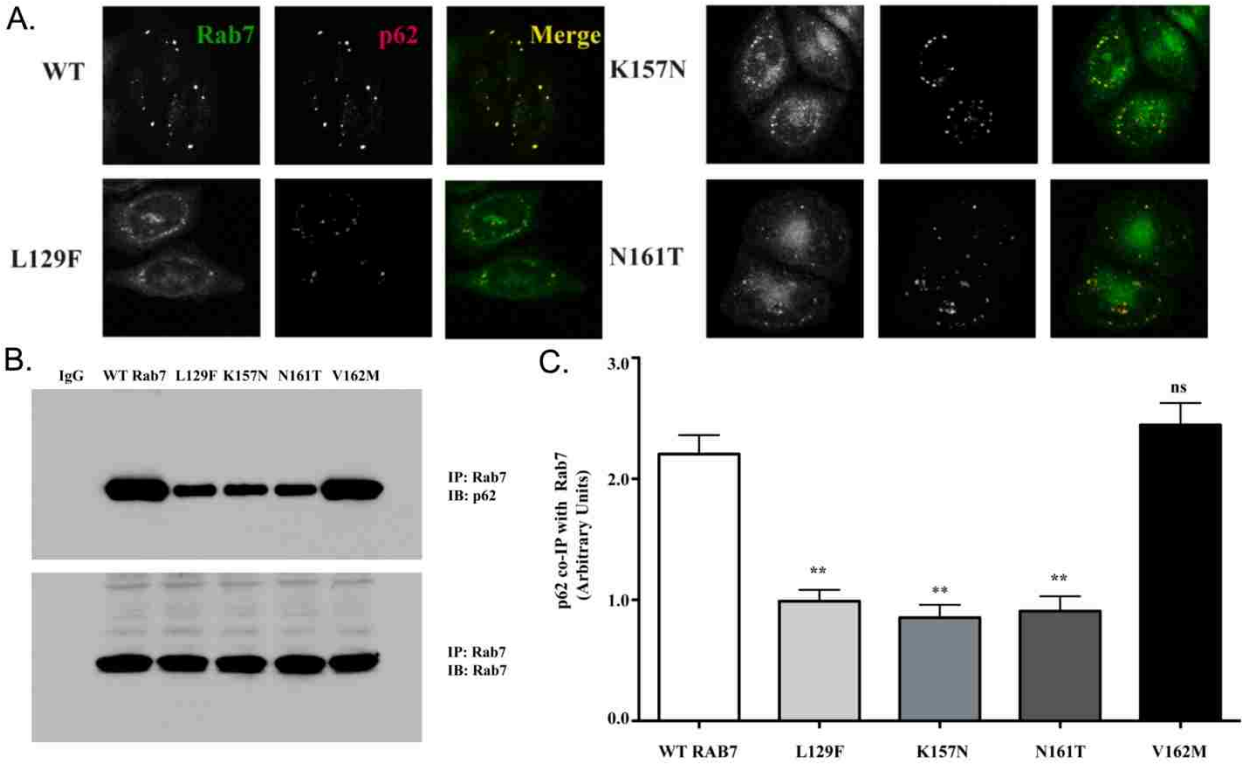

Figure 36: Rab7CMT2B mutants differentially colocalize with and interact with proteasome linker p62. **(A)** Stable cell lines expressing GFP-tagged wild-type Rab7 or Rab7CMT2B mutants (green) were immunostained for p62 (red). **(B)** Cell lysates were prepared from stable cell lines expressing wild-type Rab7 or Rab7CMT2B mutants. Rab7 was immunoprecipitated from each cell lysate and immunoblotted for co-precipitation of p62. As a control for equal immunoprecipitation and loading the same samples were also immunoblotted for Rab7. **(C)** Quantification of three independent experiments as detailed under (B).

The role of p62 in TrkA trafficking in CMT2B mutants suggests an intersection with autophagy. A recent report showed that Rab7V162M mutant colocalized with p62 in enlarged vesicles and increased the anterograde transport of these autophagosomes indicating an alteration in autophagic flux (105). This calls for an in depth analysis on the putative role of p62 in altering the endosomal traffic in CMT2B disease conditions.

Chapter 7: Discussion

Genome wide analysis of CMT disease have identified many important gene products that play crucial role in axonal trafficking and misregulated functions of which lead to CMT pathology (106-113,113-116). The Charcot-Marie-Tooth Type 2B disease specifically involves mutations in conserved amino acid residues of the late endocytic regulator Rab7. The four missense mutations of Rab7 implicated in the disease show similar biochemical properties that have been associated with the proteins being predominantly in the GTP-bound state (29, 30).

Rab7CMT2B mutants alter endocytic transport

Charcot-Marie-Tooth type 2B disease occurs due to L129F, K157N, N161T and V162M substitutions in the ubiquitously expressed Rab7 protein. A perplexing mystery of the Rab7 mutations is that only the peripheral nerves are affected even though Rab7 is a ubiquitous protein. This has been attributed to the presence of one or more specific effectors of Rab7 that affect unique pathways in the peripheral neurons to cause the disease (48). The Rab7CMT2B mutants being predominantly in the GTP-bound state have been suggested to cause more rapid degradation of the endocytosed growth factor receptor (117),however, the results suggest slowed membrane cycling of Rab7CMT2B mutants, which is directly linked to slowed trafficking and degradation of endocytosed growth factor receptors, leading to enhanced and prolonged endosomal signaling. A possible explanation for slowed transport is a differential interaction of Rab7CMT2B mutants with downstream effector proteins. Previous studies have indicated enhanced interaction of Rab7L129F and Rab7V162M mutants with cholesterol sensor ORP1L,

Vps13C, and clathrin heavy chain (47). A recent report also suggests enhanced interaction of all the four Rab7CMT2B mutants with peripherin, a neuronal intermediate filament which alters its assembly dynamics (118). The Rab7CMT2B mutants have also been found to phosphorylate and alter the assembly of vimentin, another intermediate filament component (119).

Evidence for altered effector binding and differential phenotypes between other CMT2B mutants is provided by other published studies and this thesis. Rab7K157N mutant does not interact with the retromer complex, Vps35/29/26. This was the first report of a loss of function for the Rab7K157N disease mutant and led to the postulate that neuronal degeneration might result from altered retromer regulation of endosomal membrane protein sorting. The Rab7CMT2B mutants, including the K157N mutant, are autosomal dominant mutants; CMT2B patients harboring the K157N mutation would still possess the wild-type Rab7, but the disease mutant would affect the kinetics of VPS35/29/26 recruitment, leading to reduced efficiency of endosomal protein sorting, which could be detrimental in the very long axons that are affected in CMT2B patients (38). On early endosomes, Rab7 functions in cargo sorting by recruiting the retromer complex (Vps26/ 29/35), which enables retrieval of cation-independent mannose 6-phosphate receptor, TGN38, Wntless among other cargo from early endosomes to the Golgi (38, 120, 121) **(Figure 5)**. Interaction of retromer with Snx proteins and actin-binding proteins couples sorting with membrane tubulation (121, 122). Dysregulation of retromer is associated with neurologic diseases, including Alzheimer's disease, underscoring the importance of the Rab7-retromer link.

In fact, work in this thesis also shows a loss of function of Rab7V162M mutant based on its diminished interaction with the Rab7 interactor alpha proteasomal subunit, XAPC7. XAPC7 has been shown to be a negative regulator of endocytic transport (80), and the impaired interaction with Rab7V162M mutant caused a relatively faster degradation of internalized growth factor receptor compared with the other disease mutants. In cytototoxic T-lymphocytes, Rab7V162M mutant showed more tightly clustered lytic granules around the centrosome compared with those of the wild-type, although increased dynein recruitment was not observed (123). It maybe postulated that such allele-specific differences may account for kinetic differences between the mutants and help to reveal mechanistic information about Rab7-effector interactions. However, allele specific differences in the ability of the Rab7CMT2B mutants to bind various effectors cannot solely be at the root of the common pathology seen in all Rab7CMT2B mutations. The effects that are common to the different alleles (*e.g.* altered EGFR signaling/degradation) are most likely to be informative regarding the pathologic mechanisms.

Rab7CMT2B mutants alter endosomal signaling

This thesis shows that Rab7CMT2B mutants alter endosomal signaling. Here it is demonstrated that the Rab7CMT2B mutants enhance ERK signaling in response to both NGF and EGF triggered signaling through cognate receptors. This enhanced ERK signaling is likely to be dependent on the endosomal membrane residence time of the activated TrkA and EGFR, which is in turn regulated by Rab7. Being predominantly in the GTP-bound state the Rab7CMT2B mutants would be expected to promote more rapid degradation of the TrkA containing signaling endosomes. Consequently, the net effect of

slowed trafficking of the activated TrkA caused by Rab7CMT2B mutants present on endosomes is entirely consistent with the observed enhancement of phosphorylated ERK1/2 in all cell types. Brief stimulation of PC12 cells expressing the disease causing Rab7CMT2B mutants with NGF did not significantly affect Akt phosphorylation. There have been reports of the presence of activated Akt in various cell organelles such as nucleus, Golgi apparatus, cell surface and mitochondria, although not endosomes (124, 125). Therefore, consistent with previous work showing Akt signaling predominates at the plasma membrane (67,95), the data show Akt signaling does not emanate from endosomes containing activated TrkA.

An intriguing question that remains is the role played by the MAP kinase phosphatases (MKPs) in regulating the level of phosphorylated ERK1/2. MKP3 expression is triggered by the translocation of the activated ERK to the nucleus, is maximal around 3h after NGF stimulation and the upregulation can last as long as five days in PC12 cells (126). MKP3 is cytoplasmic and acts specifically on ERK (127). Because the disease associated Rab7CMT2B mutants lead to significantly higher levels of activated ERK1/2, the negative regulatory function that is normally met through the MKP activity is likely compromised in CMT2B disease. The results suggest that the impaired neurite growth, which is an important disease phenotype, may be due in part to retardation of shuttling of the phosphorylated ERK1/2 to the nucleus, which is normally a prerequisite for upregulation of MKP3 expression and down regulation of ERK signaling (97).

The strong persistence of phosphorylated ERK1/2 24h after brief NGF stimulation was reported previously in PC12 cells expressing the GDP-bound Rab7T22N mutant (67). The expression of the Rab7T22N mutant, which is stabilized in inactive state, did not

however preclude nuclear localization of the activated ERK1/2. Furthermore, inhibition of Rab7 activity by overexpressing the Rab7T22N was shown to trigger neurite outgrowth in PC12 cells following brief NGF stimulation (67). In contrast, it is demonstrated that the Rab7 mutants associated with CMT2B disease led to accumulation of the phosphorylated ERK1/2 in the cytosol rather than the nucleus. This may explain the inhibitory effect of the Rab7CMT2B mutants on neurite outgrowth as recently observed (117).

Sensory neurons have very long axons and endocytosis typically occurs at the distal axonal terminal. Signaling endosomes must therefore traverse a long way to the cell body via retrograde transport and consequently misregulation of the Rab7 cycle under diseased conditions (e.g. mutant versions of Rab7) would lead to altered trafficking and deficits in the translocation of activated ERK1/2. This could account for the more pronounced effects of these mutants in cells bearing longer neurites (>0.50μm) (117). The accumulation of activated ERK1/2 in the cytoplasm suggests that the CMT2B associated mutants retard kinase shuttling to the nucleus, which is required to upregulate the genes responsible for differentiation of sensory neurons. An alternative explanation stems from a recent study showing the enhanced trafficking of Rab7CMT2B positive endosomes/autophagosomes in the anterograde direction rather than the usual retrograde direction that might increase the membrane residence time of the MAPK signaling scaffold and account for the enhanced cytoplasmic signaling observed in this study (105). The data shed new light on the mechanism mediating the deficits in neurite outgrowth in Charcot-Marie-Tooth disease.

Previous studies have shown that overexpression of the constitutively active Rab7Q67L mutant causes a perinuclear accumulation of endosomes that delays the delivery of EGFR to the late endosomes and subsequent EGFR degradation. Additionally, ERK signaling was enhanced, whereas p38 signaling decreased (101). It was also seen the Rab7CMT2B-positive endosomes to be more concentrated in the perinuclear region although not quite as tightly clustered as the Rab7Q67L-positive endosomes, which might partially explain the enhanced p38 and ERK activation and slower EGFR degradation. Also the positioning of the signaling endosomes decorated by the Rab7CMT2B mutants seems to play a crucial role in determining the signal output. Enhanced endosomal p38 and ERK1/2 activation may reflect slowed membrane sequestration of the internalized activated growth factor receptor into intralumenal vesicles. The relatively higher membrane residence time of Rab7CMT2B mutants suggested by FRAP experiments accounts for an increased residence time of the MAPK scaffold, in turn accounting for the enhanced ERK1/2 and p38 activation following growth factor stimulation of Rab7CMT2B mutant expressing cells. In PC12 cells, EGF stimulation results in transient MAPK activation in contrast to NGF signaling, where sustained activation of MAPK continues signaling by phosphorylating transcription factors. These differential consequences of signaling determine the proliferative (EGF-induced) and differentiation (NGF-induced) capacity of the cell (128). Interestingly, EGFR family members have also been shown to function in concert, autonomously or non-autonomously, to regulate the development of the peripheral nervous system (129-132). Hence, impaired trafficking of internalized epidermal growth factor receptors can reduce nuclear signaling and expression of immediate early genes to cause an overall developmental defect. The

experiments conducted in this dissertation work show a similar defect in nuclear shuttling of activated ERK1/2 upon NGF stimulation in PC12 cells expressing the Rab7CMT2B mutants (68). All four Rab7CMT2B mutants showed differential nuclear to cytoplasmic distribution of activated ERK upon NGF stimulation of TrkA receptors compared to the wild-type. The effects of EGF stimulation in non-neuronal HeLa and neuronal PC12 cells were also analyzed. Indeed, nuclear distribution of the signaling MAPKs was reduced, as also observed for TrkA signaling (133). The data are consistent with a prolonged half-life of activated pEGFR due to delayed trafficking to lysosomes, linked to the prolonged membrane residence time of the mutant Rab7 proteins and a concomitant increased membrane residence time of the MAPK scaffold.

Rab7CMT2B mutants show impaired nuclear signaling

This thesis also shows a reduced nuclear signaling with lower Elk-1 driven gene activity and lower transcription of c-*fos* and *Egr-1* in the disease mutants, most likely due to the impaired nuclear shuttling of activated p38 and ERK1/2 in the disease mutants. It is worth noting that another member of the Egr family, Egr-2 is mutant in CMT1D and 4E types. Interestingly, Egr-1 and Egr-2 show 92% sequence homology in the zinc binding finger structure (134) that might explain a common mechanism operative in different types of CMT disease.

Elk-1 uses different DNA binding modes to regulate distinct classes of target genes involved in cellular processes ranging from cytoskeletal regulation to apoptosis (135). For example, transcription of SMN1 is dependent on ETS-domains in Elk-1 rather than

on serum response factor element recognition, as well as on glycogen synthase kinase 3(136, 137). This may explain why no impact of the CMT2B mutants on *SMN1* transcription was observed. Mcl-1 is a prosurvival factor that regulates autophagy in mature neurons via a Rab7-Beclin-dependent pathway (136, 138). Although *Mcl-1* is also subject to transcriptional regulation by Elk-1, reductions in *Mcl-1* transcription were too slight to reach statistical significance in our experimental system but might be more critical in a neuronal context with long axons.

Rab7CMT2B mutants differentially interact with p62 and show slower deubiquitination of TrkA receptors

The co-immunoprecipitation studies demonstrate an altered interaction of p62 with the Rab7CMT2B mutants. SQSTM1/p62 lies at the nexus of TrkA endocytic trafficking and autophagy. Hence a correlative alteration of these two machineries in CMT2B disease cannot be ruled out. In fact a recent report suggests modulation of the endocytic and autophagic flux by the Rab7CMT2B mutants that substantially increase the transport of these vesicles in the anterograde direction compared with the wild-type Rab7. The speed of TrkA transport was significantly decreased in the vesicles containing the Rab7CMT2B mutants (105). This thesis also suggests a slower process of deubiquitination of the TrkA receptors in the Rab7CMT2B mutants which would suggest an impaired shuttling of the ubiquitylated TrkA from the late endosomes to the proteasome for deubiquitination by the p62 and hence a delay in TrkA transport and lysosomal degradation.

Conclusion

Overall, the results suggest an impaired trafficking and altered endosomal and nuclear signaling in cells expressing the Rab7CMT2B mutants and lay the foundation for a better understanding of the disease pathology. Rab7, although a ubiquitous protein, affects principally the peripheral nervous system in CMT2B disease. The more pronounced effect of the CMT2B mutants in reducing nuclear translocation of p38 and ERK1/2 in PC12 cells might be attributed to neuronal cell-specific effectors and/or a greater sensitivity to defects in endocytic trafficking, as suggested previously (31, 48).

In conclusion, the study throws light on the pathogenic mechanism leading to Charcot-Marie-Tooth Type2B disease by defining the enhanced Rab7-dependent activation of TrkA and EGFR and the consequent alteration of downstream MAPK signaling pathways that leads to altered nuclear signaling and overall impaired transport.

Future Directions

Charcot-Marie-Tooth disease typically manifests in the second or third decade of life. Impaired trafficking of growth factor receptors may over time alter the balance between proliferative and differentiation signals that cause axonal shortening and eventual loss of contacts necessary for viability. Peripheral axons can grow as long as 1meter, and impairment in long distance transport from the axonal tip to the cell body through differential interaction of Rab7 with specific effector proteins may impair endosomal traffic and in turn affect endosomal and nuclear signaling to cause progressive neurodegeneration. Dynein-/dynactin-mediated perinuclear positioning of late endosomes have also been shown to depend on the membrane-associated scaffolding protein, huntingtin (Htt), which when mutant causes Huntington's disease, though the link between Htt and Rab7 remains unclear (31, 139). Htt and the huntingtin associated protein of 40 kDa (HAP40) are known effectors of Rab5 that facilitate transfer between microtubule-and actin-based networks. Parallel *in vitro* studies testing Rab7 did not provide evidence for a direct Rab7-Htt or a Rab7-HAP40 interaction, although huntingtin-associated protein 1 (HAP1) binds dynactin-p150-Glued (31). Therefore, it is speculated that Htt interaction with the Rab7 dynein/dynactin complex may occur through HAP1**.** In light of the disease relevance, further study of the potential interfaces between Htt,HAP1 and Rab7 is warranted. Although no difference was found in the interaction between Rab7CMT2B mutants and its effector the RILP that bridges between endosomes and the dynein-dynactin motor complex (29), future work should carefully examine the role played by the kinesin motors in enhancing the anterograde transport of

these Rab7CMT2B mutant-vesicles as recently reported (105). This might help investigate the molecular basis of CMT2B pathology.

The similarities between CMT diseases and hereditary spastic paraplegia, together with the recent identification of single nucleotide polymorphisms or SNPs in Rab7 that are linked to late onset Alzheimer disease (140), suggest that these findings may be more broadly relevant to other neurodegenerative diseases.

Appendices

Appendix A: Small molecule intervention of Rab7 activity

Therapeutic interventions relevant to CMT2B disease remain unexplored. To date there is only one report that suggests therapeutic intervention with the small molecule mood stabilizer drug, valproic acid. In DRG neurons expressing the Rab7CMT2B mutants, valproic acid was found to improve defective neurite formation via the c-Jun N terminal Kinase (JNK) signaling pathway (141). Valproic acid is a histone deacetylase inhibitor that promotes neuronal differentiation through extracellular signal regulated kinase (ERK) and glycogen synthase kinase 3 (GSK 3) pathways (142). Direct interventions of Rab GTPases through modulation of membrane association, nucleotide binding or exchange and inhibition of protein-protein interaction remain unexploited. There is only one report that used a systematic screen for Rab7 guanine nucleotide binding inhibitors where purified proteins immobilized on beads were used to assay for fluorescent GTP binding by flow cytometry **(Appendix A)** (31). As mentioned earlier, the inhibitor of Rab7 identified in our lab reports an inhibition of GTP binding of 80% and GDP binding of 60% *in vitro* (87). Inhibition of Rab7 guanine nucleotide binding would be expected to significantly impair its interaction with effector proteins in cells by this novel approach. Targeting the activity of Rab7CMT2B mutants that predominantly occur in the GTP-bound active state would hence regulate the signaling pathways that get altered due to impaired trafficking in axons.

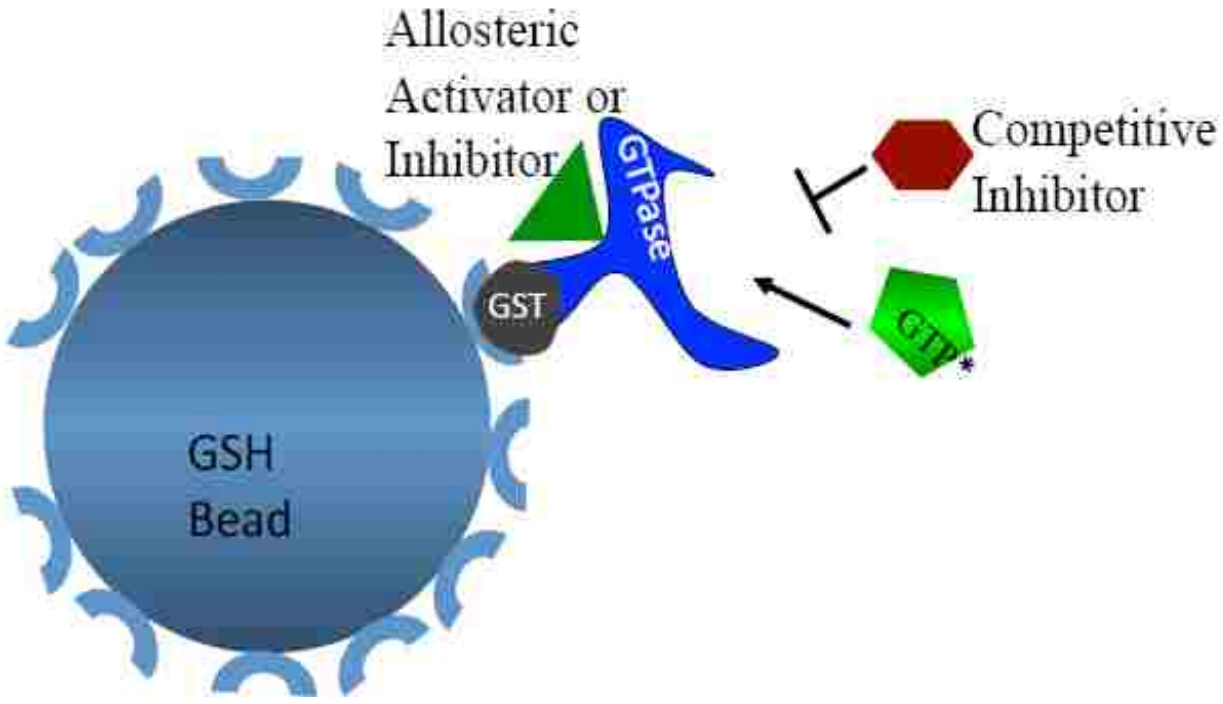

Appendix A: Bead based flow cytometry assay to analyze the effect of small molecule inhibition of Rab7 activity

Appendix B: Rab GTPase activation in response to growth factor stimulation measured in flow cytometry based assay

A robust bead-based assay is devised to quantitatively monitor GTPase protein-protein interactions and also assess Rab GTPase activation in response to growth factor stimulation (**Figure 11**). The assay is novel, adaptable to multiplexing and sensitive enough for measuring GTPase activity in small cell lysate samples. The assay provided the first concrete evidence for an upregulation in Rab5 and Rab7 GTPase activity in response to growth factor (EGF) signaling. While there have been reports that Rab7 is phosphorylated in response to EGF stimulation it has long been assumed that EGF and its receptor are constitutively endocytosed. The time course of increased Rab5 and Rab7 activation is directly correlated with the known time course of endocytosis. Rab5 is required for early events in endocytosis from the plasma membrane to early endosomes and Rab7 being required at later stages when cargo moves from early endosomes to late endosomes and lysosomes.

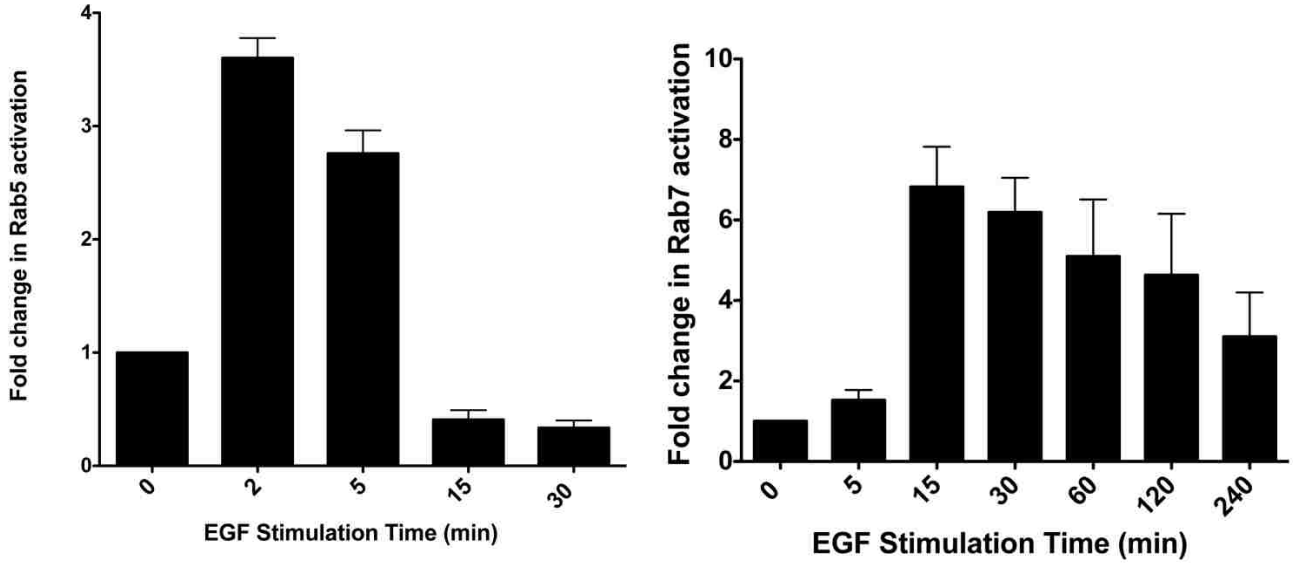

Appendix B: Quantitative Flow Cytometry Assay for measuring Rab GTPase activation status in cells. Bar graphs: Purified GST-effector proteins (EEA1 for Rab5 and RILP for Rab7) were bound to GSH beads overnight in HPSE buffer (HPS, 1mM EDTA, and 0.1% BSA). Cells were serum-starved and stimulated with 10ng/ml EGF for 2min to 4h and cell lysates prepared in RIPA buffer. Lysates were immediately incubated with effector beads, and bound, active Rab5 or Rab7 GTPases were quantified using fluorescently conjugated antibodies against Rab5 or Rab7. Negative controls with irrelevant antibody were measured in parallel and subtracted prior to calculation of fold change. n=3.

Appendix C: Effector Binding Assay Reveals Cellular Inhibition of Rab GTPases by CID1067700

As detailed above, a flow cytometry assay was established based on effector binding that can specifically measure Rab5 and Rab7 in the GTP-bound states. The assay was used to definitively demonstrate that the compound is effective in inhibiting Rab5 and Rab7 in cells. The findings confirm that the observed inhibition of EGFR degradation in cell based assays is a direct consequence of GTPase inhibition.

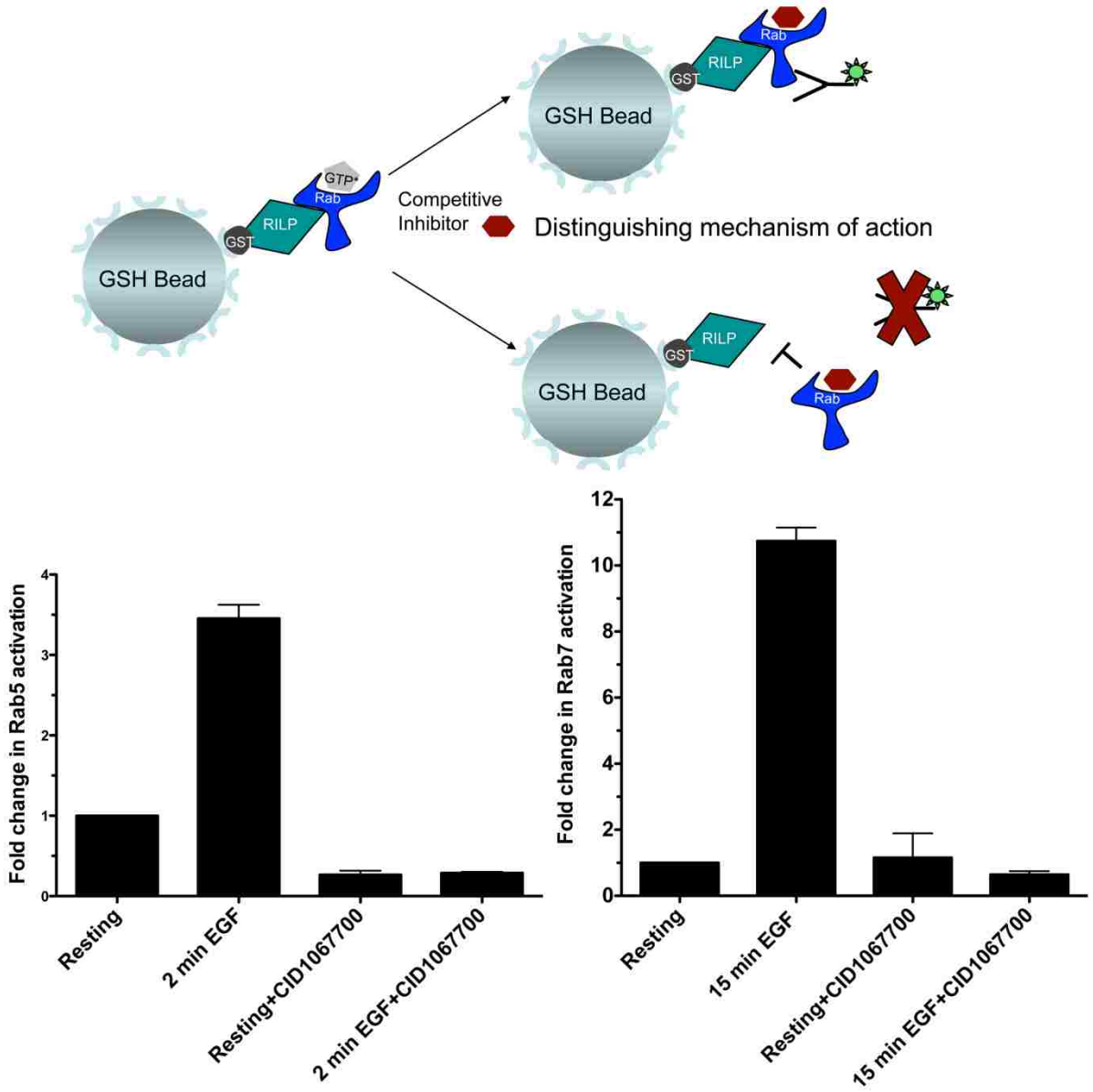

Appendix C. A novel competitive inhibitor of Rab7 blocks Rab GTPase activation in cells. Cells were serum-starved and EGF-stimulated with or without CID1067700, a competitive inhibitor of Rab7. A flow cytometric effector binding assay was used to quantify the levels of active Rab5 (EEA1 used as effector) and Rab7 (RILP used as effector). n=3.

Appendix D: CID1067700 impair EGFR degradation in HeLa cells stably expressing GFP-tagged Rab7

HeLa cells were serum starved for 2h followed by EGF stimulation in a time dependent manner. Cells treated with CID1067700 showed slower EGFR degradation.

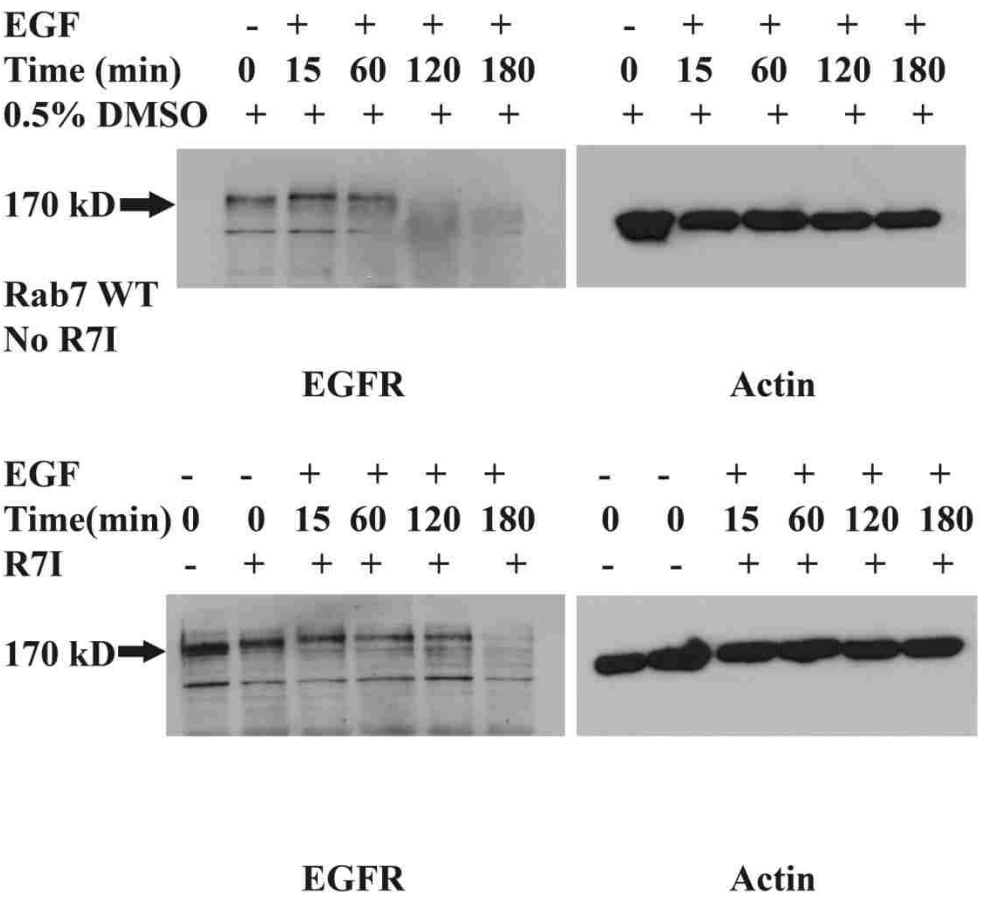

Appendix D: A novel competitive inhibitor of Rab7, CID1067700 impairs EGFR in cells. Cells were serum-starved and EGF-stimulated with or without CID1067700, a competitive inhibitor of Rab7. Following EGF stimulation for the indicated time points cells were lysed and samples were immunoblotted and probed for anti-EGFR antibody.

Appendix E: Rab7 inhibitor CID1067700, inhibits autophagy

To further investigate the role of CID1067700 in impairing Rab7 activity, cells were starved for 2h followed by 1h treatment with CID1067700 and its structural analogs, CID 46916263 and CID 1251121. The levels of LC3-II, an indicator of autophagy were quantified. The Rab7 small molecule inhibitor showed higher level of accumulation of LC3-II.

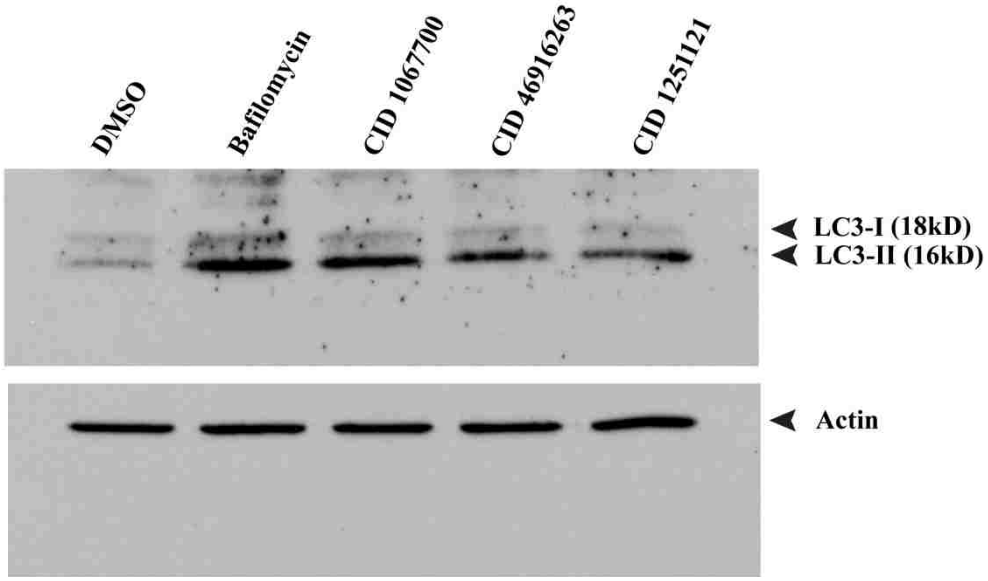

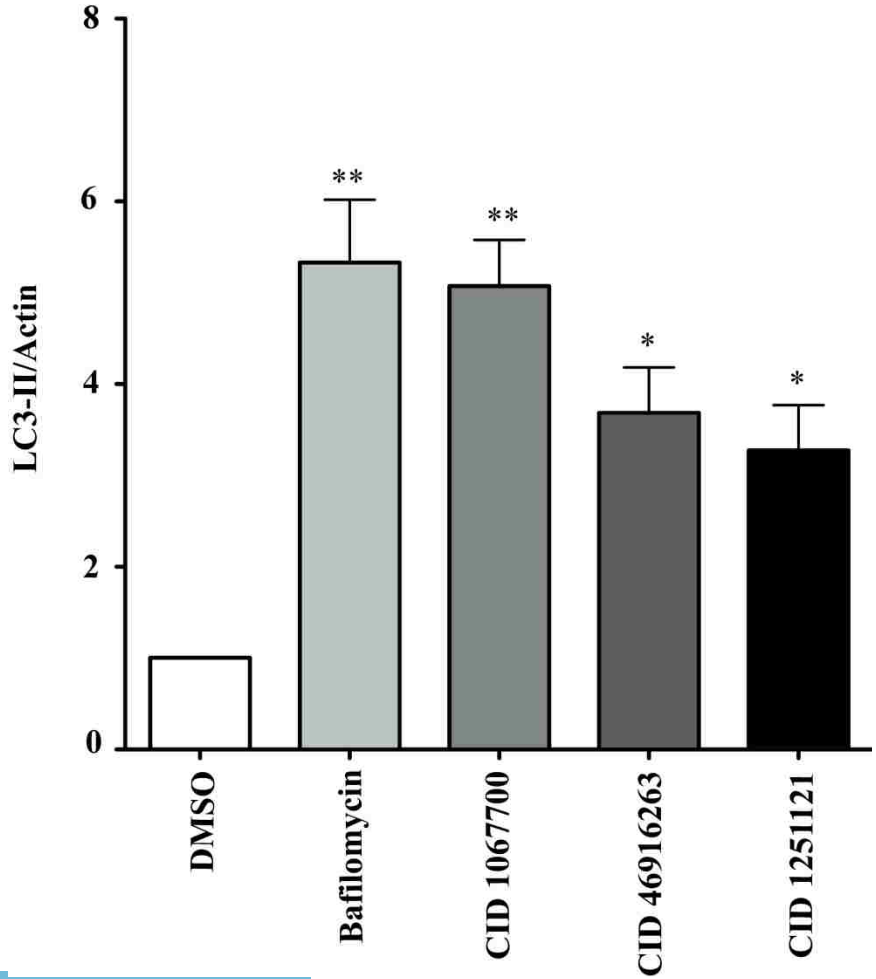

Appendix E: Rab7 inhibitor CID1067700 inhibits autophagy. A) HeLa cells starved for 2h with Earle's Balanced Salt Solution (EBSS) were treated with CID1067700, CID46916263 and CID1251121 for 1h. Cells were lysed and probed with anti LC3 antibody. **B)** Densitometric quantification of the blots were quantified by Image J analysis. LC3-II levels were normalized against actin. Differences are represented as ± S.E.M. Asterisks denote $p<0.05$ based on one-way ANOVA with Dunnett's post-test and relative to Rab7 wild-type control.

Conclusion

The detailed mechanisms of alteration of endocytic trafficking and signaling in CMT2B disease are still beginning to be appreciated. However therapeutic intervention of Rab7 might help ameliorate the trafficking defects observed in CMT2B disease but this endeavor is still at its nascent stage. To date, CID1067700 is the only small molecule inhibitor functionally characterized that has the potential to modulate Rab7 activity as a competitive inhibitor (87). This is promising as Rab7CMT2B mutants predominantly exist in the GTP-bound state and any therapeutic intervention to regulate the GTP loading on the nucleotide binding pocket of these Rab7CMT2B mutants would be expected to help prevent the molecular trafficking events that go awry in CMT2B disease. Future studies should focus on testing the efficacy of this molecule on animal models recapitulating the CMT2B disease and translate to clinical trials.

References

1. Barisic, N., Claeys, K. G., Sirotkovic-Skerlev, M., Lofgren, A., Nelis, E., De Jonghe, P. and Timmerman, V. Charcot-Marie-Tooth disease: a clinico-genetic confrontation. Annhum Genet. 2008; **72:** 416-441.
2. Shy, M. E., Garbern, J. Y. and Kamholz, J.hereditary motor and sensory neuropathies: a biological perspective. Lancet Neurol. 2002; **1:** 110-118.
3. Young, P. and Suter, U. The causes of Charcot-Marie-Tooth disease. Cell Mol Life Sci. 2003; **60:** 2547-2560.
4. Bienfait,h. M., Baas, F., Koelman, J.h., dehaan, R. J., van Engelen, B. G., Gabreels-Festen, A. A., Ongerboer de Visser, B. W., Meggouh, F., Weterman, M. A., De Jonghe, P., Timmerman, V. and de Visser, M. Phenotype of Charcot-Marie-Tooth disease Type 2. Neurology. 2007; **68:** 1658-1667.
5. Mersiyanova, I. V., Perepelov, A. V., Polyakov, A. V., Sitnikov, V. F., Dadali, E. L., Oparin, R. B., Petrin, A. N. and Evgrafov, O. V. A new variant of Charcot-Marie-Tooth disease type 2 is probably the result of a mutation in the neurofilament-light gene. Am Jhum Genet. 2000; **67:** 37-46.
6. Kuhlenbaumer, G., Young, P.,hunermund, G., Ringelstein, B. and Stogbauer, F. Clinical features and molecular genetics ofhereditary peripheral neuropathies. J Neurol. 2002; **249:** 1629-1650.

7. Nave, K. A., Sereda, M. W. and Ehrenreich,h. Mechanisms of disease: inherited demyelinating neuropathies--from basic to clinical research. Nat Clin Pract Neurol. 2007; **3:** 453-464.

8. Ajroud-Driss, S., Deng,h. X. and Siddique, T. Recent advances in the genetics ofhereditary axonal sensory-motor neuropathies type 2. Curr Neurol Neurosci Rep. 2011; **11:** 262-273.

9. Zuchner, S. and Vance, J. M. Mechanisms of disease: a molecular genetic update onhereditary axonal neuropathies. Nat Clin Pract Neurol. 2006; **2:** 45-53.

10. Azzedine,h., Senderek, J., Rivolta, C. and Chrast, R. Molecular genetics of charcot-marie-tooth disease: from genes to genomes. Mol Syndromol. 2012; **3:** 204-214.

11. Thomas, P. K. andharding, A. E. Inherited neuropathies: the interface between molecular genetics and pathology. Brain Pathol. 1993; **3:** 129-133.

12. Azzedine,h., Ravise, N., Verny, C., Gabreels-Festen, A., Lammens, M., Grid, D., Vallat, J. M., Durosier, G., Senderek, J., Nouioua, S.,hamadouche, T., Bouhouche, A., Guilbot, A., Stendel, C., Ruberg, M., Brice, A., Birouk, N., Dubourg, O., Tazir, M. and LeGuern, E. Spine deformities in Charcot-Marie-Tooth 4C caused by SH3TC2 gene mutations. Neurology. 2006; **67:** 602-606.

13. Thomas, P. K. and Calne, D. B. Motor nerve conduction velocity in peroneal muscular atrophy: evidence for geneticheterogeneity. J Neurol Neurosurg Psychiatry. 1974; **37:** 68-75.

14. Bouche, P., Gherardi, R., Cathala,h. P., Lhermitte, F. and Castaigne, P. Peroneal muscular atrophy. Part 1. Clinical and electrophysiological study. J Neurol Sci. 1983; **61:** 389-399.

15. Rossi, A., Paradiso, C., Cioni, R., Rizzuto, N. and Guazzi, G. Charcot-Marie-Tooth disease: study of a large kinship with an intermediate form. J Neurol. 1985; **232:** 91-98.

16. Patzko, A. and Shy, M. E. Update on Charcot-Marie-Tooth disease. Curr Neurol Neurosci Rep. 2011; **11:** 78-88.

17. Dubourg, O., Azzedine,h., Verny, C., Durosier, G., Birouk, N., Gouider, R., Salih, M., Bouhouche, A., Thiam, A., Grid, D., Mayer, M., Ruberg, M., Tazir, M., Brice, A. and LeGuern, E. Autosomal-recessive forms of demyelinating Charcot-Marie-Tooth disease. Neuromolecular Med. 2006; **8:** 75-86.

18. Gentil, B. J. and Cooper, L. Molecular basis of axonal dysfunction and traffic impairments in CMT. Brain Res Bull. 2012; **88:** 444-453.

19. Alto, N. M., Soderling, J. and Scott, J. D. Rab32 is an A-kinase anchoring protein and participates in mitochondrial dynamics. J Cell Biol. 2002; **158:** 659-668.

20. Bui, M., Gilady, S. Y., Fitzsimmons, R. E., Benson, M. D., Lynes, E. M., Gesson, K., Alto, N. M., Strack, S., Scott, J. D. and Simmen, T. Rab32 modulates apoptosis onset and mitochondria-associated membrane (MAM) properties. J Biol Chem. 2010; **285:** 31590-31602.

21. Auer-Grumbach, M.hereditary sensory neuropathies. Drugs Today (Barc). 2004; **40:** 385-394.

22. Auer-Grumbach, M., Mauko, B., Auer-Grumbach, P. and Pieber, T. R. Molecular genetics ofhereditary sensory neuropathies. Neuromolecular Med. 2006; **8:** 147-158.

23. Schwartz, S. L., Cao, C., Pylypenko, O., Rak, A. and Wandinger-Ness, A. Rab GTPases at a glance. J Cell Sci. 2007; **120:** 3905-3910.

24. Axelrod, F. B. and Gold-von Simson, G.hereditary sensory and autonomic neuropathies: types II, III, and IV. Orphanet J Rare Dis. 2007; **2:** 39.

25. Verhoeven, K., De Jonghe, P., Coen, K., Verpoorten, N., Auer-Grumbach, M., Kwon, J. M., FitzPatrick, D., Schmedding, E., De Vriendt, E., Jacobs, A., Van Gerwen, V., Wagner, K.,hartung,h. P. and Timmerman, V. Mutations in the small GTP-ase late endosomal protein RAB7 cause Charcot-Marie-Tooth type 2B neuropathy. Am Jhum Genet. 2003; **72:** 722-727.

26. Houlden,h., King, R.h., Muddle, J. R., Warner, T. T., Reilly, M. M., Orrell, R. W. and Ginsberg, L. A novel RAB7 mutation associated with ulcero-mutilating neuropathy. Ann Neurol. 2004; **56:** 586-590.

27. Meggouh, F., Bienfait,h. M., Weterman, M. A., de Visser, M. and Baas, F. Charcot-Marie-Tooth disease due to a de novo mutation of the RAB7 gene. Neurology. 2006; **67:** 1476-1478.

28. Zhang, M., Chen, L., Wang, S. and Wang, T. Rab7: roles in membrane trafficking and disease. Biosci Rep. 2009; **29:** 193-209.

29. Spinosa, M. R., Progida, C., De Luca, A., Colucci, A. M., Alifano, P. and Bucci, C. Functional characterization of Rab7 mutant proteins associated with Charcot-Marie-Tooth type 2B disease. J Neurosci. 2008; **28:** 1640-1648.

30. De Luca, A., Progida, C., Spinosa, M. R., Alifano, P. and Bucci, C. Characterization of the Rab7K157N mutant protein associated with Charcot-Marie-Tooth type 2B. Biochem Biophys Res Commun. 2008; **372:** 283-287.

31. Agola, J. O., Jim, P. A., Ward,h.h., Basuray, S. and Wandinger-Ness, A. Rab GTPases as regulators of endocytosis, targets of disease and therapeutic opportunities. Clin Genet. 2011; **80:** 305-318.

32. Wang, T.,ming, Z., Xiaochun, W. andhong, W. Rab7: role of its protein interaction cascades in endo-lysosomal traffic. Cell Signal. 2011; **23:** 516-521.

33. Sun, Q., Westphal, W., Wong, K. N., Tan, I. and Zhong, Q. Rubicon controls endosome maturation as a Rab7 effector. Proc Natl Acad Sci U S A. 2010; **107:** 19338-19343.

34. Zhong, Y., Wang, Q. J., Li, X., Yan, Y., Backer, J. M., Chait, B. T.,heintz, N. and Yue, Z. Distinct regulation of autophagic activity by Atg14L and Rubicon associated with Beclin 1-phosphatidylinositol-3-kinase complex. Nat Cell Biol. 2009; **11:** 468-476.

35. Sun, Q., Zhang, J., Fan, W., Wong, K. N., Ding, X., Chen, S. and Zhong, Q. The RUN domain of rubicon is important forhVps34 binding, lipid kinase inhibition, and autophagy suppression. J Biol Chem. 2011; **286:** 185-191.

36. Lin, M. G. and Zhong, Q. Interaction between small GTPase Rab7 and PI3KC3 links autophagy and endocytosis: A new Rab7 effector protein sheds light on membrane trafficking pathways. Small GTPases. 2011; **2:** 85-88.

37. Frasa, M. A., Maximiano, F. C., Smolarczyk, K., Francis, R. E., Betson, M. E., Lozano, E., Goldenring, J., Seabra, M. C., Rak, A., Ahmadian, M. R. and Braga, V. M. Armus is a Rac1 effector that inactivates Rab7 and regulates E-cadherin degradation. Curr Biol. 2010; **20:** 198-208.

38. Seaman, M. N.,harbour, M. E., Tattersall, D., Read, E. and Bright, N. Membrane recruitment of the cargo-selective retromer subcomplex is catalysed by the small GTPase Rab7 and inhibited by the Rab-GAP TBC1D5. J Cell Sci. 2009; **122:** 2371-2382.

39. Peralta, E. R., Martin, B. C. and Edinger, A. L. Differential effects of TBC1D15 and mammalian Vps39 on Rab7 activation state, lysosomal morphology, and growth factor dependence. J Biol Chem. 2010; **285:** 16814-16821.

40. Wu, Y. W., Goody, R. S., Abagyan, R. and Alexandrov, K. Structure of the disordered C terminus of Rab7 GTPase induced by binding to the Rab geranylgeranyl transferase catalytic complex reveals the mechanism of Rab prenylation. J Biol Chem. 2009; **284:** 13185-13192.

41. Wu, Y. W., Tan, K. T., Waldmann,h., Goody, R. S. and Alexandrov, K. Interaction analysis of prenylated Rab GTPase with Rab escort protein and GDP dissociation inhibitor explains the need for both regulators. Proc Natl Acad Sci U S A. 2007; **104:** 12294-12299.

42. Wu, Y. W., Oesterlin, L. K., Tan, K. T., Waldmann,h., Alexandrov, K. and Goody, R. S. Membrane targeting mechanism of Rab GTPases elucidated by semisynthetic protein probes. Nat Chem Biol. 2010; **6:** 534-540.

43. Asbury, A. K. Sensory neuronopathy. Semin Neurol. 1987; **7:** 58-66.

44. Bucci, C., Thomsen, P., Nicoziani, P., McCarthy, J. and van Deurs, B. Rab7: a key to lysosome biogenesis. Mol Biol Cell. 2000; **11:** 467-480.

45. Stenmark,h. and Gillooly, D. J. Intracellular trafficking and turnover of phosphatidylinositol 3-phosphate. Semin Cell Dev Biol. 2001; **12:** 193-199.

46. Stenmark,h. and Olkkonen, V. M. The Rab GTPase family. Genome Biol. 2001; **2:** REVIEWS3007.

47. McCray, B. A., Skordalakes, E. and Taylor, J. P. Disease mutations in Rab7 result in unregulated nucleotide exchange and inappropriate activation.hum Mol Genet. 2010; **19:** 1033-1047.

48. Cogli, L., Piro, F. and Bucci, C. Rab7 and the CMT2B disease. Biochem Soc Trans. 2009; **37:** 1027-1031.

49. Cao, C., Backer, J. M., Laporte, J., Bedrick, E. J. and Wandinger-Ness, A. Sequential actions of myotubularin lipid phosphatases regulate endosomal PI(3)P and growth factor receptor trafficking. Mol Biol Cell. 2008; **19:** 3334-3346.

50. Previtali, S. C., Quattrini, A. and Bolino, A. Charcot-Marie-Tooth type 4B demyelinating neuropathy: deciphering the role of MTMR phosphatases. Expert Rev Mol Med. 2007; **9:** 1-16.

51. Wiley,h. S. and Burke, P. M. Regulation of receptor tyrosine kinase signaling by endocytic trafficking. Traffic. 2001; **2:** 12-18.

52. Beattie, E. C.,howe, C. L., Wilde, A., Brodsky, F. M. and Mobley, W. C. NGF signals through TrkA to increase clathrin at the plasma membrane and enhance clathrin-mediated membrane trafficking. J Neurosci. 2000; **20:** 7325-7333.

53. Howe, C. L., Valletta, J. S., Rusnak, A. S. and Mobley, W. C. NGF signaling from clathrin-coated vesicles: evidence that signaling endosomes serve as a platform for the Ras-MAPK pathway. Neuron. 2001; **32:** 801-814.

54. Shao, Y., Akmentin, W., Toledo-Aral, J. J., Rosenbaum, J., Valdez, G., Cabot, J. B.,hilbush, B. S. andhalegoua, S. Pincher, a pinocytic chaperone for nerve growth factor/TrkA signaling endosomes. J Cell Biol. 2002; **157:** 679-691.

55. Zweifel, L. S., Kuruvilla, R. and Ginty, D. D. Functions and mechanisms of retrograde neurotrophin signalling. Nat Rev Neurosci. 2005; **6:** 615-625.

56. Lu, A., Tebar, F., Alvarez-Moya, B., Lopez-Alcala, C., Calvo, M., Enrich, C., Agell, N., Nakamura, T., Matsuda, M. and Bachs, O. A clathrin-dependent pathway leads to KRas signaling on late endosomes en route to lysosomes. J Cell Biol. 2009; **184:** 863-879.

57. Nada, S.,hondo, A., Kasai, A., Koike, M., Saito, K., Uchiyama, Y. and Okada, M. The novel lipid raft adaptor p18 controls endosome dynamics by anchoring the MEK-ERK pathway to late endosomes. EMBO J. 2009; **28:** 477-489.

58. York, R. D., Yao,h., Dillon, T., Ellig, C. L., Eckert, S. P., McCleskey, E. W. and Stork, P. J. Rap1 mediates sustained MAP kinase activation induced by nerve growth factor. Nature. 1998; **392:** 622-626.

59. Delcroix, J. D., Valletta, J. S., Wu, C.,hunt, S. J., Kowal, A. S. and Mobley, W. C. NGF signaling in sensory neurons: evidence that early endosomes carry NGF retrograde signals. Neuron. 2003; **39:** 69-84.

60. Kuruvilla, R., Ye,h. and Ginty, D. D. Spatially and functionally distinct roles of the PI3-K effector pathway during NGF signaling in sympathetic neurons. Neuron. 2000; **27:** 499-512.

61. Cullen, P. J., Cozier, G. E., Banting, G. and Mellor,h. Modular phosphoinositide-binding domains--their role in signalling and membrane trafficking. Curr Biol. 2001; **11:** R882-93.

62. Christoforidis, S., McBride,h. M., Burgoyne, R. D. and Zerial, M. The Rab5 effector EEA1 is a core component of endosome docking. Nature. 1999; **397:** 621-625.

63. Kruttgen, A., Saxena, S., Evangelopoulos, M. E. and Weis, J. Neurotrophins and neurodegenerative diseases: receptors stuck in traffic? J Neuropathol Exp Neurol. 2003; **62:** 340-350.

64. Howe, C. L. and Mobley, W. C. Long-distance retrograde neurotrophic signaling. Curr Opin Neurobiol. 2005; **15:** 40-48.

65. Rajagopal, R., Ishii, S. and Beebe, D. C. Intracellular mediators of transforming growth factor beta superfamily signaling localize to endosomes in chicken embryo and mouse lenses in vivo. BMC Cell Biol. 2007; **8:** 25.

66. Schroeder, B., Weller, S. G., Chen, J., Billadeau, D. and McNiven, M. A. A Dyn2-CIN85 complex mediates degradative traffic of the EGFR by regulation of late endosomal budding. EMBO J. 2010; **29:** 3039-3053.

67. Saxena, S., Bucci, C., Weis, J. and Kruttgen, A. The small GTPase Rab7 controls the endosomal trafficking and neuritogenic signaling of the nerve growth factor receptor TrkA. J Neurosci. 2005; **25:** 10930-10940.

68. BasuRay, S., Mukherjee, S., Romero, E., Wilson, M. C. and Wandinger-Ness, A. Rab7 mutants associated with Charcot-Marie-Tooth disease exhibit enhanced NGF-stimulated signaling. PLoS One. 2010; **5:** e15351.

69. Villen, J., Beausoleil, S. A., Gerber, S. A. and Gygi, S. P. Large-scale phosphorylation analysis of mouse liver. Proc Natl Acad Sci U S A. 2007; **104:** 1488-1493.

70. Guo, A., Villen, J., Kornhauser, J., Lee, K. A., Stokes, M. P., Rikova, K., Possemato, A., Nardone, J., Innocenti, G., Wetzel, R., Wang, Y., MacNeill, J., Mitchell, J., Gygi, S. P., Rush, J., Polakiewicz, R. D. and Comb, M. J. Signaling networks assembled by oncogenic EGFR and c-Met. Proc Natl Acad Sci U S A. 2008; **105:** 692-697.

71. Raiborg, C. and Stenmark,h. The ESCRT machinery in endosomal sorting of ubiquitylated membrane proteins. Nature. 2009; **458:** 445-452.

72. Geetha, T., Seibenhener, M. L., Chen, L., Madura, K. and Wooten, M. W. p62 serves as a shuttling factor for TrkA interaction with the proteasome. Biochem Biophys Res Commun. 2008; **374:** 33-37.

73. Geetha, T. and Wooten, M. W. TrkA receptor endolysosomal degradation is both ubiquitin and proteasome dependent. Traffic. 2008; **9:** 1146-1156.

74. Bronfman, F. C., Escudero, C. A., Weis, J. and Kruttgen, A. Endosomal transport of neurotrophins: roles in signaling and neurodegenerative diseases. Dev Neurobiol. 2007; **67:** 1183-1203.

75. Chavrier, P., Parton, R. G.,hauri,h. P., Simons, K. and Zerial, M. Localization of low molecular weight GTP binding proteins to exocytic and endocytic compartments. Cell. 1990; **62:** 317-329.

76. Gama, L. and Breitwieser, G. E. Generation of epitope-tagged proteins by inverse polymerase chain reaction mutagenesis. Methods Mol Biol. 2002; **182:** 77-83.

77. Grimes, M. L., Zhou, J., Beattie, E. C., Yuen, E. C.,hall, D. E., Valletta, J. S., Topp, K. S., LaVail, J.h., Bunnett, N. W. and Mobley, W. C. Endocytosis of activated TrkA: evidence that nerve growth factor induces formation of signaling endosomes. J Neurosci. 1996; **16:** 7950-7964.

78. Bernd, P. and Greene, L. A. Association of 125I-nerve growth factor with PC12 pheochromocytoma cells. Evidence for internalization viahigh-affinity receptors only and for long-term regulation by nerve growth factor of bothhigh- and low-affinity receptors. J Biol Chem. 1984; **259:** 15509-15516.

79. Press, B., Feng, Y.,hoflack, B. and Wandinger-Ness, A. Mutant Rab7 causes the accumulation of cathepsin D and cation-independent mannose 6-phosphate receptor in an early endocytic compartment. J Cell Biol. 1998; **140:** 1075-1089.

80. Dong, J., Chen, W., Welford, A. and Wandinger-Ness, A. The proteasome alpha-subunit XAPC7 interacts specifically with Rab7 and late endosomes. J Biol Chem. 2004; **279:** 21334-21342.

81. Mukherjee, S., Dong, J.,heincelman, C., Lenhart, M., Welford, A. and Wandinger-Ness, A. Functional analyses and interaction of the XAPC7 proteasome subunit with Rab7. Methods Enzymol. 2005; **403:** 650-663.

82. Stein, M. P., Feng, Y., Cooper, K. L., Welford, A. M. and Wandinger-Ness, A.human VPS34 and p150 are Rab7 interacting partners. Traffic. 2003; **4:** 754-771.

83. Jordens, I., Fernandez-Borja, M., Marsman, M., Dusseljee, S., Janssen, L., Calafat, J., Janssen,h., Wubbolts, R. and Neefjes, J. The Rab7 effector protein RILP controls lysosomal transport by inducing the recruitment of dynein-dynactin motors. Curr Biol. 2001; **11:** 1680-1685.

84. Tohgo, A., Pierce, K. L., Choy, E. W., Lefkowitz, R. J. and Luttrell, L. M. beta-Arrestin scaffolding of the ERK cascade enhances cytosolic ERK activity but inhibits ERK-mediated transcription following angiotensin AT1a receptor stimulation. J Biol Chem. 2002; **277:** 9429-9436.

85. Tessema, M., Simons, P. C., Cimino, D. F., Sanchez, L., Waller, A., Posner, R. G., Wandinger-Ness, A., Prossnitz, E. R. and Sklar, L. A. Glutathione-S-transferase-green fluorescent protein fusion protein reveals slow dissociation fromhigh site density beads and measures free GSH. Cytometry A. 2006; **69:** 326-334.

86. Schwartz, S. L., Tessema, M., Buranda, T., Pylypenko, O., Rak, A., Simons, P. C., Surviladze, Z., Sklar, L. A. and Wandinger-Ness, A. Flow cytometry for real-time measurement of guanine nucleotide binding and exchange by Ras-like GTPases. Anal Biochem. 2008; **381:** 258-266.

87. Agola, J. O.,hong, L., Surviladze, Z., Ursu, O., Waller, A., Strouse, J. J., Simpson, D. S., Schroeder, C. E., Oprea, T. I., Golden, J. E., Aube, J., Buranda, T., Sklar, L. A. and Wandinger-Ness, A. A competitive nucleotide binding inhibitor: in vitro characterization of Rab7 GTPase inhibition. ACS Chem Biol. 2012; **7:** 1095-1108.

88. Mitra, S., Cheng, K. W. and Mills, G. B. Rab GTPases implicated in inherited and acquired disorders. Semin Cell Dev Biol. 2011; **22:** 57-68.

89. Feng, Y., Press, B., Chen, W., Zimmerman, J. and Wandinger-Ness, A. Expression and properties of Rab7 in endosome function. Methods Enzymol. 2001; **329:** 175-187.

90. Jian, X., Cavenagh, M., Gruschus, J. M., Randazzo, P. A. and Kahn, R. A. Modifications to the C-terminus of Arf1 alter cell functions and protein interactions. Traffic. 2010; **11:** 732-742.

91. Sorkin, A. and von Zastrow, M. Endocytosis and signalling: intertwining molecular networks. Nat Rev Mol Cell Biol. 2009; **10:** 609-622.

92. Di Fiore, P. P. and De Camilli, P. Endocytosis and signaling. an inseparable partnership. Cell. 2001; **106:** 1-4.

93. Perlson, E., Maday, S., Fu, M. M., Moughamian, A. J. andholzbaur, E. L. Retrograde axonal transport: pathways to cell death? Trends Neurosci. 2010; **33:** 335-344.

94. Baloh, R.h., Schmidt, R. E., Pestronk, A. and Milbrandt, J. Altered axonal mitochondrial transport in the pathogenesis of Charcot-Marie-Tooth disease from mitofusin 2 mutations. J Neurosci. 2007; **27:** 422-430.

95. Zhang, Y., Moheban, D. B., Conway, B. R., Bhattacharyya, A. and Segal, R. A. Cell surface Trk receptors mediate NGF-induced survival while internalized receptors regulate NGF-induced differentiation. J Neurosci. 2000; **20:** 5671-5678.

96. Goh, L. K.,huang, F., Kim, W., Gygi, S. and Sorkin, A. Multiple mechanisms collectively regulate clathrin-mediated endocytosis of the epidermal growth factor receptor. J Cell Biol. 2010; **189:** 871-883.

97. Colucci-D'Amato, L., Perrone-Capano, C. and di Porzio, U. Chronic activation of ERK and neurodegenerative diseases. Bioessays. 2003; **25:** 1085-1095.

98. Vieira, A. V., Lamaze, C. and Schmid, S. L. Control of EGF receptor signaling by clathrin-mediated endocytosis. Science. 1996; **274:** 2086-2089.

99. Xue, L. and Lucocq, J. ERK2 signalling from internalised epidermal growth factor receptor in broken A431 cells. Cell Signal. 1998; **10:** 339-348.

100. Fukuda, M., Gotoh, Y., Tachibana, T., Dell, K.,hattori, S., Yoneda, Y. and Nishida, E. Induction of neurite outgrowth by MAP kinase in PC12 cells. Oncogene. 1995; **11:** 239-244.

101. Taub, N., Teis, D., Ebner,h. L.,hess, M. W. andhuber, L. A. Late endosomal traffic of the epidermal growth factor receptor ensures spatial and temporal fidelity of mitogen-activated protein kinase signaling. Mol Biol Cell. 2007; **18:** 4698-4710.

102. Feng, Y., Press, B. and Wandinger-Ness, A. Rab 7: an important regulator of late endocytic membrane traffic. J Cell Biol. 1995; **131:** 1435-1452.

103. Whitmarsh, A. J., Shore, P., Sharrocks, A. D. and Davis, R. J. Integration of MAP kinase signal transduction pathways at the serum response element. Science. 1995; **269:** 403-407.

104. Sanchez, P., De Carcer, G., Sandoval, I. V., Moscat, J. and Diaz-Meco, M. T. Localization of atypical protein kinase C isoforms into lysosome-targeted endosomes through interaction with p62. Mol Cell Biol. 1998; **18:** 3069-3080.

105. Zhang, K., Fishel Ben Kenan, R., Osakada, Y., Xu, W., Sinit, R. S., Chen, L., Zhao, X., Chen, J. Y., Cui, B. and Wu, C. Defective Axonal Transport of Rab7 GTPase Results in Dysregulated Trophic Signaling. J Neurosci. 2013; **33:** 7451-7462.

106. Chance, P. F. Molecular basis ofhereditary neuropathies. Phys Med Rehabil Clin N Am. 2001; **12:** 277-291.

107. Chance, P. F. Genetic evaluation of inherited motor/sensory neuropathy. Suppl Clin Neurophysiol. 2004; **57:** 228-242.

108. Yoshioka, R., Dyck, P. J. and Chance, P. F. Geneticheterogeneity in Charcot-Marie-Tooth neuropathy type 2. Neurology. 1996; **46:** 569-571.

109. Saito, M.,hayashi, Y., Suzuki, T., Tanaka,h.,hozumi, I. and Tsuji, S. Linkage mapping of the gene for Charcot-Marie-Tooth disease type 2 to chromosome 1p (CMT2A) and the clinical features of CMT2A. Neurology. 1997; **49:** 1630-1635.

110. Keller, M. P. and Chance, P. F. Inherited neuropathies: from gene to disease. Brain Pathol. 1999; **9:** 327-341.

111. Keller, M. P. and Chance, P. F. Inherited peripheral neuropathy. Semin Neurol. 1999; **19:** 353-362.

112. Dubourg, O., Barhoumi, C., Azzedine,h., Birouk, N., Brice, A., Bouche, P. and Leguern, E. Phenotypic and genetic study of a family withhereditary sensory neuropathy and prominent weakness. Muscle Nerve. 2000; **23:** 1508-1514.

113. Gemignani, F. and Marbini, A. Charcot-Marie-Tooth disease (CMT): distinctive phenotypic and genotypic features in CMT type 2. J Neurol Sci. 2001; **184:** 1-9.

114. Georgiou, D. M., Zidar, J., Korosec, M., Middleton, L. T., Kyriakides, T. and Christodoulou, K. A novel NF-L mutation Pro22Ser is associated with CMT2 in a large Slovenian family. Neurogenetics. 2002; **4:** 93-96.

115. Lus, G., Nelis, E., Jordanova, A., Lofgren, A., Cavallaro, T., Ammendola, A., Melone, M. A., Rizzuto, N., Timmerman, V., Cotrufo, R. and De Jonghe, P. Charcot-Marie-Tooth disease with giant axons: a clinicopathological and genetic entity. Neurology. 2003; **61:** 988-990.

116. Rotthier, A., Baets, J., De Vriendt, E., Jacobs, A., Auer-Grumbach, M., Levy, N., Bonello-Palot, N., Kilic, S. S., Weis, J., Nascimento, A., Swinkels, M., Kruyt, M.

C., Jordanova, A., De Jonghe, P. and Timmerman, V. Genes forhereditary sensory and autonomic neuropathies: a genotype-phenotype correlation. Brain. 2009; **132:** 2699-2711.

117. Cogli, L., Progida, C., Lecci, R., Bramato, R., Kruttgen, A. and Bucci, C. CMT2B-associated Rab7 mutants inhibit neurite outgrowth. Acta Neuropathol. 2010; **120:** 491-501.

118. Cogli, L., Progida, C., Thomas, C. L., Spencer-Dene, B., Donno, C., Schiavo, G. and Bucci, C. Charcot-Marie-Tooth type 2B disease-causing RAB7A mutant proteins show altered interaction with the neuronal intermediate filament peripherin. Acta Neuropathol. 2013; **125:** 257-272.

119. Cogli, L., Progida, C., Bramato, R. and Bucci, C. Vimentin phosphorylation and assembly are regulated by the small GTPase Rab7a. Biochim Biophys Acta. 2013; **1833:** 1283-1293.

120. Rojas, R., van Vlijmen, T., Mardones, G. A., Prabhu, Y., Rojas, A. L., Mohammed, S.,heck, A. J., Raposo, G., van der Sluijs, P. and Bonifacino, J. S. Regulation of retromer recruitment to endosomes by sequential action of Rab5 and Rab7. J Cell Biol. 2008; **183:** 513-526.

121. McGough, I. J. and Cullen, P. J. Recent advances in retromer biology. Traffic. 2011; **12:** 963-971.

122. Harbour, M. E., Breusegem, S. Y., Antrobus, R., Freeman, C., Reid, E. and Seaman, M. N. The cargo-selective retromer complex is a recruitinghub for protein complexes that regulate endosomal tubule dynamics. J Cell Sci. 2010; **123:** 3703-3717.

123. Daniele, T.,hackmann, Y., Ritter, A. T., Wenham, M., Booth, S., Bossi, G., Schintler, M., Auer-Grumbach, M. and Griffiths, G. M. A role for Rab7 in the movement of secretory granules in cytotoxic T lymphocytes. Traffic. 2011; **12:** 902-911.

124. Filippa, N., Sable, C. L.,hemmings, B. A. and Van Obberghen, E. Effect of phosphoinositide-dependent kinase 1 on protein kinase B translocation and its subsequent activation. Mol Cell Biol. 2000; **20:** 5712-5721.

125. Sasaki, K., Sato, M. and Umezawa, Y. Fluorescent indicators for Akt/protein kinase B and dynamics of Akt activity visualized in living cells. J Biol Chem. 2003; **278:** 30945-30951.

126. Camps, M., Nichols, A., Gillieron, C., Antonsson, B., Muda, M., Chabert, C., Boschert, U. and Arkinstall, S. Catalytic activation of the phosphatase MKP-3 by ERK2 mitogen-activated protein kinase. Science. 1998; **280:** 1262-1265.

127. Bermudez, O., Marchetti, S., Pages, G. and Gimond, C. Post-translational regulation of the ERK phosphatase DUSP6/MKP3 by the mTOR pathway. Oncogene. 2008; **27:** 3685-3691.

128. Marshall, C. J. Specificity of receptor tyrosine kinase signaling: transient versus sustained extracellular signal-regulated kinase activation. Cell. 1995; **80:** 179-185.

129. Maklad, A., Nicolai, J. R., Bichsel, K. J., Evenson, J. E., Lee, T. C., Threadgill, D. W. andhansen, L. A. The EGFR is required for proper innervation to the skin. J Invest Dermatol. 2009; **129:** 690-698.

130. Lin, W., Sanchez,h. B., Deerinck, T., Morris, J. K., Ellisman, M. and Lee, K. F. Aberrant development of motor axons and neuromuscular synapses in erbB2-deficient mice. Proc Natl Acad Sci U S A. 2000; **97:** 1299-1304.

131. Golding, J. P., Trainor, P., Krumlauf, R. and Gassmann, M. Defects in pathfinding by cranial neural crest cells in mice lacking the neuregulin receptor ErbB4. Nat Cell Biol. 2000; **2:** 103-109.

132. Riethmacher, D., Sonnenberg-Riethmacher, E., Brinkmann, V., Yamaai, T., Lewin, G. R. and Birchmeier, C. Severe neuropathies in mice with targeted mutations in the ErbB3 receptor. Nature. 1997; **389:** 725-730.

133. BasuRay, S., Mukherjee, S., Romero, E. G., Seaman, M. N. and Wandinger-Ness, A. Rab7 mutants associated with Charcot-Marie-Tooth disease cause delayed growth factor receptor transport and altered endosomal and nuclear signaling. J Biol Chem. 2013; **288:** 1135-1149.

134. Joseph, L. J., Le Beau, M. M., Jamieson, G. A. J., Acharya, S., Shows, T. B., Rowley, J. D. and Sukhatme, V. P. Molecular cloning, sequencing, and mapping of EGR2, ahuman early growth response gene encoding a protein with "zinc-binding finger" structure. Proc Natl Acad Sci U S A. 1988; **85:** 7164-7168.

135. Odrowaz, Z. and Sharrocks, A. D. ELK1 uses different DNA binding modes to regulate functionally distinct classes of target genes. PLoS Genet. 2012; **8:** e1002694.

136. Demir, O., Aysit, N., Onder, Z., Turkel, N., Ozturk, G., Sharrocks, A. D. and Kurnaz, I. A. ETS-domain transcription factor Elk-1 mediates neuronal survival: SMN as a potential target. Biochim Biophys Acta. 2011; **1812:** 652-662.

137. Makhortova, N. R.,hayhurst, M., Cerqueira, A., Sinor-Anderson, A. D., Zhao, W. N.,heiser, P. W., Arvanites, A. C., Davidow, L. S., Waldon, Z. O., Steen, J. A., Lam, K., Ngo,h. D. and Rubin, L. L. A screen for regulators of survival of motor neuron protein levels. Nat Chem Biol. 2011; **7:** 544-552.

138. Germain, M., Nguyen, A. P., Le Grand, J. N., Arbour, N., Vanderluit, J. L., Park, D. S., Opferman, J. T. and Slack, R. S. MCL-1 is a stress sensor that regulates autophagy in a developmentally regulated manner. EMBO J. 2011; **30:** 395-407.

139. Caviston, J. P. andholzbaur, E. L. Microtubule motors at the intersection of trafficking and transport. Trends Cell Biol. 2006; **16:** 530-537.

140. Vardarajan, B. N., Bruesegem, S. Y.,harbour, M. E., St George-Hyslop, P., Seaman, M. N. and Farrer, L. A. Identification of Alzheimer disease-associated variants in genes that regulate retromer function. Neurobiol Aging. 2012; **33:** 2231.e15-2231.e30.

141. Yamauchi, J., Torii, T., Kusakawa, S., Sanbe, A., Nakamura, K., Takashima, S.,hamasaki,h., Kawaguchi, S., Miyamoto, Y. and Tanoue, A. The mood stabilizer valproic acid improves defective neurite formation caused by Charcot-Marie-Tooth disease-associated mutant Rab7 through the JNK signaling pathway. J Neurosci Res. 2010; **88:** 3189-3197.

142. Hao, Y., Creson, T., Zhang, L., Li, P., Du, F., Yuan, P., Gould, T. D., Manji,h. K. and Chen, G. Mood stabilizer valproate promotes ERK pathway-dependent cortical neuronal growth and neurogenesis. J Neurosci. 2004; **24:** 6590-6599.

****